Some Problems on the Analysis and Control of Electrical Networks with Constant Power Loads

Juan Eduardo Machado Martínez

NNT : 2019SACLS445

Thèse de doctorat

Some Problems on the Analysis and Control of Electrical Networks with Constant Power Loads

Thèse de doctorat de l'Université Paris-Saclay
préparée à L'Université Paris-Sud

École doctorale n°580 Sciences et Technologies de l'Information et de la Communication (STIC)
Spécialité de doctorat : Automatique

Thèse présentée et soutenue à Gif-sur-Yvette, le 22 novembre 2019, par

JUAN EDUARDO MACHADO MARTÍNEZ

Composition du Jury :

Françoise Lamnabhi-Lagarrigue Directeur de Recherche, L2S (CNRS, UMR 8506)	Présidente
Aleksandar Stankovic Professor, Tufts University	Rapporteur
John W. Simpson-Porco Assistant Professor, University of Waterloo	Rapporteur
Robert Griñó Professor, Universitat Politècnica de Catalunya	Examinateur
Luca Greco Maître de conférences, Université Paris-Sud (UMR 8506)	Examinateur
Roméo Ortega Directeur de Recherche, L2S (CNRS, UMR 8506)	Directeur de thèse

Abstract

The continuously increasing demand of electrical energy has led to the conception of power systems of great complexity that may extend even through entire countries. In the vast majority of large-scale power systems the main primary source of energy are fossil fuels. Nonetheless, environmental concerns are pushing a major change in electric energy production practices, with a marked shift from fossil fuels to renewables and from centralized architectures to more distributed ones. One of the main challenges that distributed power systems face are the stability problems arising from the presence of the so-called *Constant Power Loads* (CPLs). These loads, which are commonly found in information and communication technology facilities, are known to reduce the effective damping of the circuits that energize them, which can cause voltage oscillations or even voltage collapse. In this thesis, the main contributions are focused in understanding and solving diverse problems found in the analysis and control of electrical power systems containing CPLs. The contributions are listed as follows. (i) Simply verifiable conditions are proposed to certify the *non existence* of steady states in general, multi-port, alternating current (AC) networks with a distributed array of CPLs. These conditions, which are based on Linear Matrix Inequalities (LMIs), allow to discard the values of the loads' powers that would certainly produce a voltage collapse in the whole network. (ii) For general models of some modern power systems, including High-Voltage Direct Current (HVDC) transmission networks and microgrids, it is shown that if equilibria exist, then there is a characteristic high-voltage equilibrium that dominates, entry-wise, all the other ones. Furthermore, for the case of AC power systems under the standard decoupling assumption, this characteristic equilibrium is shown to be long-term stable. (iii) A class of port-Hamiltonian systems, in which the control variables act directly on the power balance equation, is explored. These systems are shown to be shifted passive when their trajectories are constrained to easily definable sets. The latter properties are exploited to analyze the stability of their—intrinsically non zero—equilibria. It is also shown that the stability of multi-port DC electrical networks and synchronous generators, both with CPLs, can be naturally studied with the proposed framework. (iv) The problem of regulating the output voltage of the versatile DC buck-boost converter feeding an *unknown* CPL is addressed. One of the main obstacles for conventional linear control design stems from the fact that the system's model is non-minimum phase with respect to each of its state variables. As a possible solution to this problem, this thesis reports a nonlinear, adaptive controller that is able to render a desired equilibrium asymptotically stable; furthermore an estimate of the region of attraction can be computed. (v) The last contribution concerns the active damping of a DC small-scale power system with a CPL. Instead of connecting impractical, energetically inefficient passive elements to the existing network, the addition of a controlled DC-DC power converter is explored. The main

contribution reported here is the design of a nonlinear, observer-based control law for the converter. The novelty of the proposal lies in the non necessity of measuring the network's electrical current nor the value of the CPL, highlighting its practical applicability. The effectiveness of the control scheme is further validated through experiments on a real DC network.

To Anna Karen.

Acknowledgements

First, I want to express my deepest and most sincere gratitude to Professor Romeo Ortega, who so kindly accepted my request to become his PhD student around four years ago. All his support, encouragement and valuable advice throughout this years — both in the professional and personal realm — are something for which I will be forever indebted. I would like to also thank here Sra. Amparo, who showed nothing but kindness and sincere care towards me and my little family.

I thank all my co-authors — I have been so lucky to work side-by-side with such talented and kind people.

I thank the jury members of my thesis defense, Dr. Françoise Lamnabhi-Lagarrigue, Prof. Aleksandar Stankovic, Prof. Robert Griñó, Prof. John Simpson-Porco, Dr. Luca Greco, for dedicating their valuable time to read my thesis and for giving me such insightful remarks aimed at improving my work.

I thank the Mexican *Consejo Nacional de Ciencia y Tecnología* (CONACyT) for funding this thesis.

I thank the project Ecos-Nord between Mexico and France (No. M14M02) for funding a research stay in Mexico City and in Guadalajara, where I worked under the guidance of Prof. Gerardo Espinosa and Prof. Emmanuel Nuño; I acknowledge their kind support too.

I thank Antonio, Elena and William for their encouragement, constant advice and kindness.

I thank all my labmates — Rafael, Pablo, Missie, Mohammed, Mattia, Alessio, Bowen, Dongjun, Adel — and many more, for their honest friendship. A special mention goes to Rafael, Pablo and Missie for helping me getting installed at L2S and for tirelessly assisting me in completing the (many) associated administrative tasks. A heartfelt thanks goes to Adel, for his generous time and feedback while preparing my thesis defense.

Lastly — and most importantly — I thank all my family. I thank my wife, Anna Karen, for jumping into this adventure with closed eyes but with the confidence that together we can overcome whatever obstacle comes in the way. You have given me the greatest gift I could ever ask — our beautiful Lucas — and I am the luckiest for sharing my life with you two. I thank my parents, Maricela and Juan, who have always been there for me and have had to make incredible sacrifices so I could have a good life. To my little brother and sister, thank you for always supporting my

dreams even if they imply living far away from each other. To my grandmother, Hermelinda, for being my No. 1 supporter, thank you.

Hubo alguien quien me amó como a un hijo y a quien amé como a una madre. Lucía, con extrema tristeza escribo que tu hermosa vida se extinguió antes de que pudieras ver culminados mis estudios, pero yo sé desde el fondo de mi corazón que ese pasado 22 de noviembre tu amor sin barreras me ayudó a defender con éxito mi tesis. Honraré tu memoria viviendo una vida de la cual tú estarías orgullosa. Gracias por tu amor incondicional. Siempre me haces falta. Te amo.

Sincerely,
Juan E. Machado
La Paz (BCS), Mexico - December 2019.

Contents

Part I

PROLOGUE

Chapter 1

Overview

The energy needs of a modern society are mainly supplied in the form of electrical energy [4]. The commercial use of electricity began in the late 1870's with very small scale networks that provided enough energy to supply arc lamps for lighthouse illumination and street lighting [56]. In order to satisfy the ever increasing demand of electrical energy, industrially developed societies have built large and complex power systems that can extend through entire countries [4, 56].

Electric energy is traditionally produced in thermal power plants, where a combustion process of *fossil fuels* release thermal energy that is transformed into consumer-useful electric energy. The most common fuels used in the commercial production of electricity are coal, natural gas, nuclear fuel and oil [56, 67, 40]. The combustion of fossil fuels in electric power plants represents a major contributor of greenhouse gases emission to the atmosphere [67, 90, 15, 29]. Furthermore, it is considered that the emission of greenhouse gases from human activity is one of the biggest responsible factors in climate change and global warming [15, 63, 87].

A number of strategies have been proposed to reduce greenhouse gas emissions in the electric industry, for example, to increase the number of nuclear plants or to remove the carbon dioxide from exhaust gases of traditional thermal generation [67]. A radical alternative to these options consists in changing from traditional fossil-fueled electric plants to renewable energies-based ones. Renewable energies are energy sources that are continually replenished by nature and derived directly from the sun (e.g. thermal, photo-electric), indirectly from the sun (e.g. wind, hydropower, biomass), or from other natural movements and mechanisms of the environment (e.g. geothermal) [36].

Renewable energy markets have been continuously growing during the last years. The deployment of established technologies, such as hydro, as well as newer technologies, such as wind and solar, has risen quickly, which has increased confidence in the technologies and reduced costs [36].

The increasing penetration of renewable energy markets may require a major shift to current electric production practices. The thermal power plants of a traditional electric system are generally large in terms of power and located far from the end-consumers. To efficiently transport the electricity through large distances, the operation voltages must be tapped up to very high levels using a complex system of substations and transmission grids. Conversely, renewable energy sources tend to be very small in terms of capacity with respect to thermal power plants, which implies that in order to supply the same amount of electric energy, many renewable energy

sources must be installed. Nonetheless, due to a low energy density, these sources are situated in a distributed array rather than a centralized one as in traditional power plants [67].

Recent advances in power electronics have elucidated possible answers to the question of how to better integrate renewable sources into the conventional power system. A proposal that has gained much attention is the concept of *microgrid* [62]. A microgrid consists of a collection of generation units—mostly based on renewable energy sources—residential loads and energy storage elements that can be operated either interconnected/disconnected to/from the main grid [62]. The reader is referred to [96, 97] for a more extensive discussion on microgrids.

1.1 The problem

In many electric power distribution systems and particularly in microgrids, stability problems may occur when a major proportion of the loads are electronic equipment. This kind of equipment is usually powered by cascade distributed architectures which are characterized by the presence of different voltage levels and power electronic converters. These converters act as interfaces between sections of different voltages in which, at last stage, loads are a combination of power electronic converters tightly regulating their output voltage, behaving as Constant Power Loads (CPLs). This architectures are common in information and communication technology facilities where the many telecom switches, wireless communication base stations, and data center servers act as CPLs [38, 59, 122]. It is well-known that CPLs introduce a destabilizing effect that gives rise to significant oscillations or even voltage collapse [38], and hence they are considered to be the most challenging component of the standard load model—referred to as the ZIP model [106, 30] in power system stability analysis.

Stability assessment in networks containing CPLs is a defying challenge, mainly because of the nonlinearities introduced by the dynamics of this kind of load, but also by the nonlinear nature of electronic converters itself. Additionally, the uncertainties associated with renewable energies and the interconnection of several subsystems further aggravate the problem. Hence, the overall system stability can be difficult to be ensured, even if individual subsystems are stable [109].

Considering the relevant economical and environmental implications of understanding the conditions ensuring the stable and safe operation of networks containing Constant Power Loads, this thesis is concerned with this objective

1.2 A general literature review

The main objective of a power system is to provide electric energy to the consumers in a reliable manner, with a minimum cost, minimum ecological impact, and with specified quality standards [56, 67]. Stability analysis of a power system is concerned with the system's ability to withstand perturbations and still be able to fulfill its main objective [4]. Typical disturbances in power systems are, for example, changes in the demand, outages of power plants, or failures in the transmission system [56]. Given the high complexity of the power system of a modern society, the problem

of guaranteeing a safe and stable operation of the system is still an active research field [39, 61, 98, 117, 41].

A *sine qua non* condition to perform stability analyses, and for the correct operation of power systems, is the *existence of a steady state* that, moreover, should be robust in the presence of perturbations [56]. The analysis of these equilibria is complicated by the presence of CPLs, which introduce "strong" nonlinearities. This motivates the development of new methods to analyze their the existence of steady states. In [69, 9, 14] some analysis of *existence* of equilibria is carried out, whereas in [106], sufficient conditions are derived for all operating points of purely resistive networks with constant power loads to lie in a desirable set. It should be pointed out that the power systems community debates now new definitions of stability, which move away from the equilibrium-disturbance-equilibrium paradigm [57]. However, analysis of equilibria in direct current and alternating current systems is still an active research field; see, *e.g.*, [74] and [123].

Stability analysis has been carried out in [3, 9] using linearization methods, see also [69]. In [10], and recently in [20], the Brayton-Moser potential theory [16] is employed, where, however, constraints on individual grid components are imposed. Moreover, as shown in [69], the provided estimate of the region of attraction (ROA) of the equilibria based on the Brayton-Moser potential is rather conservative.

Regarding the *stabilization* of networks with CPLs, there are two main approaches, respectively referred as *passive* and *active damping* methods. For a passive stabilization, additional hardware is connected to the network, *e.g.*, a resistor may be connected in parallel with the CPL or a larger capacitive effect can be obtained by including additional filters [59, 21]. However, the main drawback of these approaches is that they are typically energetically inefficient and the added cost or size may not be practical. On the other hand, active damping methods aim at achieving the same behavior of these passive components through the modification of existing or added control loops [59, 122, 68, 46, 7].

1.3 Main contributions and outline

The main contributions of this thesis are on the analysis and control of networks containing constant power loads and they can be listed as follows.

C1 The problem of *existence of equilibria* of a general class of alternating current networks that have a distributed array of constant power loads is addressed. This thesis provides algebraic, *necessary* conditions on the power values of the loads for the existence of equilibria, that is, if these conditions are met, then the network does not admit a sinusoidal equilibrium regime. By exploiting the framework of *quadratic forms* [86, 118] these conditions are expressed in terms of the feasibility of simple linear matrix inequalities (LMIs) for which reliable software is available. Additionally, a refinement is made for the case of one-ported networks where a condition that is both *necessary* and *sufficient* for the existence of equilibria is reported.

C2 It is shown that general models of alternating current and direct current networks with constant power loads, *e.g.*, multi-terminal high voltage transmission systems and microgrids, are described in steady state by a nonlinear vector

field that, when is associated to a set of ordinary differential equations, exhibits properties of monotonicity. These properties are then used to establish that if the aforementioned models admit steady state solutions, then one of them dominates, component-wise, all the other ones. Furthermore, for the case of alternating current networks under some rather standard *decoupling* assumptions, this equilibrium is shown to be *voltage regular*; see [65, 45].

C3 A class of port-Hamiltonian systems in which the control variables act directly on the power balance equation is explored; these systems are then coined *power-controlled Hamiltonian systems* . In these dynamical systems, the equilibrium points are intrinsically non-zero, which hampers the use of the known passivity properties of more conventional port-Hamiltonian systems (with constant input matrix) to analyze their stability. The conditions under which these systems are *shifted passive* are studied; this is further used to perform a stability analysis on the system's equilibria. Interestingly, in case that the Hamiltonian is quadratic, an estimate of the region of attraction can be provided. These results are applied to study the stability of a general class of direct current electrical networks with constant power loads, and of a synchronous generator modeled by the improved swing equation connected to a constant power load.

C4 The problem of regulating the output voltage of the widely popular and versatile DC buck-boost converter is addressed; the converter is assumed to supply energy to a CPL. The bilinear model describing this network is shown to be non-minimum phase with respect to each of the state variables, which complicates the design of linear controllers. A novel nonlinear, adaptive control law is designed following the Interconnection and Damping Assignment Passivity-Based Control (IDA-PBC) design methodology. The controller is rendered adaptive by incorporating an online estimator of the—practically difficult to measure—value of the constant power load.

C5 The stabilization of a DC microgrid whose main electric power source is connected to a constant power load is explored. The source is assumed be non-controllable and hence the network is first augmented by adding a controllable power converter. Then, an adaptive observer-based nonlinear control law, that provably achieves the overall network's stabilization, is proposed to control the converter. The design is particularly challenging due to the existence of states that are difficult to measure in a practical scenario—the current of the DC network—and due to the unknown power consumption of the load. The theoretical developments have been validated through physical experiments on a real small-scale, DC network; these experimental results are also reported in the thesis.

The rest of the thesis is structured as follows. Some preliminaries on nonlinear dynamical systems and power systems are presented in Chapter 2. The main contributions, from C1 to C5, are reported in chapters 3 to 7, respectively. The thesis is concluded with Chapter 8, which contains a brief summary and a discussion on plausible future research.

1.4 Publications

This thesis is based on the following articles, some of which have already been published or are under review.

J1 Juan E. Machado, Robert Griñó, Nikita Barabanov, Romeo Ortega, and Boris Polyak, "On Existence of Equilibria of Multi-Port Linear AC Networks With Constant-Power Loads,", *IEEE Transactions on Circuits and Systems I: Regular Papers*, Vol. 64, No. 10, pp. 2772–2782, 2017.

J2 Wei He, Romeo Ortega, Juan E. Machado, and Shihua Li, "An Adaptive Passivity-Based Controller of a Buck-Boost Converter With a Constant Power Load," *Asian Journal of Control*, Vo. 21, No. 2, pp. 1–15, 2018.

J3 Pooya Monshizadeh, Juan E. Machado, Romeo Ortega, and Arjan van der Schaft, "Power-Controlled Hamiltonian Systems: Application to Electrical Systems with Constant Power Loads," *Automatica*, 2019. (to appear)

J4 Alexey Matveev, Juan E. Machado, Romeo Ortega, Johannes Schiffer, and Anton Pyrkin, "On the Existence and Long-Term Stability of Voltage Equilibria in Power Systems with Constant Power Loads," *IEEE Transactions on Automatic Control*, 2019. (provisionally accepted)

J5 Juan E. Machado, Romeo Ortega, Alessandro Astolfi, José Arocas-Pérez, Anton Pyrkin, Alexey Bobtsov, and Robert Griñó, "Active Damping of a DC Network with a Constant Power Load: An Adaptive Observer-based Design," *IEEE Transactions on Control Systems Technology*, 2019. (submitted)

Chapter 2

Preliminaries and models

Synopsis This chapter presents the notation and theoretical foundations that are used throughout the thesis. The content regarding nonlinear dynamical systems reported in Section 2.2 is the base of the stability analysis of Chapters 4 and 5 and of the control design that is reported in Chapters 6 and 7. The concepts of passivity presented in section 2.2.2 and the port-Hamiltonian framework introduced in section 2.2.3 are also extensively used in the latter chapter. The brief introduction to electric power systems in Section 2.3 is helpful to better understand the developments that are presented in Chapters 3 and 4.[1]

2.1 Notation and mathematical foundations

Sets and Numbers: The sets of natural, real and complex numbers are denoted by $\mathbb{N}$, $\mathbb{R}$, and $\mathbb{C}$, respectively. The notation $x \in A \subset \mathbb{R}$ means that x is a member of A and that A is a subset of $\mathbb{R}$. A complex number $z \in \mathbb{C}$ is usually written in its Cartesian form as $z = a + \mathbf{j}b$, where $a, b \in \mathbb{R}$ and $\mathbf{j} = \sqrt{-1}$ is the imaginary unit, $\text{conj}(z)$ denotes its complex conjugate, and the real and imaginary parts of z are denoted by $\text{Re}(z)$ and $\text{Im}(z)$, respectively. For a set $\mathcal{V}$, with a finite number of elements, $|\mathcal{V}|$ denotes its cardinality.

Vectors and Matrices: The Euclidean n-space is denoted by $\mathbb{R}^n$ and any $x \in \mathbb{R}^n$ is written as an $n \times 1$ matrix $x = \text{col}(x_1, x_2, ..., x_n)$; the notation $\text{col}(x_i)$ or $\text{stack}(x_i)$ is considered equivalent in the text. The positive orthant of $\mathbb{R}^n$ is denoted by $\mathcal{K}_+^n = \{x \in \mathbb{R}^n : \ x_i > 0 \ \forall i\}$. The n-vectors of all unit and all zero entries are written as 1_n and 0_n, respectively; whenever clear from the context, the sub-index n may be dropped. The $n \times n$ identity matrix is I_n. Given $x \in \mathbb{R}^n$, $\text{diag}(x)$ denotes a diagonal matrix with x on the diagonal; an equivalent notation is $\text{diag}(x_i)$. For $x \in \mathbb{R}^n$, $\|x\|_1 = \sum_{i=1}^n |x_i|$, $\|x\|_2 = (\sum_{i=1}^n x_i^2)^{1/2}$, and $\|x\|_\infty = \max_i |x_i|$. Inequalities between real, n-vectors is meant component-wise.

An $m \times n$ matrix A of real (complex) entries is denoted by $A \in \mathbb{R}^{m \times n}$ ($A \in \mathbb{C}^{m \times n}$). For $A \in \mathbb{R}^{m \times n}$, its transpose is $A^\top$. For $B \in \mathbb{C}^{m \times n}$, its conjugate transpose is $B^{\mathtt{H}}$. For a square, symmetric matrix A, its smallest and largest eigenvalues are denoted by $\lambda_{\mathtt{m}}(A)$ and $\lambda_{\mathtt{M}}(A)$, respectively. The nullspace of a matrix is denoted by $\ker(A)$. For

[1] The structure and content of this chapter borrows heavily from the analogous chapters of the theses [96, 105, 78, 131], yet primary bibliographic sources are signaled whenever necessary.

$A_1, A_2, ..., A_k \in \mathbb{R}^{n\times n}$, $\text{diag}(A_1, A_2, ..., A_k)$ is a block-diagonal matrix of appropriate size.

Functions: The notation $f : A \subset \mathbb{R} \to \mathbb{R}$ means that f maps the domain A into $\mathbb{R}$. A function f of argument x is denoted by $x \mapsto f(x)$ yet, for ease of notation, $f(x)$ may be used to represent the function itself. For a vector field $f : \mathbb{R}^n \to \mathbb{R}^m$, the partial derivative of f_i with respect to x_j is equivalently written as $\frac{\partial f_i(x)}{\partial x_j}$ and $\nabla_{x_j} f_i(x)$. The Jacobian matrix of f is written as $\nabla f(x)$; the argument x is omitted whenever clear from the context and, for the particular case when $m = 1$, $\nabla f(x)$ represents the transposed gradient of f. For a map $\mathcal{F} : \mathbb{R}^n \to \mathbb{R}^{n\times m}$ and the distinguished vector $\bar{x} \in \mathbb{R}^n$, $\bar{\mathcal{F}} = \mathcal{F}(x)|_{x=\bar{x}}$; analogously, for $f : \mathbb{R}^n \to \mathbb{R}^k$, $\nabla \bar{f} = \nabla f(x)|_{x=\bar{x}}$. In the text, every function is assumed to be sufficiently smooth.

Graph Theory[2]: A *finite*, *undirected*, *graph* is defined as a pair $\mathfrak{G} = (\mathcal{V}, \mathcal{E})$ where $\mathcal{V} = \{1, 2, ..., n\}$ is the set of vertices (also referred as nodes, or buses), $\mathcal{E} \subset \mathcal{V} \times \mathcal{V}$ is the set of edges (or branches, or lines). The set of edges consists of elements of the form (i, j) such that $i, j = 1, 2, ..., n$ and $i \neq j$.[3] Two vertices $i, j \in \mathcal{V}$ are said to be *adjacent* if $\{i, j\} \in \mathcal{E}$; in this case, the edge $\{i, j\}$ is said to be *incident* with vertices i and j. The *neighborhood* $\mathcal{N}_i \subset \mathcal{V}$ of a vertex $i \in \mathcal{V}$ is the set $\{j \in \mathcal{V} : \{i, j\} \in \mathcal{E}\}$. A *path* of length m in $\mathfrak{G}$ is a sequence of distinct vertices $\{v_{i_0}, v_{i_1}, ..., v_{i_m}\} \subset \mathcal{V}$ such that for $k = 0, 1, ..., m - 1$, the vertices v_{i_k} and $v_{i_{k+1}}$ are adjacent, that is, $\{v_{i_k}, v_{i_{k+1}}\} \in \mathcal{E}$; the vertices v_{i_0} and v_{i_m} are called the *end vertices* of the path. A graph $\mathfrak{G}$ is said to be *connected* if, for every pair of (different) vertices in $\mathcal{V}$, there is a path that has them as its end vertices; notice that the graphs considered in this thesis do not admit self loops, *i.e.*, for any $i \in \mathcal{V}$, $\{i, i\} \notin \mathcal{E}$.

Although this thesis deals only with simple graphs, the following discussion is pertinent for the analysis carried in Section 2.3. An orientation o of the edges set $\mathcal{E}$ assigns a direction to the edges in the sense that $o : \mathcal{E} \to \{-1, 1\}$, with $o(i, j) = -o(j, i)$. An edge is said to originate in i (tail) and terminate in j (head) if $o(i, j) = 1$, and vice versa if $o(i, j) = -1$. Assume that the edges of a simple graph $\mathfrak{G}$ have been *arbitrarily* oriented and that a unique number $\ell \in \{1, 2, ..., |\mathcal{E}|\}$ is assigned to each edge $\{i, j\} \in \mathcal{E}$, then the node-to-edge, *incidence matrix*, $\mathcal{B} \in \mathbb{R}^{n\times|\mathcal{E}|}$, is defined as

$$\mathcal{B} = [d_{i\ell}]\,,\ d_{i\ell} = \begin{cases} \text{-1} & \text{if } i \text{ is the tail of the edge associated to } \ell, \\ 1 & \text{if } i \text{ is the head of the edge associated to } \ell, \\ 0 & \text{otherwise.} \end{cases} \tag{2.1}$$

Notice that for $x \in \mathbb{R}^n$, $\mathcal{B}^\top x \in \mathbb{R}^{|\mathcal{E}|}$ is the vector of edge-wise differences $x_i - x_j$. Assume now that, together with the edge and vertex sets, a function $w : \mathcal{E} \to \mathbb{R}$ is given that associates a value to each edge, then the resulting graph, denoted as $\mathfrak{G} = (\mathcal{V}, \mathcal{E}, w)$, is a *weighted graph*. The *weighted* graph Laplacian matrix associated with the weighted graph $\mathfrak{G} = (\mathcal{V}, \mathcal{E}, w)$ is defined as

$$L = \mathcal{B}W\mathcal{B}^\top \in \mathbb{R}^{n\times n}, \tag{2.2}$$

where W is a $|\mathcal{E}| \times |\mathcal{E}|$ diagonal matrix, with $w(\ell)$, $\ell = 1, 2, ..., |\mathcal{E}|$, on the diagonal.

[2]The information of this section has been taken from [72, Chapter 2].

[3]The notation $\{i, j\}$ is used in the sequel to identify the pair $(i, j) \in \mathcal{E}$ and $(j, i) \in \mathcal{E}$ as the same edge.

The discussion on weighted, simple graphs is wrapped-up with the following claim, which is instrumental in this thesis; see [72, Chapter 2].

(i) If the graph is connected, then $\ker(\mathcal{B}^\top) = \ker(L) = \operatorname{span}(1_n)$, and all $n-1$ non-zero eigenvalues of L are strictly positive.

More information about graph theory can be found in [13] and [12].

2.2 Nonlinear dynamical systems

Let $\mathcal{J} \subset \mathbb{R}$ be an interval and $\mathcal{X} \subset \mathbb{R}^n, \mathcal{U} \subset \mathbb{R}^m$ open subsets. Let $f : \mathcal{J} \times \mathcal{X} \times \mathcal{U} \to \mathbb{R}^n$ and $h : \mathcal{J} \times \mathcal{X} \times \mathcal{U} \to \mathbb{R}^k$ be *continuously differentiable*. The dynamical systems that are studied in this work are represented by a system of first-order ordinary differential equations (ODEs) of the form

$$\begin{aligned} \dot{x}(t) &= f(t, x(t), u(t)), \\ y(t) &= h(t, x(t), u(t)), \end{aligned} \tag{2.3}$$

where the dot denotes differentiation with respect to the independent variable t, which in the text represents the time, the dependent variable is the state vector x, u is an input signal, which is used to represent either a control signal or a disturbance, and y may codify variables of particular interest as, for example, physically measurable variables. A system in the form of equation (2.3) is accompanied, but usually not written together, by a third equation, namely

$$x(t_0) = x_0, \quad (t_0, x_0) \in \mathcal{J} \times \mathcal{X}, \tag{2.4}$$

which is called an *initial condition*. In the text, the initial condition is always specified when making reference to *particular* solutions of (2.3). For the purposes of the thesis, the set $\mathcal{J}$ is usually represented by an interval of the form $[a, \infty)$.

In some scenarios, the ODEs under study do not depend explicitly on t and do not include the input nor the output vectors. In that case, the second equation in (2.3) is dropped and the independent variable t and the input u are omitted from the arguments of f, giving the following reduced form of (2.3).

$$\dot{x}(t) = f(x(t)). \tag{2.5}$$

The ODEs written in this form are referred as *autonomous* or *time-invariant* systems. A particular property of time-invariant systems is that they are invariant with respect to shifts in the time origin t_0; notice that changing the time variable from t to $\tau = t - t_0$ does not change the right hand side of (2.5). Hence, without loss of generality, it is assumed throughout that $\mathcal{J} = [0, \infty)$ and that $t_0 \equiv 0$, unless specified otherwise.

An important concept used in the text is that of *equilibrium point*. For the system (2.5) notice that if $f(x_0) = 0$ for some $x_0 \in \mathbb{R}^n$, then the constant function $\phi : \mathbb{R} \to \mathbb{R}^n$ defined by $\phi(t) \equiv x_0$ is a solution of (2.5). This kind of solutions are also referred as *steady state*, a *rest point*, or a zero (of the associated vector field). Given the possibly nonlinear nature of the vector field f, a given system may have a single equilibrium point, finite or infinitely many of them, or none. An equilibrium

point can be either *isolated*, which means that there are no other equilibrium points in its vicinity, or there could also be a *continuum* of them.

When the input vector is considered in (2.3), but still in the time-invariant context, the concept of equilibrium pair is also relevant. The pair $(\bar{x}, \bar{u}) \in \mathcal{X} \times \mathcal{U}$ is said to be an *equilibrium pair* of (2.3) if and only if for a given $\bar{x} \in \mathcal{X}$ there exists $\bar{u} \in \mathcal{U}$ such that $f(\bar{x}, \bar{u}) = 0_n$.

2.2.1 Stability in the sense of Lyapunov

The following stability concept and results are stated for autonomous ODEs under the assumption that $x \equiv 0_n$ is an equilibrium point. This is done without loss of generality since if $\bar{x} \in \mathbb{R}^n \setminus \{0_n\}$ is an equilibrium point of (2.5), then the equivalent system $\dot{z}(t) = f(z)$, with $z(t) := x(t) - \bar{x}$, has an equilibrium at the origin.

Definition 2.1. The equilibrium point $x = 0_n$ of (2.5) is

- stable if, for each $\epsilon > 0$, there exists $\delta > 0$ such that
$$\|x(0)\| < \delta \;\Rightarrow\; \|x(t)\| < \epsilon,\ \forall t \geq 0$$
- unstable if it is not stable, and
- asymptotically stable if it is stable and δ can be chosen such that
$$\|x(0)\| < \delta \;\Rightarrow\; \lim_{t\to\infty} x(t) = 0.$$

The following theorem and its proof can be found in [54, Chapter 4].

Theorem 2.1. Let the origin be an equilibrium point of (2.5) and let $\mathcal{D} \subset \mathcal{X}$ be an open set containing it. Let $V : \mathcal{D} \to \mathbb{R}$ be a continuously differentiable function such that

$$V(0) = 0 \text{ and } V(x) > 0 \text{ in } \mathcal{D} \setminus \{0_n\} \tag{2.6}$$
$$\dot{V}(x) \leq 0 \text{ in } \mathcal{D}. \tag{2.7}$$

Then, the origin is stable. Moreover, if

$$\dot{V}(x) < 0 \text{ in } \mathcal{D} \setminus \{0_n\} \tag{2.8}$$

then the origin is asymptotically stable.

A continuously differentiable function $V(x)$ satisfying (2.6) and (2.7) is called a *Lyapunov function* and we may refer to it as *strict* Lyapunov function if the stronger condition (2.8) is met. In many physical systems however the condition (2.8) may not be met, nonetheless, asymptotic stability can still be concluded by means of LaSalle's invariance principle which is presented next; see [54, Chapter 4.2] for a proof of Theorem 2.2.

Definition 2.2. A set $\mathcal{M}$ is said to be *invariant* if

$$x(0) \in \mathcal{M} \;\Rightarrow\; x(t) \in \mathcal{M},\ \forall t,$$

and positively invariant if

$$x(0) \in \mathcal{M} \;\Rightarrow\; x(t) \in \mathcal{M},\ \forall t > 0.$$

Theorem 2.2. Let $\Omega \subset \mathcal{X}$ be a compact set that is positively invariant with respect to (2.5). Let $V : \mathcal{X} \to \mathbb{R}$ be continuously differentiable function satisfying (2.7). Let $\mathcal{F}$ be the set of all points in $\mathcal{X}$ where $\dot{V}(x) = 0$. Let $\mathcal{M}$ be the largest invariant set in $\mathcal{F}$. Then every solution starting in Ω approaches $\mathcal{M}$ as $t \to \infty$.

Definition 2.3. Let $\phi(t, x_0)$ denote a solution of (2.5) with initial condition $x_0 \in \mathcal{X}$. Assume that $\bar{x} \in \mathcal{X}$ is an equilibrium point. Then, the *region (or domain) of attraction* of $\bar{x}$ is defined as the set of points $s \in \mathcal{X}$ for which $\phi(t, s)$ is defined for all $t \geq 0$ and $\lim_{t\to\infty} \phi(t, s) = \bar{x}$.

Lyapunov functions can be used to obtain subsets of the region of attraction. Indeed, let $\mathcal{D} \subset \mathcal{X}$ be open and suppose $\bar{x} \in \mathcal{D}$ is an equilibrium point. Assume that $V : \mathcal{D} \to \mathbb{R}$ is a strict Lyapunov function for $\bar{x}$ and that $\Omega_c = \{x \in \mathcal{D} : \ V(x) \leq c\}$ is a bounded set. Then, Ω_c is positively invariant and every solution with initial condition $x_0 \in \Omega_c$ approaches $\bar{x}$ as t goes to infinity. Consequently, Ω_c is contained in the region of attraction of $\bar{x}$.

2.2.2 Passive systems

The topics of this and the following subsection are heavily referred in Chapter 5; see [94] and [95] for more details about passive and port-Hamiltonian systems.

The following two concepts concern systems of the form (2.3) under the assumption that neither f nor h depend explicitly on t, and that $k \equiv m$, *i.e.*, that the size of the input and output vectors is the same.

Definition 2.4. A dynamic system of the form $\dot{x} = f(x, u)$ and $y = h(x, u)$ is said to be *passive* if there exists a differentiable *storage function* $S : \mathcal{X} \to \mathbb{R}$, with $S(x) \geq 0$ for all $x \in \mathcal{X}$, satisfying the *differential dissipation inequality*

$$\dot{S}(x) \leq u^\top y, \tag{2.9}$$

along all solutions $x \in \mathcal{X}$ corresponding to input functions $u \in \mathcal{U}$.

For physical systems, the right-hand of inequality (2.9) is usually interpreted as the *supplied power*, and $S(x)$ as the *stored energy*. The system is called *lossless* if (2.9) is satisfied with an equality. Hence, a passive system cannot store more energy than it is supplied with and, in the lossless case, the stored energy is exactly equal to the supplied one [95, Chapter 7].

Definition 2.5. Consider the dynamic system $\dot{x} = f(x, u)$ with input u and output $y = h(x, u)$. Let $(\bar{x}, \bar{u}) \in \mathcal{E}$ denote an equilibrium pair of the system and define $\bar{y} := h(\bar{x}, \bar{u})$. Then the system is said to be *shifted passive* if there exists a function $\mathcal{S} : \mathcal{X} \to \mathbb{R}$, $\mathcal{S}(x) \geq 0$ for all $x \in \mathcal{X}$, such that

$$\dot{\mathcal{S}}(x) \leq (u - \bar{u})^\top (y - \bar{y}) \tag{2.10}$$

along all solutions $x \in \mathcal{X}$.

Remark 2.1. Shifted passivity is a particular case of the more general property of *incremental passivity* [32, 85], *i.e.,* the latter implies the former. Incremental passivity is established with respect to *two arbitrary* input-output pairs of the system, whereas in shifted passivity only one input-output pair is arbitrary and the other

one is fixed to a given non-zero equilibrium $(\bar{x}, \bar{u}) \in \mathcal{E}$. While incremental passivity is used for well-posedness results in closed-loop configurations and for deriving the convergence of solutions to each other, the more modest requirement of shifted passivity is used to analyze the system behavior for non-zero constant input, and in particular its stability with respect to the corresponding non-zero equilibrium.
Shifted passivity with respect to *any* $(\bar{x}, \bar{u})$ was coined in [6] as *equilibrium independent passivity*.

2.2.3 Port-Hamiltonian systems

In this work, a *port-Hamiltonian system* is a dynamical system admitting the form [95, Chapter 4.2]

$$\begin{aligned} \dot{x} &= (J(x) - R(x))\,\nabla H(x) + g(x)u, \quad x \in \mathcal{X},\ u \in \mathcal{U} \\ y &= g^\top(x)\nabla H(x), \end{aligned} \tag{2.11}$$

where the $n \times n$ matrices $J(x) = -J^\top(x)$ and $R(x) = R^\top(x)$ have entries depending smoothly on x. The matrix $J(x)$ is referred as the *interconnection matrix* and $R(x)$ is called the *damping matrix*. The continuously differentiable function $H : \mathcal{X} \to \mathbb{R}$ is the *Hamiltonian*.[4] The specific output y defined is usually referred as *natural output*.

Remark 2.2. Port-Hamiltonian systems are passive. Indeed, assume that the Hamiltonian $H(x) \geq 0$ for all $x \in \mathcal{X}$ and compute

$$\begin{aligned} \dot{H}(x) &= (\nabla H(x))^\top \left[(J(x) - R(x))\,\nabla H(x) + g(x)u\right] \\ &= -(\nabla H(x))^\top R(x)\nabla H(x) + u^\top y \\ &\leq u^\top y, \end{aligned}$$

which establish the passivity claim with respect the input-output pair (u, y) and storage function H . The interpretation of this is that the increase in the stored energy $H(x)$ is always smaller than or equal to the supplied power $u^\top y$.

Theorem 2.3. For a port-Hamiltonian system assume that $H(x)$ is convex. Then the system is *shifted passive* if the matrices J, R and g are all constant.

The proof of this theorem, which can be deduced from [49, Remark 3], relies on the use of the storage function

$$\mathcal{H}(x) = H(x) - (x - \bar{x})^\top \nabla H(\bar{x}) - H(\bar{x}). \tag{2.12}$$

This function is referred here as *shifted Hamiltonian* and it is closely related to the *Bregman distance* with respect to an equilibrium point; see [17]. These concepts are used in Chapter 5 of this thesis to establish shifted passivity of a class of port-Hamiltonian systems in which the matrix $g(x)$ is not necessarily constant.

[4] Recall that for a scalar function H, its transposed gradient is denoted by ∇H.

2.3 Electric Power Grids

This work treats both direct current (DC) and alternating current (AC) electric power systems. In a DC system, the relevant variables of interest are voltages and currents and at a steady state they shall remain *constant* with respect to time. The variables of interest are the same in AC power systems, nonetheless at a steady state they have a sinusoidal characteristic of the form $A\sin(w_0 t + \theta)$, where A is the *amplitude*, w_0 is the *angular frequency*, and θ is the *phase*. However, a given sinusoidal signal $x(t) = A\sin(w_0 t + \theta)$ is more conveniently represented as the complex number $Ae^{\mathbf{j}\theta}$, which is called the *phasor* of $x(t)$; see [31, Chapter 7.2] for more details on phasorial representation of sinusoidal signals.

An AC power grid is modeled in steady state as an simple, connected and complex-weighted graph $\mathfrak{G} = (\mathcal{V}, \mathcal{E}, w)$, where $\mathcal{V}$ is the set of buses[5] and $\mathcal{E} \subset \mathcal{V} \times \mathcal{V}$ is the set of transmission lines. The buses are partitioned in two mutually exclusive sets as $\mathcal{V} = \mathcal{L} \cup \mathcal{S}$ with $\mathcal{L}$ being the *load* buses and $\mathcal{S}$ the *generation* buses and their cardinality is conveniently expressed by the numbers $n := |\mathcal{L}|$ and $m := |\mathcal{S}|$, for a total of $n + m$ buses. The weight function of the graph, w, is defined as complex-valued *admittance* $w(\{i, j\}) := g_{ij} + \mathbf{j}b_{ij} \in \mathbb{C}$, where g_{ij} is the *conductance* and b_{ij} the *susceptance* of the line associated to the edge $\{i, j\}$; these parameters codify the resistive and inductive effects of said line, respectively. The incidence matrix of the network is denoted as $\mathcal{B} \in \mathbb{R}^{(n+m)\times|\mathcal{E}|}$ and is built assuming an arbitrary orientation of the network's associated graph.

The phasors of voltage and current of the j-th element in $\mathcal{L}$ are denoted, respectively, as $V_j^\ell \in \mathbb{C}$ and $I_j^\ell \in \mathbb{C}$. Conversely, the variables $V_i^s \in \mathbb{C}$ and $I_i^s \in \mathbb{C}$ respectively denote those same phasors for each $i \in \mathcal{S}$. In addition, each transmission line $\{j, k\}$ has an associated voltage difference v_{jk}[6] and a current $i_{jk} \in \mathbb{C}$.

Regarding the elements of $\mathcal{L}$ consider the following remark.

Remark 2.3. For each load $j \in \mathcal{L}$ there exists a function $\mathfrak{F}_j : \mathbb{C} \times \mathbb{C} \to \mathbb{C}$ such that

$$\mathfrak{F}_j(V_j^\ell, I_j^\ell) = 0. \tag{2.13}$$

The structure of $\mathfrak{F}_j$ depends on the model adopted; here, the conventional ZIP-load model is used: ZIP is a composition of a constant impedance (Z), constant current (I) and *constant power* (P) load. Nonetheless, the focus is, primarily, on constant power loads, hence, the other two terms are dropped in certain cases. Particularly, in Chapter 3, the loads are assumed to be purely constant power loads and $\mathfrak{F}_j$ takes the form

$$\mathfrak{F}_j(V_j^\ell, I_j^\ell) := V_j^\ell \mathrm{conj}(I_j^\ell) + S_j,\ j \in \mathcal{L}, \tag{2.14}$$

where $S_j \in \mathbb{C}$ is the load's complex power, whose real $P_j := \mathrm{Re}(S_j)$ and imaginary $Q_j := \mathrm{Im}(S_j)$ parts are called *active* and *reactive* power; a detailed explanation of the physical meaning of these terms can be found in [31, Chapter 7.7]. In the literature of power systems, these kind of buses are referred as PQ buses.

Regarding the elements of $\mathcal{S}$, consider the following assumption.

[5] In Chapter 3, the buses are referred as ports.

[6] For convenience, the directions of reference for this difference are taken as the same as those used in the definition of the incidence matrix.

Assumption 2.1. There exists, in $\mathcal{S}$, a unique bus for which the voltage phasor is known *a priori*, that is, the phase angle and the magnitude are both specified.[7] In addition, for the other elements in $\mathcal{S}$ a standard PV model can be adopted; in the latter kind of buses, referred as voltage-controlled buses, the active power injection and the magnitude of the voltage phasor are assumed to be known.

The aforementioned partition of $\mathcal{V}$ allows the incidence matrix $\mathcal{B}$ to be row-partitioned as

$$\mathcal{B} = \begin{bmatrix} \mathcal{B}_L \\ \mathcal{B}_S \end{bmatrix}, \tag{2.15}$$

where $\mathcal{B}_L \in \mathbb{R}^{n\times|\mathcal{E}|}$ is the loads-to-lines incidence matrix and $\mathcal{B}_S \in \mathbb{R}^{m\times|\mathcal{E}|}$ is the sources-to-lines incidence matrix. Then, from Kirchhoff's and Ohm's laws the following equivalences are established.

$$\begin{aligned} \operatorname{col}(v_{jk})_{(j,k)\in\mathcal{E}} &= \mathcal{B}^\top \begin{bmatrix} \operatorname{col}(V_i^\ell)_{i\in\mathcal{L}} \\ \operatorname{col}(V_i^s)_{i\in\mathcal{S}} \end{bmatrix}, \\ \mathcal{B}\operatorname{col}(i_{jk})_{(j,k)\in\mathcal{E}} &= \begin{bmatrix} \operatorname{col}(I_i^\ell)_{i\in\mathcal{L}} \\ \operatorname{col}(I_i^s)_{i\in\mathcal{S}} \end{bmatrix}, \\ \operatorname{col}\left(i_{jk}\right)_{\{j,k\}\in\mathcal{E}} &= \operatorname{diag}\left(y_{jk}\right)_{\{j,k\}\in\mathcal{E}} \operatorname{col}\left(v_{jk}\right)_{\{j,k\}\in\mathcal{E}}. \end{aligned} \tag{2.16}$$

After the elimination of $\operatorname{col}\left(i_{jk}\right)_{\{j,k\}\in\mathcal{E}}$ and $\operatorname{col}\left(v_{jk}\right)_{\{j,k\}\in\mathcal{E}}$ from (2.16), it follows that

$$Y \begin{bmatrix} \operatorname{col}(V_i^\ell)_{i\in\mathcal{L}} \\ \operatorname{col}(V_i^s)_{i\in\mathcal{S}} \end{bmatrix} = \begin{bmatrix} \operatorname{col}(I_i^\ell)_{i\in\mathcal{L}} \\ \operatorname{col}(I_i^s)_{i\in\mathcal{S}} \end{bmatrix}, \tag{2.17}$$

where the matrix $Y := \mathcal{B}\operatorname{diag}(y_{jk})_{(j,k)\in\mathcal{E}}\mathcal{B}^\top$ admits the block-decomposition

$$\begin{aligned} Y &= \begin{bmatrix} \mathcal{B}_L\operatorname{diag}(y_{jk})_{\{j,k\}\in\mathcal{E}}\mathcal{B}_L^\top & \mathcal{B}_L\operatorname{diag}(y_{jk})_{\{j,k\}\in\mathcal{E}}\mathcal{B}_S^\top \\ \mathcal{B}_S\operatorname{diag}(y_{jk})_{\{j,k\}\in\mathcal{E}}\mathcal{B}_L^\top & \mathcal{B}_S\operatorname{diag}(y_{jk})_{\{j,k\}\in\mathcal{E}}\mathcal{B}_S^\top \end{bmatrix}, \\ &=: \begin{bmatrix} Y_{11} & Y_{12} \\ Y_{12}^\top & Y_{22} \end{bmatrix}, \end{aligned} \tag{2.18}$$

due to (2.15). Since the network is assumed to be connected, it can be shown that the Hermitian parts of the matrices

$$Y_{11} = \mathcal{B}_L\operatorname{diag}(y_{jk})_{\{j,k\}\in\mathcal{E}}\mathcal{B}_L^\top$$

and

$$Y_{22} = \mathcal{B}_S\operatorname{diag}(y_{jk})_{\{j,k\}\in\mathcal{E}}\mathcal{B}_S^\top$$

are positive semi-definite, respectively.

Remark 2.4. For power networks in which all the elements in $\mathcal{L}$ are PQ buses (see Remark 2.3) and $\mathcal{S}$ is uniquely conformed by a slack node, the matrices Y_{11} and Y_{22} can be shown to be positive definite if each transmission line is assumed to be "lossy", *i.e.*, if $g_{ij} > 0$ for all $\{i,j\} \in \mathcal{E}$; the latter scenario is the one considered in Chapter 3 and the condition $Y_{11} > 0$ is reflected in the expression (3.2) of said chapter. The described scenario regarding the conforming elements of $\mathcal{L}$ and $\mathcal{S}$ is pertinent for the analysis of existence of equilibria in AC distribution networks as studied, for example, in [123] and [14].

[7] This type of bus is referred as a *slack* node in [67, Section 3.6.2].

Combining (2.17) and (2.18), the following expression is isolated

$$Y_{11}\text{col}(V_i^\ell)_{i\in\mathcal{L}} + Y_{12}\text{col}(V_i^s)_{i\in\mathcal{S}} = \text{col}(I_i^\ell)_{i\in\mathcal{L}}, \tag{2.19}$$

which combined with an specific load model, for example (2.14), provides the *AC power flow* equations of the network. The solvability of the power flow equations is necessary and sufficient for the existence of a sinusoidal steady state of specific frequency ω_0. For the purposes of Chapter 3, the model (2.19) is used. However, a simplified expression that is used in Chapter 4 is developed next.

Assume that $\mathcal{L}$ is conformed of PQ buses only. Denote the load voltage phasor in a polar form as $V_i^\ell = E_i e^{\mathbf{j}\theta_i}$ and write $Y_{11} = G + \mathbf{j}B$,[8] where $G \in \mathbb{R}^{n\times n}$ is the conductance matrix, and $B \in \mathbb{R}^{n\times n}$ is the susceptance matrix. Then, a widely used expression of the power flow equations reads as[9]

$$\begin{aligned} P_i &= \sum_{j\in\mathcal{L}} B_{ij}E_iE_j\sin(\theta_i-\theta_j) + \sum_{j\in\mathcal{L}} G_{ij}E_iE_j\cos(\theta_i-\theta_j), \quad i\in\mathcal{L} \\ Q_i &= -\sum_{j\in\mathcal{L}} B_{ij}E_iE_j\cos(\theta_i-\theta_j) + \sum_{j\in\mathcal{L}} G_{ij}E_iE_j\sin(\theta_i-\theta_j), \quad i\in\mathcal{L}. \end{aligned} \tag{2.20}$$

By invoking the so-called *decoupling assumption* (see [56, Chapter 14.3.3] and [99, Assumption 1]), reading as

(i) the phase angle differences $\theta_i - \theta_j$ are constant and approximately zero,

and further assuming that the transmission lines are purely inductive, *i.e.*, $G = 0 \in \mathbb{R}^{n\times n}$, then (2.20) can be simplified as

$$\begin{aligned} P_i &= \sum_{j\in\mathcal{L}} B_{ij}E_iE_j\sin(\theta_i-\theta_j) \quad i\in\mathcal{L} \\ Q_i &= -\sum_{j\in\mathcal{L}} B_{ij}E_iE_j, \quad i\in\mathcal{L}. \end{aligned} \tag{2.21}$$

These are called the *decoupled power flow equations* and each of them may be referred as to active power flow and reactive power flow, respectively. Notice that the second equation in (2.21) is equivalent to

$$Q_i = E_i\sum_{j\in\mathcal{L}} B_{ij}(E_i - E_j), \tag{2.22}$$

which is an expression used in Chapter 4 to analyze the existence of equilibria assuming a ZIP-load model for the reactive power Q_i.[10]

Remark 2.5. The power flow equations of DC power systems can be obtained as a particular case of the AC power flow. Indeed, if in the latter equations the fundamental frequency is assumed to be $\omega_0 = 0$, then all the signals become *real* constants and the complex, phasorial notation can be dropped. The buses representing sources

[8] The subindices $(\cdot)_{11}$ are dropped in the matrices G and B for simplicity reasons.

[9] See the developments presented in [67, Chapter 3.5] and [105, Chapter 2.2].

[10] This expression can be derived by recalling the properties of the incidence matrix discussed by the end of Section 2.1.

would now be DC voltage-controlled, *i.e.,* assigning a constant voltage value to the source buses, and for every transmission line the admittance value would have only its real part, *i.e.*, the conductance. The DC equivalent of the constant power load (2.14) would now specify only the active power and the reactive power would be zero. Consequently, the combination of (2.14) and (2.19) would provide a set of *real, quadratic* equations for either $\mathrm{col}(V_i^\ell)_{i\in\mathcal{L}}$ or $\mathrm{col}(I_i^\ell)_{i\in\mathcal{L}}$.

Part II

EQUILIBRIA ANALYSIS: EXISTENCE AND STABILITY

Chapter 3

Equilibria of LTI-AC Networks with CPLs

Synopsis Given a multi-port, linear AC network with instantaneous *constant power loads*, this chapter identifies a set of active and reactive load powers for which there is *no steady state* operating condition—in this case it is said that the power load is *inadmissible*. The identification is given in terms of feasibility of simple linear matrix inequalities, hence it can be easily verified with existing software. For one- or two-port networks the proposed feasibility test is *necessary and sufficient* for load power admissibility with the test for the former case depending only on the network data. Two benchmark numerical examples illustrate the results.

3.1 Introduction

This chapter explores the problem of existence of equilibria of linear time-invariant (LTI), multi-port AC circuits with instantaneous constant power loads (CPLs). This type of analysis is essential to identify proper operative conditions of the network and could be further used in the controller design of the different equipment in it.

Existence of equilibria for AC networks containing CPLs has been studied within the context of the well-known power-flow (or load-flow) equations. In [5], sufficient conditions for the existence of solutions are given, under the assumption that the CPLs constrains only the active power term. Within the same context, in [23] sufficient conditions for existence and uniqueness of solutions are given for radial networks, *i.e.*, with a single energy source, considering a simultaneous treatment of the active and reactive power terms of the loads. More recently, in [73], using the implicit function theorem, sufficient conditions for the existence of equilibria are given for a lossless network. In Section IV of the same paper, the authors propose *necessary* conditions for existence of equilibria based on convex relaxation techniques. Using this approach, the authors give an index on how the power values should be modified so the network could *potentially* attain an equilibrium regime. The paper [107] explores, for general multi-port, resistive networks with constant power devices and of arbitrary topology, a sufficient condition on the circuit parameters which guarantees that any load flow solution, if exists, belongs to a specified set. Back to AC networks, in [14], using fixed-point theorems, sufficient conditions for existence of a unique equilibrium state are derived. In [126], sufficient conditions for the solvability of the power-flow equations are given using bifurcation theory.

Sufficient conditions for existence of a unique high-voltage power flow solution of lossless networks are proposed in [103, 104]; an iterative algorithm to approximate this solution is also considered. More recently, in [52], the authors show that the load flow equations of unbalanced, polyphase power systems can be written as a set of quadratic equations of several variables; under certain assumptions the authors then propose a decoupling of this algebraic system and provide conditions for their solvability.

In this chapter, *necessary* conditions on the CPLs active and reactive powers, for existence of equilibria of general multi-port AC networks, are proposed. If these conditions are not satisfied, the loads are called inadmissible. For one- or two-port networks with free reactive (or active) power these conditions are also *sufficient*—providing a full characterization of the power that can be extracted from the AC network through the CPLs. Using the framework of *quadratic forms*—see [86] and [118]—these conditions are expressed in terms of the feasibility of simple linear matrix inequalities (LMIs), for which reliable software is available. Moreover, for single-port networks, the admissibility test depends only on the network data, avoiding the need for an LMI analysis.

The contributions presented here are an extension, to the case of AC networks, of the results on DC power systems reported in [9]; see also [91]. The extension is non-trivial for two main reasons: (i) The mappings associated with the quadratic equations, whose solvability has to be studied in this problem, have *complex* domain and co-domain—in contrast with the ones of DC networks where these sets are real. It is shown, however, that these complex quadratic equations are equivalent to a set of real quadratic ones that can, in certain practical scenarios, have twice the number of unknowns than equations, stymieing the application of the tools used for DC networks, which treat the case of same number of equations and unknowns. (ii) The characterization of CPLs in AC networks involve the simultaneous treatment of an active and reactive component, whereas in DC networks only active power is considered.

The remainder of the chapter is structured as follows. In Section 3.2 the problem addressed in the chapter is formulated and the difference with respect to DC networks is highlighted. Section 3.3 contains three lemmata that are instrumental to establish the main results. Section 3.4 gives necessary conditions for existence of equilibria for multi-port networks. In Section 3.5 necessary and sufficient conditions for the case of one- or two-port networks are studied and in Section 3.6 these previous results are used to provide a characterization of the admissible and inadmissible loads, while in Section 3.7 the results are illustrated with two benchmark examples. The chapter is wrapped-up in Section 3.8 with a brief summary. To enhance readability all proofs are given in technical appendices at the end of the chapter.

3.2 Problem Formulation

3.2.1 Mathematical model of AC networks with CPLs

This chapter deals with LTI AC electrical networks with CPLs working in sinusoidal steady state at a frequency $\omega_0 \geq 0$; see Fig. 3.1. The description of this regime in

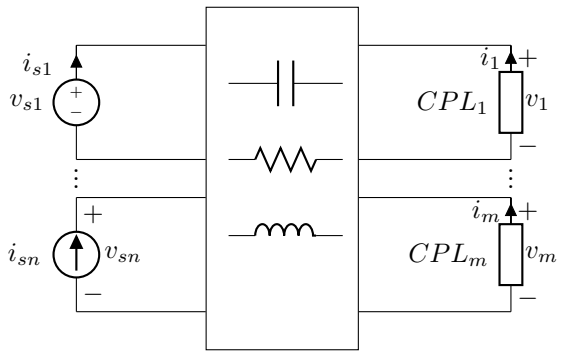

Figure 3.1: Schematic representation of multi-port AC LTI electrical networks with n external voltage and current sources feeding m CPLs.

the frequency domain is[1]

$$V(\mathbf{j}\omega_0) = G(\mathbf{j}\omega_0)I(\mathbf{j}\omega_0) + K(\mathbf{j}\omega_0), \tag{3.1}$$

where[2] $V \in \mathbb{C}^m$ and $I \in \mathbb{C}^m$ are the vectors of generalized Fourier transforms of the port voltages and injected currents, respectively, and $K \in \mathbb{C}^m$ captures the effect of the AC sources, all evaluated at the frequency ω_0. Equation (3.1) can also be seen as the Thevenin equivalent model of the m-port AC linear network including the voltage and current sources and, then, $G \in \mathbb{C}^{m\times m}$ should be interpreted as the frequency domain impedance matrix of the network at the frequency ω_0.

In virtue of Remark 2.4 in the previous chapter, the following expression holds.

$$G(\mathbf{j}\omega) + G^{\mathtt{H}}(\mathbf{j}\omega) > 0, \ \forall\omega \in \mathbb{R}; \tag{3.2}$$

the reader is reminded that $(\cdot)^{\mathtt{H}}$ denotes the complex conjugate transpose.

The complex power of the i-th CPL is defined as the complex number

$$S_i := P_i + \mathbf{j}Q_i, \ \ i \in \{1, \dots m\}, \tag{3.3}$$

where $P_i \in \mathbb{R}$ and $Q_i \in \mathbb{R}$ are the active and reactive power at the $i-$th port, respectively. Then, the CPLs constraint the network through the nonlinear relation

$$V_i \,\mathrm{conj}(I_i) + S_i = 0, \tag{3.4}$$

where conj$(\cdot)$ is the complex conjugate. In equation (3.4), and throughout the rest of the chapter, the qualifier $i \in \{1, \dots m\}$ is omitted.

It is established then that a necessary and sufficient condition for the existence of a sinusoidal steady–state (at a given frequency ω_0) is that the *complex* equations (3.1), (3.3) and (3.4) have a solution, which is the question addressed in this chapter.

[1] A comprehensive development of this description is followed in the chapter of preliminaries; see, particularly, Assumption 2.1 and Remark 2.4.

[2] To simplify the notation the argument $\mathbf{j}\omega_0$ is omitted in the sequel.

3.2.2 Compact representation and comparison with DC networks

Notice that, eliminating the voltage vector V, the system of equations (3.1), (3.3) and (3.4) can be compactly represented by the set of *complex* quadratic equations

$$f_i(I) = 0, \tag{3.5}$$

where the complex mappings $f_i : \mathbb{C}^m \to \mathbb{C}$ are defined as

$$f_i(I) := I^{\mathrm{H}} \left(e_i e_i^\top G\right) I + I^{\mathrm{H}} K_i e_i + S_i, \tag{3.6}$$

where $e_i \in \mathbb{R}^m$ is the i-th Euclidean basis vector. The fact that the mappings $f_i(\cdot)$ have complex domain and co-domain represents a major technical difficulty to establish conditions for existence of solutions of equations (3.5), (3.6).

This situation should be contrasted with the case of DC networks where the mappings have real domain and co-domain. Indeed, there exists a *constant* steady state if and only if the *real* quadratic equations $\vartheta_i(\mathtt{I}) = 0$ have a real solution, with the mappings $\vartheta_i : \mathbb{R}^m \to \mathbb{R}$ given by

$$\vartheta_i(\mathtt{I}) := \mathtt{I}^\top [e_i e_i^\top G(0)] \mathtt{I} + \mathtt{I}^\top \mathtt{s}_i e_i + P_i, \tag{3.7}$$

where $\mathtt{I} \in \mathbb{R}^m$ are the currents, $G(0) \in \mathbb{R}^{m \times m}$ is the DC gain of the impedance matrix, and $\mathtt{s}_i \in \mathbb{R}$ are the external (voltage or current) DC sources; see [9].

3.2.3 Considered scenario and characterization of the loads

Finding conditions for the solvability of equations (3.5) and (3.6), for arbitrary P_i, Q_i, G and K, is a nonlinear analysis daunting task. In practical scenarios, however, the values of P_i and-or Q_i are *fixed* and conditions on G and K, such that an equilibrium exists, are looked for.[3] Interestingly, it is shown next that this makes the problem mathematically tractable. The powers P_i and Q_i for which an equilibrium exists are said to be *admissible*, otherwise, they are called *inadmissible*.

To state the problem formulation in a compact manner, define the vectors

$$\begin{aligned} P &:= \mathrm{col}(P_1, \ldots, P_m) \in \mathbb{R}^m \\ Q &:= \mathrm{col}(Q_1, \ldots, Q_m) \in \mathbb{R}^m \\ S &:= \mathrm{col}(S_1, \ldots, S_m) \in \mathbb{C}^m, \end{aligned}$$

which are assumed *given*. Then, the conditions under which P and-or Q belong to either one of the following sets are identified.

- $\mathcal{P}^{\mathtt{I}}_{\mathtt{FAQ}} \subset \mathbb{R}^m$ denotes the set of P that are inadmissible for all Q. That is, if $P \in \mathcal{P}^{\mathtt{I}}_{\mathtt{FAQ}}$ there is no steady state no matter what Q is.
- $\mathcal{Q}^{\mathtt{I}}_{\mathtt{FAP}} \subset \mathbb{R}^m$ is the set of Q that are inadmissible for all P. That is, if $Q \in \mathcal{Q}^{\mathtt{I}}_{\mathtt{FAP}}$ there is no steady state no matter what P is.
- $\mathcal{S}^{\mathtt{I}} \subset \mathbb{R}^m \times \mathbb{R}^m$ represents the set of (P, Q) that are inadmissible. That is, if $(P, Q) \in \mathcal{S}^{\mathtt{I}}$ there is no steady state.

[3] Nominal values of G and K are usually available too.

The first contribution is the definition of LMIs—parameterised in P and Q—whose feasibility *implies* that P and-or Q belong to either one of the aforementioned sets.

A second contribution is that, for the case of one- or two-port networks, *i.e.*, $m \leq 2$, a *full characterization* of the following sets is provided.

- $\mathcal{P}^{\mathtt{A}}_{\mathtt{FSQ}} \subset \mathbb{R}^m$ set of P that are admissible for some Q. That is, if $P \in \mathcal{P}^{\mathtt{A}}_{\mathtt{FSQ}}$ there is a Q (that can be computed) for which there is a steady state.
- $\mathcal{Q}^{\mathtt{A}}_{\mathtt{FSP}} \subset \mathbb{R}^m$ set of Q that are admissible for some P. That is, if $Q \in \mathcal{P}^{\mathtt{A}}_{\mathtt{FSP}}$ there is a P (that can be computed) for which there is a steady state.
- (For $m = 1$) $\mathcal{S}^{\mathtt{A}} \subset \mathbb{R}^m \times \mathbb{R}^m$ set of (P, Q) that are admissible. That is, if $(P, Q) \in \mathcal{S}^{\mathtt{A}}$ there is a steady state.

By full characterization of the sets it is meant that

$$\begin{aligned} \mathcal{P}^{\mathtt{A}}_{\mathtt{FSQ}} \cup \mathcal{P}^{\mathtt{I}}_{\mathtt{FAQ}} &= \mathbb{R}^m \qquad (\text{for } m \leq 2) \\ \mathcal{Q}^{\mathtt{A}}_{\mathtt{FSP}} \cup \mathcal{Q}^{\mathtt{I}}_{\mathtt{FAP}} &= \mathbb{R}^m \qquad (\text{for } m \leq 2) \\ \mathcal{S}^{\mathtt{A}} \cup \mathcal{S}^{\mathtt{I}} &= \mathbb{R}^m \times \mathbb{R}^m \qquad (\text{for } m = 1). \end{aligned}$$

In other words, that the conditions of admissibility for P or Q are *necessary and sufficient*.

From the practical viewpoint, the inadmissibility sets $\mathcal{P}^{\mathtt{I}}_{\mathtt{FAQ}}$ and $\mathcal{Q}^{\mathtt{I}}_{\mathtt{FAP}}$ allows to rule out "bad" Ps and Qs, respectively. The set $\mathcal{S}^{\mathtt{I}}$ is useful in the scenario when the devices at the ports transfer constant power with a specified power factor $\mathrm{PF_i} = \frac{P_i}{S_i}$, in which case S is fixed. Another scenario of practical interest where the set $\mathcal{S}^{\mathtt{I}}$ is instrumental is when P is fixed (possibly some elements zero) and some Q_i are fixed and the others are free. The main question in this case is if some specific values of the free Q_i can *enlarge* the set of admissible P.

Finally, for $m \leq 2$, the sets $\mathcal{P}^{\mathtt{A}}_{\mathtt{FSQ}}$ and $\mathcal{Q}^{\mathtt{A}}_{\mathtt{FSP}}$ provide a complete answer to the admissibility question when P is fixed and Q is free and, vice versa, when Q is fixed and P is free, respectively. Additionally, for the special case $m = 1$, a full characterization of the set $\mathcal{S}^{\mathtt{A}}$ is provided. See Section 3.5 for an illustration of these scenarios in two numerical examples.

3.3 Three Preliminary Lemmata

This section presents three lemmata that are instrumental to establish the main results of the chapter. The first lemma shows that the m complex quadratic equations (3.5) and (3.6) admit a solution if and only if a system of $2m$ *real* quadratic equations with $2m$ unknowns are solvable. In AC networks the complex power has active and reactive components, which in some practical situations may give rise to a new situation where the number of equations is different from the number of unknowns. The second lemma gives necessary conditions for the solvability of such a system of equations and is an extension of Lemma 1 of [9], where these numbers are the same. Finally, the third lemma shows that these conditions are also *sufficient* if the number of equations is smaller than three—provided an additional assumption is verified. The latter always holds true in DC networks, but it has to be verified in the AC case.

3.3.1 A real representation of (3.5), (3.6)

To streamline the presentation of the following lemma, define the real mappings $g_i, h_i : \mathbb{R}^{2m} \to \mathbb{R}$

$$\begin{aligned} g_i(d) &:= d^\top \hat{A}_i d + 2d^\top \hat{b}_i + 2P_i \\ h_i(d) &:= d^\top \hat{B}_i d + 2d^\top \hat{q}_i + 2Q_i, \end{aligned} \tag{3.8}$$

where

$$\begin{aligned} d &:= \begin{bmatrix} \mathrm{Re}\{I\} \\ \mathrm{Im}\{I\} \end{bmatrix}, \hat{b}_i := \begin{bmatrix} \mathrm{Re}\{K_i\}e_i \\ \mathrm{Im}\{K_i\}e_i \end{bmatrix}, \hat{q}_i := \begin{bmatrix} \mathrm{Im}\{K_i\}e_i \\ -\mathrm{Re}\{K_i\}e_i \end{bmatrix} \\ \hat{A}_i &:= \begin{bmatrix} e_i e_i^\top \left(\mathrm{Re}\{G\} + \mathrm{Re}\{G\}^\top\right) & e_i e_i^\top \left(-\mathrm{Im}\{G\} + \mathrm{Im}\{G\}^\top\right) \\ e_i e_i^\top \left(\mathrm{Im}\{G\} - \mathrm{Im}\{G\}^\top\right) & e_i e_i^\top \left(\mathrm{Re}\{G\} + \mathrm{Re}\{G\}^\top\right) \end{bmatrix} \\ \hat{B}_i &:= \begin{bmatrix} e_i e_i^\top \left(\mathrm{Im}\{G\} + \mathrm{Im}\{G\}^\top\right) & e_i e_i^\top \left(\mathrm{Re}\{G\} - \mathrm{Re}\{G\}^\top\right) \\ e_i e_i^\top \left(-\mathrm{Re}\{G\} + \mathrm{Re}\{G\}^\top\right) & e_i e_i^\top \left(\mathrm{Im}\{G\} + \mathrm{Im}\{G\}^\top\right) \end{bmatrix}. \end{aligned} \tag{3.9}$$

Lemma 3.1. The set of complex mappings $f_i : \mathbb{C}^m \to \mathbb{C}$ given in (3.6) verifies

$$\begin{aligned} g_i(d) &= \mathrm{Re}\{f_i(I)\} \\ h_i(d) &= \mathrm{Im}\{f_i(I)\}. \end{aligned} \tag{3.10}$$

Consequently,

$$\exists I \in \mathbb{C}^m \mid f_i(I) = 0 \;\Leftrightarrow\; \exists\, d \in \mathbb{R}^{2m} \mid g_i(d) = h_i(d) = 0.$$

□□□

The proof of this lemma can be established by direct, but lengthy, computations.

3.3.2 Necessary condition for the solution of quadratic equations

Lemma 3.2. Consider the real mappings $v_k : \mathbb{R}^n \to \mathbb{R}$ where[4] $k \in \bar{\ell} := \{1, 2, \ldots, \ell\}$,

$$v_k(x) := x^\top A_k x + 2x^\top b_k + c_k, \tag{3.11}$$

$x \in \mathbb{R}^n$, $b_k \in \mathbb{R}^n$, $c_k \in \mathbb{R}$, and A_k are symmetric $n \times n$ matrices with $n \geq 2$—not necessarily equal to ℓ. Define the following $(n+1) \times (n+1)$ real matrices

$$\mathcal{A}_k := \begin{bmatrix} A_k & b_k \\ b_k^\top & c_k \end{bmatrix}. \tag{3.12}$$

Then, the following implication is true.

$$\exists\, t_k \in \mathbb{R} \mid \sum_{k=1}^{\ell} t_k \mathcal{A}_k > 0 \;\Rightarrow\; \{x \in \mathbb{R}^n \mid v_k(x) = 0,\ \forall k\} = \varnothing. \tag{3.13}$$

□□□

Remark 3.1. Lemma 3.2, which gives *necessary* conditions for existence of solutions of ℓ quadratic equations with n unknowns, is an extension of Lemma 1 presented in [9]; therein, the *particular case* $n = \ell$ is treated.

[4] In the sequel, the clarification that $k \in \bar{l}$ is omitted.

3.3.3 Sufficient condition for the solution of two equations

Lemma 3.3. Consider two mappings $v_1(x), v_2(x)$ as given in (3.11) and two matrices $\mathcal{A}_1, \mathcal{A}_2$ as in (3.12). Assume there exists $s_1, s_2 \in \mathbb{R}$, such that

$$s_1 A_1 + s_2 A_2 > 0. \tag{3.14}$$

Then, the following implication is true.

$$\begin{aligned} &\exists\, t_1, t_2 \in \mathbb{R} \mid t_1\mathcal{A}_1 + t_2\mathcal{A}_2 > 0 \\ \Leftarrow\ &\{x \in \mathbb{R}^n \mid v_1(x) = v_2(x) = 0\} = \varnothing. \end{aligned} \tag{3.15}$$

□□□

Remark 3.2. Lemma 3.3, which gives *sufficient* conditions for existence of solutions of *two* quadratic equations with n unknowns, is related with Proposition 3 of [9] where the condition (3.14) is not explicitly stated because it is always satisfied in DC networks. However, as explained in Section 3.5, this is not always the case for AC networks. Notice that the need for (3.14) is clearly stated in Theorem 2.2 of [86]. Moreover, as indicated in Remark 3.1, in Proposition 3 of [9] only the particular case $n = \ell$ is treated.

Remark 3.3. Invoking Lemma 3.2, it can be seen that the "only if" condition (3.15) for two-port equations is actually an "if and only if"—with the "if" part holding even without (3.14).

3.4 Necessary Conditions For Existence of a Steady State for m-port Networks

A direct application of Lemmata 3.1 and 3.2 provides a way to determine the *inadmissibility* of P and-or Q from the feasibility of parameterised LMIs. Also, an interpretation of the results in terms of the extracted active power is given.

3.4.1 An LMI-based inadmissibility condition

Proposition 3.1. Fix $P, Q \in \mathbb{R}^m$. If there exist $T = \operatorname{diag}(t_i)_{i=1}^m \in \mathbb{R}^{m\times m}$ and $\bar{T} = \operatorname{diag}(\bar{t}_i)_{i=1}^m \in \mathbb{R}^{m\times m}$ such that

$$R_P(T) + R_Q(\bar{T}) > 0, \tag{3.16}$$

where $R_P(T)$ and $R_Q(\bar{T})$ are $(2m+1)\times(2m+1)$ real matrices given by

$$R_P(T) := \begin{bmatrix} T\mathrm{Re}\{G\} + \mathrm{Re}\{G\}^\top T & -T\mathrm{Im}\{G\} + \mathrm{Im}\{G\}^\top T & T\mathrm{Re}\{K\} \\ T\mathrm{Im}\{G\} - \mathrm{Im}\{G\}^\top T & T\mathrm{Re}\{G\} + \mathrm{Re}\{G\}^\top T & T\mathrm{Im}\{K\} \\ \mathrm{Re}\{K\}^\top T & \mathrm{Im}\{K\}^\top T & 2P^\top T\mathbf{1}_m \end{bmatrix} \tag{3.17}$$

and

$$R_Q(\bar{T}) := \begin{bmatrix} \bar{T}\mathrm{Im}\{G\} + \mathrm{Im}\{G\}^\top \bar{T} & \bar{T}\mathrm{Re}\{G\} - \mathrm{Re}\{G\}^\top \bar{T} & \bar{T}\mathrm{Im}\{K\} \\ -\bar{T}\mathrm{Re}\{G\} + \mathrm{Re}\{G\}^\top \bar{T} & \bar{T}\mathrm{Im}\{G\} + \mathrm{Im}\{G\}^\top \bar{T} & -\bar{T}\mathrm{Re}\{K\} \\ \mathrm{Im}\{K\}^\top \bar{T} & -\mathrm{Re}\{K\}^\top \bar{T} & 2Q^\top \bar{T}\mathbf{1}_m \end{bmatrix}. \tag{3.18}$$

Then, there is no *sinusoidal* steady state for the network. □□□

Remark 3.4. In Proposition 3.1 the values of P and Q are fixed *a priori*, then the positivity condition (3.16) is a simple LMI in $(T, \bar{T})$ for which reliable software is available. Otherwise, it represents a *bilinear* matrix inequality in $(T, \bar{T}, P, Q)$, whose solution is far from trivial.

3.4.2 Bound on the extracted active power

In this subsection it is assumed that the active power flows only from the network to the loads, then an upper bound on the admissible overall extracted power is provided.

To streamline the result, define the $2m \times 2m$ real, symmetric matrix

$$M := \begin{bmatrix} \mathrm{Re}\{G\} + \mathrm{Re}\{G\}^\top & -\mathrm{Im}\{G\} + \mathrm{Im}\{G\}^\top \\ -\mathrm{Im}\{G\}^\top + \mathrm{Im}\{G\} & \mathrm{Re}\{G\} + \mathrm{Re}\{G\}^\top \end{bmatrix}, \tag{3.19}$$

that, in view of (3.2), is *positive definite*.

Proposition 3.2. Suppose that all the CPLs extract active power from the network, that is $P_i \geq 0$. A *necessary* condition for the existence of a sinusoidal steady state is that the overall extracted power is upper bounded as follows

$$\sum_{i=1}^{m} P_i \leq \frac{1}{2} \begin{bmatrix} \mathrm{Re}\{K\} \\ \mathrm{Im}\{K\} \end{bmatrix}^\top M^{-1} \begin{bmatrix} \mathrm{Re}\{K\} \\ \mathrm{Im}\{K\} \end{bmatrix}. \tag{3.20}$$

□□□

The condition above is similar to the necessary condition for existence of a *constant* steady state regime for LTI DC networks with CPLs presented in Proposition 2 of [9]. The condition for DC networks is the existence of a *positive definite* diagonal matrix T such that

$$\sum_{i=1}^{m} t_i P_i \leq \frac{1}{2} (TK)^\top [TG(0) + G^\top(0)T]^{-1} TK. \tag{3.21}$$

To compare this bound with (3.20) recall that in the DC case $\omega_0 = 0$ and the vector of external sources K is real—whose elements were denoted as $\mathtt{s}_i$ in (3.7). Therefore, (3.20) reduces to (3.21) but with $T = I_m$. The presence of the free matrix T makes the bound for DC networks tighter.

3.5 Necessary and Sufficient Conditions for Load Admissibility for One- or Two-port Networks

To make the conditions for existence of a steady state not only necessary, but also *sufficient*, in this section the case of one- or two-port networks, *i.e.*, $m \leq 2$, is considered. In [9], Proposition 3, a similar scenario is treated for DC networks. However, as indicated in Remark 3.2, this proposition is inapplicable in the AC case, hence the need to invoke Lemma 3.3, which requires the verification of condition (3.14).

As done in the previous section, the scenarios where P is fixed and Q is *free* or, vice versa, where Q is fixed and P is *free*, are considered. Lastly, for the particular case of $m = 1$, both P and Q are assumed fixed. The latter case is presented first, since it is a natural complement to Proposition 3.1 [for $m = 1$].

3.5.1 Single-port networks with fixed active *and* reactive power

The next result pertains to *single-port* networks and gives two different necessary and sufficient conditions for *a pair* (P, Q) to be admissible. The first condition is given in the spirit of Proposition 3.1, that is, it relates the existence of a sinusoidal steady state with the feasibility of an LMI. In addition, a radically different condition is given exclusively in terms of the data of the problem.

Proposition 3.3. For a *one-port* network fix P *and* Q. Then, the following three statements are *equivalent*.

- The system admits a sinusoidal steady state.
- There are no real scalars T and $\bar{T}$ such that

$$R_P(T) + R_Q(\bar{T}) > 0. \tag{3.22}$$

- The inequality

$$|K|^2 \geq 2\left(|S||G| + \mathrm{Re}\{\mathrm{conj}(S)G\}\right), \tag{3.23}$$

holds true, where $|\cdot|$ is the magnitude of the complex number. □□□

It is important to underscore that inequality (3.23) is written only in terms of the *original parameters* of the system, that is G, K and S, and it does not include additional variables. Also, this inequality reduces to the necessary and sufficient condition for existence of equilibria for LTI DC circuits for the case $m = 1$ presented in [91], Section II.

3.5.2 Two-port networks with free active or reactive power

Suppose that the network is constrained to satisfy the active power demand but the reactive power is *unconstrained*, *i.e.*, the reactive power term Q can be arbitrarily assigned. Now, as seen from (3.8), the quadratic mappings $g_i(d)$ are independent of the reactive power Q and the quadratic mappings $h_i(d)$ are independent of the active power P. Since the Q is free the equations $h_i(d) = 0$ are trivialised, reducing to the definition

$$Q_i := -\frac{1}{2}(\bar{d}^\top \hat{B}_i \bar{d} + \bar{d}^\top \hat{c}_i),$$

where $\bar{d} \in \mathbb{R}^{2m}$ is the solution of the equations $g_i(\bar{d}) = 0$. The case where the network is constrained to satisfy a given reactive power, with unconstrained active power, is analogous to the scenario just described and now the existence of a sinusoidal steady state is equivalent to the solvability of the system $h_i(d) = 0$.

For two-port networks there are only two quadratic equations, in which case, Lemma 3.3 states that their solvability is *equivalent* to the feasibility of its associated LMI—provided condition (3.14) is satisfied.

Proposition 3.4. For a two-port network, fix P and suppose Q is unconstrained. The following two statements are *equivalent*.

- The network admits a sinusoidal steady state.
- There is no diagonal matrix T such that $R_P(T) > 0$.

□□□

Proposition 3.5. For a two-port network, fix Q and suppose P unconstrained. *Assume* there exists $\hat{s}_1, \hat{s}_2 \in \mathbb{R}$, such that

$$\hat{s}_1 \hat{B}_1 + \hat{s}_2 \hat{B}_2 > 0. \tag{3.24}$$

The following two statements are *equivalent*.

- The network admits a sinusoidal steady state.
- There is no diagonal matrix $\bar{T}$ such that $R_Q(\bar{T}) > 0$.

□□□

Remark 3.5. Notice from the propositions above that for the case of fixed reactive power the additional assumption (3.24) is imposed on the network. This assumption is absent when the active power is fixed—a distinction that is clarified in the proofs. It is worth remarking that (3.24) is verified in both benchmark examples given in Section 3.6.

Remark 3.6. Unfortunately, for $m \geq 2$, conditions that are simultaneously *necessary and sufficient* for power load admissibility, when both P and Q are fixed, are not provided in this chapter. This stems from the fact that the proof of sufficiency relies, either on Finsler's Lemma as in Lemma 3.3 or on establishing *convexity* of the image of the mapping defined by the quadratic equations as done in Proposition 3 of [9]. To the extent of the author's knowledge, there are no general results concerning the (global) convexity of these mappings nor extensions of Finsler's Lemma when there are more than two equations. As explained in Subsection 3.2.2 this corresponds in the AC case to single-port networks, while in the DC case is applicable to two-port networks.

3.6 Admissibility and Inadmissibility Sets

The results of Propositions 3.1 and 3.3-3.5 are applied in this section to identify the sets that characterize the admissible and inadmissible loads described in Subsection 3.2.3.

3.6.1 Inadmissibility sets for m-port networks

The identification of the inadmissibility sets $\mathcal{P}^{\mathtt{I}}_{\mathtt{FAQ}}$, $\mathcal{Q}^{\mathtt{I}}_{\mathtt{FAP}}$ and $\mathcal{S}^{\mathtt{I}}$ follows as a direct corollary of Proposition 3.1. First, notice that $R_P(0) = 0$ and $R_Q(0) = 0$. Therefore, setting $\bar{T} = 0$ in (3.16), $R_P(T) > 0$ implies the non-existence of a sinusoidal steady state for the system—with a similar situation for $R_Q(\bar{T}) > 0$ and $T = 0$. Second, matrix R_P is independent of Q and matrix R_Q is independent of P. On the other hand, matrix $R_P(T) + R_Q(\bar{T})$ is dependent on both P and Q simultaneously.

In view of the observations above it is clear that the following implications hold:

- $\exists\, T$ such that $R_P(T) > 0 \;\Rightarrow\; P \in \mathcal{P}^{\mathtt{I}}_{\mathtt{FAQ}}$
- $\exists\, \bar{T}$ such that $R_Q(\bar{T}) > 0 \;\Rightarrow\; Q \in \mathcal{Q}^{\mathtt{I}}_{\mathtt{FAP}}$
- $\exists\, T,\ \bar{T}$ such that $R_P(T) + R_Q(\bar{T}) > 0 \;\Rightarrow\; (P, Q) \in \mathcal{S}^{\mathtt{I}}$.

3.6.2 Admissibility sets for one- or two-port networks

The following characterization for the admissibility sets described in Section 3.2 follows directly from Propositions 3.3-3.5.

- $(m \leq 2)$ $\nexists\, T$ such that $R_P(T) > 0 \Leftrightarrow P \in \mathcal{P}^{\mathtt{A}}_{\mathtt{FSQ}}$.
- $(m \leq 2)$ $\nexists\, \bar{T}$ such that $R_Q(\bar{T}) > 0 \Leftrightarrow Q \in \mathcal{Q}^{\mathtt{A}}_{\mathtt{FSP}}$.
- $(m = 1)$ $\nexists\, T, \bar{T}$ such that $R_P(T) + R_Q(\bar{T}) > 0 \Leftrightarrow (P, Q) \in \mathcal{S}^{\mathtt{A}}$.
- $(m = 1)$ (3.23) holds $\Leftrightarrow (P, Q) \in \mathcal{S}^{\mathtt{A}}$.

3.7 Two Illustrative Examples

3.7.1 A single-port RLC circuit

The linear RLC circuit shown in Fig. 3.2 has been previously used in studies with CPLs [9], but considering a *constant* voltage source instead of a sinusoidal AC voltage source as in the present chapter. If the voltage source is defined as

$$v_g = \sqrt{2} V_g \cos(\omega_0 t) \text{ V}, \tag{3.25}$$

then G and K, evaluated a $\mathbf{j}\omega_0$, are given by

$$G = \frac{r_1 + jL_1 w_0}{(1 + \frac{r_1}{r_c} - L_1 C_1 w_0^2) + \mathbf{j}\left(r_1 C_1 + \frac{L_1}{r_c}\right) w_0}$$
$$K = \frac{V_g}{(1 + \frac{r_1}{r_c} - L_1 C_1 w_0^2) + \mathbf{j}\left(r_1 C_1 + \frac{L_1}{r_c}\right) w_0}.$$

Using the circuit parameters from Table 3.1, and with the particular value of $r_c = 5$ kΩ, the above expressions result in

$$G = 0.0412 + j0.0238, \quad K = 24.3592 - \mathbf{j}0.6219.$$

Since $m = 1$, Proposition 3.3 gives a full characterization of the set $\mathcal{S}^{\mathtt{A}}$ for this circuit either in terms of the feasibility of the LMI (3.22) or via the simple inequality (3.23).

Fig. 3.3 shows the feasibility and infeasibility regions on the P-Q plane for the condition given in (3.22). The graph has been obtained by taking fixed values of P and Q in the discretized set $[0, 5000] \times [-12400, 4300]$. According to Proposition 3.3, any pair (P, Q) in the *infeasibility* region corresponds to an admissible pair, *i.e.*, $(P, Q) \in \mathcal{S}^{\mathtt{A}}$. On the other hand, any pair (P, Q) in the *feasibility* region corresponds to an inadmissible pair, *i.e.*, $(P, Q) \in \mathcal{S}^{\mathtt{I}}$.

In Fig. 3.4 the *exact* boundary of existence of solutions of $f_i(I) = 0$—that was computed numerically—and the feasibility boundary of the inequality (3.23) are shown; as predicted by the theory they are identical and also coincide with the boundary of of the plot shown in Fig. 3.3.

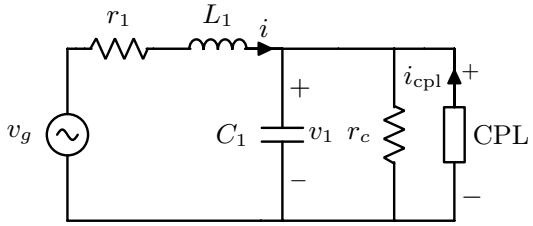

Figure 3.2: AC Linear RLC circuit with a CPL.

Table 3.1: Parameters for the circuit in Figs. 3.2 and 3.5

$r_1 = 0.04\ \Omega$	$L_1 = 78.0\ \mu$H	$C_1 = 2.0$ mF	$V_g = 24$ V
$r_2 = 0.06\ \Omega$	$L_2 = 98.0\ \mu$H	$C_2 = 1.0$ mF	$\omega_0 = 2\pi 50$ rad/s

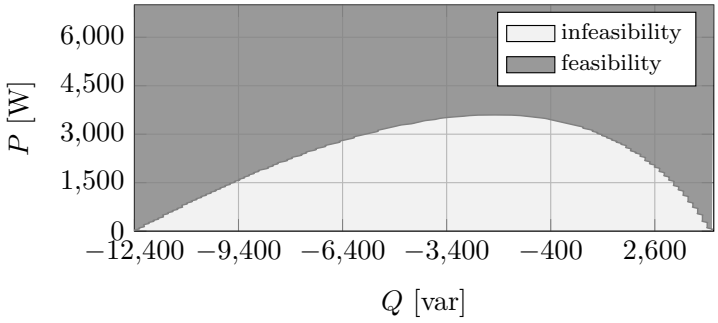

Figure 3.3: Feasibility and infeasibility regions of $R_P(T) + R_Q(\bar{T}) > 0$ for the circuit of Fig. 3.2.

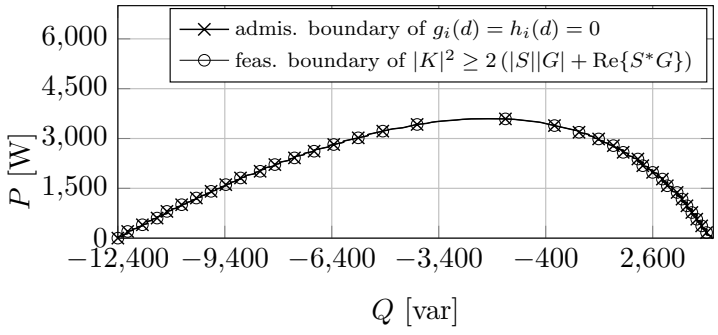

Figure 3.4: Boundary of the admissibility set $\mathcal{S}^{\mathbb{A}}$ and feasibility boundary of the inequality $|K|^2 \geq 2\,(|S||G| + \text{Re}\{\text{conj}(S)G\})$.

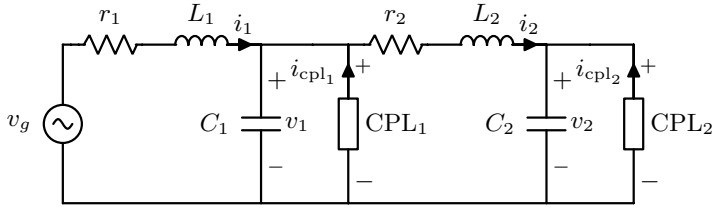

Figure 3.5: LTI AC circuit with two CPLs.

3.7.2 A two-port system

Fig. 3.5 shows an LTI circuit with two CPLs and the AC source of equation (3.25). In this case, the matrix G and the vector K are

$$G = \frac{1}{d(\mathbf{j}\omega_0)} \begin{bmatrix} n_{11}(\mathbf{j}\omega_0) & n_{12}(\mathbf{j}\omega_0) \\ n_{21}(\mathbf{j}\omega_0) & n_{22}(\mathbf{j}\omega_0) \end{bmatrix},$$
$$K = \frac{V_g}{d(\mathbf{j}\omega_0)} \begin{bmatrix} ((1 - \omega_0^2 L_2 C_2) + \mathbf{j}\omega_0 C_2 r_2) \\ 1 \end{bmatrix}$$

where

$$\begin{aligned} n_{11}(\mathbf{j}\omega_0) &= ((-C_2L_1r_2 - C_2L_2r_1)\omega_0^2 + r_1) \\ &\quad + \mathbf{j}(-C_2L_1L_2\omega_0^3 + (C_2r_1r_2 + L_1)\omega_0), \\ n_{12}(\mathbf{j}\omega_0) &= n_{21}(\mathbf{j}\omega_0) = r_1 + \mathbf{j}\omega_0 L_1, \\ n_{22}(\mathbf{j}\omega_0) &= ((-C_1L_1r_2 - C_1L_2r_1)\omega_0^2 + r_1 + r_2) \\ &\quad + \mathbf{j}(-C_1L_1L_2\omega_0^3 + (C_1r_1r_2 + L_1 + L_2)\omega_0), \\ d(\mathbf{j}\omega_0) &= (C_1C_2L_1L_2\omega_0^4 + (-C_1C_2r_1r_2 - C_1L_1 - C_2L_1 \\ &\quad - C_2L_2)\omega_0^2 + 1) + \mathbf{j}((-C_1C_2L_1r_2 - C_1C_2L_2r_1)\omega_0^3 \\ &\quad + (C_1r_1 + C_2r_1 + C_2r_2)\omega_0). \end{aligned}$$

Using the circuit parameters of Table 3.1, these matrices result in

$$G = 10^{-2} \cdot \begin{bmatrix} 4.185 + \mathbf{j}2.345 & 4.269 + j2.287 \\ 4.269 + j2.287 & 10.469 + j5.219 \end{bmatrix},$$

$$K = \begin{bmatrix} 24.526 - \mathbf{j}0.953 \\ 24.738 - \mathbf{j}1.433 \end{bmatrix}.$$

Fig. 3.6 shows the feasibility and infeasibility regions on the P_1-P_2 plane for the condition $R_P(T) > 0$. The graph was obtained by taking fixed values for P_1, P_2 in the discretized set $[0, 4000] \times [0, 2000]$. It is concluded that the dark gray area is *contained* in the set $\mathcal{P}^{\mathtt{I}}_{\mathtt{FAQ}}$. That is, for all values of P_1 and P_2 in this area, the circuit of Fig. 3.5 *does not* admit a steady state operating regime—this *independently* of the values of Q_1 and Q_2.

Fig. 3.7 shows the feasibility and infeasibility regions on the Q_1-Q_2 plane for the condition $R_Q(\bar{T}) > 0$. The gridding for Q_1, Q_2 was taken this time in the discretized set

$$[-5000, 10000] \times [-5000, 10000].$$

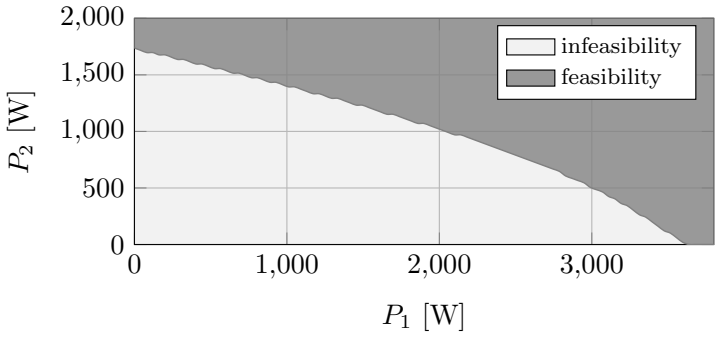

Figure 3.6: Feasibility and infeasibility regions of $R_P(T) > 0$ for the circuit of Fig. 3.5.

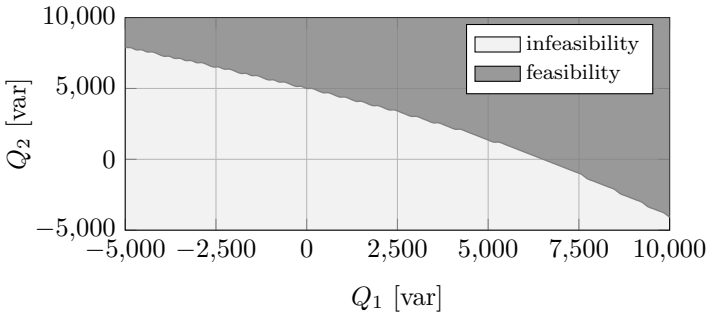

Figure 3.7: Feasibility and infeasibility regions of $R_Q(\bar{T}) > 0$ for the circuit of Fig. 3.5.

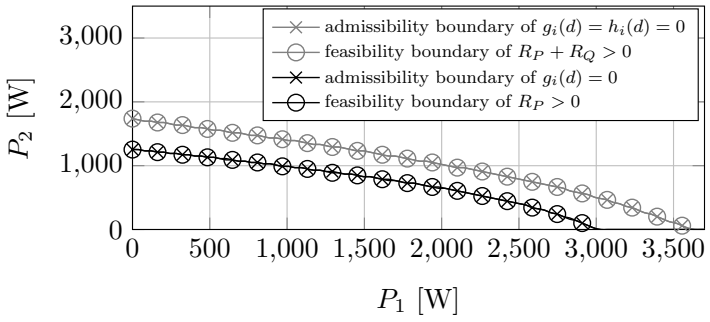

Figure 3.8: Comparison between different boundaries of admissibility and feasibility for the two-port network of Fig. 3.5 on the P_1-P_2 plane.

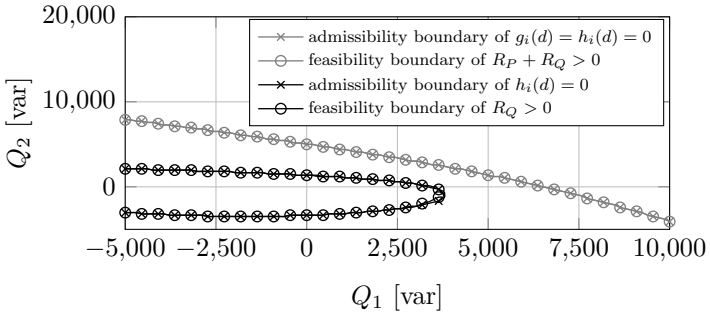

Figure 3.9: Comparison between different boundaries of admissibility and feasibility for the two-port network of Fig. 3.5 on the $Q_1 - Q_2$ plane.

The same conclusion as above applies to values of Q_1 and Q_2 in the dark gray area, which is *contained* in the set $\mathcal{Q}^{\mathtt{I}}_{\mathtt{FAP}}$.

Recall that for a two port system, non–feasibility of the LMI $R_P(T) > 0$ in Proposition 3.2 is necessary and sufficient for existence of equilibria when P is fixed and Q is free—similarly $R_Q(\bar{T}) > 0$ is the necessary and sufficient test when Q is fixed and P is free. To corroborate this fact, it is drawn with a gray line in Fig. 3.8, the *numerically exact* boundary of existence of solutions for $\mathrm{Re}\{V_i\,\mathrm{conj}(I_i)\} = -P_i$, on the plane P_1-P_2. As predicted by the theory, it exactly coincides (up to some numerical glitches) with the feasibility/infeasibility boundary of the condition $R_P(T) > 0$, drawn also in gray but with a circle marker.

Analogously, the numerically exact boundary of existence of solutions for

$$\mathrm{Im}\{V_i\,\mathrm{conj}(I_i)\} = -Q_i$$

on the plane Q_1-Q_2, is shown in Fig. 3.9 to coincide with the feasibility/infeasibility boundary for the condition $R_Q(\bar{T}) > 0$.

It should be underscored that the admissibility region for P *and* Q *is not* the union of their separate admissible regions. That is, even if values for P and Q are taken inside their respective admissible regions, *i.e.*, under the gray curves in Figs. 3.8 and 3.9, respectively, this does not imply that the system will have an equilibrium for these power values. The reason is that such boundaries were obtained solving

the real and the imaginary part of (3.4) *independently* and not simultaneously. The black curves with an 'x' marker in Figs. 3.8 and 3.9 represent the numerically exact boundaries of existence for (3.4), solving its real and imaginary parts *simultaneously*, and taking fixed values of $Q_1 = 1000$ and $Q_2 = 0$ for the former, and taking fixed values of $P_1 = 500$ and $P_2 = 500$ for the latter. It can be observed that in both cases the admissibility regions are reduced. However, they are bounded by the feasibility/infeasibility boundaries of $R_P(T) > 0$ and $R_Q(\bar{T}) > 0$.

Finally, the black curves with circle marker in Figs. 3.8 and 3.9 correspond to the feasibility/infeasibility boundaries of the LMI

$$R_P(T) + R_Q(\bar{T}) > 0$$

plotted for some fixed values of P and Q, respectively. Although not predicted by the theory, they coincide with the boundaries of numerically exact solution of the quadratic equations (3.4) for these fixed values.

3.8 Summary

For general, multi-port, linear AC networks with constant power loads, this chapter has proposed conditions that are necessary for load admissibility, *i.e.*, if this conditions are satisfied, then the network *does not* admit a sinusoidal steady state regime at certain specified frequency. For the case of one- or two-port networks and free active (or reactive) power of the CPLs' components, these conditions are also sufficient. Interestingly, for single-port networks the admissibility condition can be tested directly from the data of the problem. Similarly to the case of DC networks [9, 91] the analysis boils down to the study of solvability of a set of quadratic equations in several variables. In the DC case these equations define mappings from $\mathbb{R}^m$ to $\mathbb{R}$, while in the AC case the mappings are from $\mathbb{C}^m$ to $\mathbb{C}$, which as it has been verified here, may give rise to a different mathematical problem in certain situations; see Section 3.5.2.

Technical Appendices of the Chapter

3.A Proof of Lemma 3.2

To streamline the presentation, define the set

$$\mathcal{E}_v := \{x \in \mathbb{R}^n \mid v_k(x) = 0,\ \forall k\},$$

where $v_k(x)$ is defined in (3.11).

The proof of the implication (3.13) is established by contraposition. Therefore, suppose that $\mathcal{E}_v$ is *not empty*. It is proven next that there are no real numbers t_k such that

$$\sum_{k=1}^{\ell} t_k \mathcal{A}_k > 0. \tag{3.26}$$

Take $x \in \mathcal{E}_v$ and t_k arbitrarily. Since $v_k(x) = 0$, then $t_k v_k(x) = 0$. This implies that

$$\sum_{k=1}^{\ell} t_k v_k(x) = 0. \tag{3.27}$$

Define the vector $z := \mathrm{col}(x, 1) \in \mathbb{R}^{n+1}$. Then, using (3.12), equation (3.27) can be represented in matrix form as

$$z^\top \left(\sum_{k=1}^{\ell} t_k \mathcal{A}_k \right) z = 0. \tag{3.28}$$

Since z is a non-zero vector, (3.28) contradicts inequality (3.26) for an arbitrary selection of t_k, completing the proof.

3.B Proof of Lemma 3.3

The proof invokes Finsler's Lemma, in particular Statement I of the Main Theorem in [118] that, using the notation of Lemma 3.3, reads as follows:

$$\begin{aligned} &\exists\, t_1, t_2 \in \mathbb{R} \mid t_1 \mathcal{A}_1 + t_2 \mathcal{A}_2 > 0 \\ \Leftrightarrow\ &\{\eta \in \mathbb{R}^{n+1} \mid \eta^\top \mathcal{A}_1 \eta = \eta^\top \mathcal{A}_2 \eta = 0\} = \{\mathbf{0}\}, \end{aligned} \tag{3.29}$$

where $\mathcal{A}_1, \mathcal{A}_2$ are given by (3.12). Notice that this theorem pertains to homogeneous quadratic forms while, because of the presence of the terms $2x^\top b_k + c_k$, the equations of interest in the chapter, *e.g.*, (3.11), are non-homogeneous.

To adapt Finsler's Theorem to handle this case, define the *real* mappings $w_1, w_2 : \mathbb{R}^n \times \mathbb{R} \to \mathbb{R}$

$$\begin{aligned} w_1(x, y) &:= x^\top A_1 x + 2x^\top b_1 y + c_1 y^2 \\ w_2(x, y) &:= x^\top A_2 x + 2x^\top b_2 y + c_2 y^2 \end{aligned}$$

and the set

$$\mathcal{E}_w := \{(x, y) \in \mathbb{R}^n \times \mathbb{R} \mid w_1(x, y) = w_2(x, y) = 0\}. \tag{3.30}$$

First, it is proven that under condition (3.14), the following *equivalence* holds:

$$\mathcal{E}_v = \{x \in \mathbb{R}^n \mid v_1(x) = v_2(x) = 0\} = \varnothing \ \Leftrightarrow\ \mathcal{E}_w = \{(0_n, 0)\}. \tag{3.31}$$

($\Rightarrow$) The proof is by contraposition, therefore, suppose there is a *non-zero* vector $(\bar{x}, \bar{y}) \in \mathcal{E}_w$. Consider first the case when $\bar{y} = 0$, then $\bar{x} \neq 0$ necessarily. Since $w_1(\bar{x}, 0) = w_2(\bar{x}, 0) = 0$ This implies that

$$\bar{x}^\top A_1 \bar{x} = \bar{x}^\top A_2 \bar{x} = 0.$$

Let $s_1, s_2 \in \mathbb{R}$ arbitrary. Then, the following expression holds

$$\bar{x}^\top (s_1 A_1 + s_2 A_2)\, \bar{x} = 0. \tag{3.32}$$

However, this contradicts (3.14). Assume now that $\bar{y} \neq 0$. In this case it follows that $\frac{\bar{x}}{\bar{y}} \in \mathcal{E}_v$. Hence, $\mathcal{E}_v \neq \varnothing$, completing the proof.

($\Leftarrow$) Once again by contraposition. Hence, suppose that $\mathcal{E}_v \neq \varnothing$ and take $\bar{x} \in \mathcal{E}_v$, then $(\bar{x}, 1)$ is a *non-zero* vector in $\mathcal{E}_w$ and, consequently, $\mathcal{E}_w \neq \{0_n\}$, completing the proof.

The proof of the implication (3.15) follows next. Suppose $\mathcal{E}_v = \varnothing$. Then, the equivalence (3.31) implies that $\mathcal{E}_w = \{(0_n, 0)\}$. Recalling that

$$w_1(x, y) = \eta^\top \mathcal{A}_1 \eta, \; w_2(x, y) = \eta^\top \mathcal{A}_2 \eta$$

with $\eta := (x, y)$, Finsler's Lemma ensures the existence of $t_1, t_2 \in \mathbb{R}$ such that

$$t_1 \mathcal{A}_1 + t_2 \mathcal{A}_2 > 0. \tag{3.33}$$

Hence, the lemma is proved.

3.C Proof of Proposition 3.1

Define the following $(2m + 1) \times (2m + 1)$ real matrices

$$\hat{\mathcal{A}}_i := \begin{bmatrix} \hat{A}_i & \hat{b}_i \\ \hat{b}_i^\top & 2P_i \end{bmatrix}, \; \hat{\mathcal{B}}_i := \begin{bmatrix} \hat{B}_i & \hat{q}_i \\ \hat{q}_i^\top & 2Q_i \end{bmatrix}. \tag{3.34}$$

Notice that

$$\begin{aligned} g_i(d) &= \begin{bmatrix} d^\top & 1 \end{bmatrix} \hat{\mathcal{A}}_i \begin{bmatrix} d \\ 1 \end{bmatrix} \\ h_i(d) &= \begin{bmatrix} d^\top & 1 \end{bmatrix} \hat{\mathcal{B}}_i \begin{bmatrix} d \\ 1 \end{bmatrix}. \end{aligned} \tag{3.35}$$

Suppose there exist $t_i, \bar{t}_i$ such that[5]

$$\sum_{i=1}^{m} t_i \hat{\mathcal{A}}_i + \sum_{i=1}^{m} \bar{t}_i \hat{\mathcal{B}}_i > 0.$$

Referring to Lemma 3.2 with $\ell = 2m$, $x = d$ and

$$v_1 = g_1, \ldots, v_m = g_m, v_{m+1} = h_1, \ldots, v_{2m} = h_m,$$

it is concluded that there are no solutions for the system

$$g_i(d) = h_i(d) = 0.$$

This implies that there is no sinusoidal steady state for the network. The proof is completed noting that

$$\sum_{i=1}^{m} t_i \hat{\mathcal{A}}_i = R_P(T), \; \sum_{i=1}^{m} \bar{t}_i \hat{\mathcal{B}}_i = R_Q(\bar{T}). \tag{3.36}$$

[5]The symbol $\bar{t}_i$ is introduced for ease of reference in the subsequent material.

3.D Proof of Proposition 3.2

Consider the matrix R_P, given in (3.17), for $T = I_m$. Notice that the uppermost corner of R_P is given by M, defined in (3.19). Since $M > 0$, it follows that $R_P > 0$ if and only if the Schur complement of M is positive. The proof is completed noting that the latter is equivalent to (3.20).

3.E Proof of Proposition 3.3

The equivalence between the first two statements is a direct corollary of the last statement in Lemma 3.3, which states that for $\ell = 2$ (that is $m = 1$)

$$g_1(d) = h_1(d) = 0 \;\Leftrightarrow\; \exists\, t_1, \bar{t}_1 \mid t_1\mathcal{A}_1 + \bar{t}_1\mathcal{B}_1 > 0.$$

The proof is completed invoking the identity (3.36) with $T = t_1,\ \bar{T} = \bar{t}_1$.

The equivalence with the last statement is shown next. Towards this end, re-write the model of the network in complex form as

$$G|I|^2 + \mathrm{conj}(I)K + S = 0. \tag{3.37}$$

Inequality (3.2) implies that $G \neq 0$. Divide (3.37) by G and split it into real and imaginary parts. Then, the complex equation (3.37) is equivalent to

$$x^2 + y^2 + ax + by + P' = 0 \tag{3.38}$$
$$bx - ay + Q' = 0 \tag{3.39}$$

where

$$\frac{K}{G} := a + \mathbf{j}b, \quad \frac{S}{G} := P' + jQ', \quad I := x + jy.$$

Suppose that $a \neq 0$, then from (3.39) y is obtained as

$$y = \frac{bx + Q'}{a}. \tag{3.40}$$

Substituting the above value for y into (3.38), the following quadratic equation for x is obtained.

$$(a^2 + b^2)x^2 + \left[2bQ' + a(a^2 + b^2)\right] x + \left(Q'^2 + abQ' + a^2P'\right) = 0. \tag{3.41}$$

This equation has a *real* solution if and only if its discriminant is non-negative, that is, if and only if

$$\left(2bQ' + a(a^2 + b^2)\right)^2 \geq 4(a^2 + b^2)(Q'^2 + abQ' + a^2P').$$

Develop the left and right-hand side expressions, then the inequality above is equivalent to

$$4b^2Q'^2 + 4abQ'(a^2 + b^2) + a^2(a^2 + b^2)^2$$
$$\geq$$
$$4a^2Q'^2 + 4b^2Q'^2 + 4abQ'(a^2 + b^2) + 4a^2P'(a^2 + b^2)$$

which can be written in a simplified form as

$$(a^2+b^2)^2 - 4P'(a^2+b^2) - 4Q'^2 \geq 0.$$

This expression holds if and only if

$$(a^2+b^2) \geq 2(P' + \sqrt{P'^2+Q'^2}). \tag{3.42}$$

Notice that

$$\begin{aligned} a^2+b^2 &= \frac{|K|^2}{|G|^2}, \\ P' &= \frac{P\mathrm{Re}\{G\} + Q\mathrm{Im}\{G\}}{|G|^2}, \\ Q' &= \frac{Q\mathrm{Re}\{G\} - P\mathrm{Im}\{G\}}{|G|^2}. \end{aligned}$$

Then, inequality (3.42) can be equivalently written in the original coefficients as in in (3.23).

Now suppose that $a = 0$. If $b \neq 0$, then from (3.39) it follows that

$$x = -\frac{Q'}{b}.$$

If this value of x is substituted into (3.38), then, a quadratic equation for y is obtained:

$$b^2y^2 + b^3y + \left(Q'^2 + b^2P'\right) = 0.$$

This equation has a real solution if and only if its discriminant is non negative, that is if and only if

$$b^6 - 4b^2\left(Q'^2 + b^2P'\right) \geq 0.$$

This inequality is equivalent to

$$\left(b^2\right)^2 - 4P'(b^2) - 4Q'^2 \geq 0,$$

which holds if and only if

$$b^2 \geq 2\left(P' + \sqrt{P'^2+Q'^2}\right).$$

Clearly, the above expression corresponds with (3.42) by taking $a = 0$.

To conclude the proof, suppose that $a = 0$ and $b = 0$ simultaneously. In this case, system conformed by equations (3.38) and (3.39), has a solution if and only if $Q' = 0$ and $P' \leq 0$. This last case has little practical relevance since if $a = 0$ and $b = 0$ simultaneously, then $K = 0$, which would correspond to a single-port network without a source.

3.F Proofs of Propositions 3.4 and 3.5

The proofs follow as direct corollaries of Lemma 3.3. First, notice that

$$\begin{aligned} g_1(d) = g_2(d) = 0 \;&\Leftrightarrow\; \exists\, t_1, t_2 \text{ such that } t_1\mathcal{A}_1 + t_2\mathcal{A}_2 > 0 \\ h_1(d) = h_2(d) = 0 \;&\Leftrightarrow\; \exists\, \bar{t}_1, \bar{t}_2 \text{ such that } \bar{t}_1\mathcal{B}_1 + \bar{t}_2\mathcal{B}_2 > 0, \end{aligned}$$

and

$$\begin{aligned} t_1\mathcal{A}_1 + t_2\mathcal{A}_2 &= R_P\left(\operatorname{diag}\left(t_1, t_2\right)\right) \\ \bar{t}_1\mathcal{B}_1 + \bar{t}_2\mathcal{B}_2 &= R_Q\left(\operatorname{diag}\left(\bar{t}_1, \bar{t}_2\right)\right). \end{aligned}$$

It only remains to verify (3.14). For Proposition 3.4, it follows that

$$\hat{A}_1 + \hat{A}_2 = M,$$

with M, given in (3.19), being positive definite. Therefore, (3.14) is satisfied with $s_1 = s_2 = 1$. On the other hand, for Proposition 3.5 it is not clear when there exists $\hat{s}_1, \hat{s}_2 \in \mathbb{R}$ such that

$$\hat{s}_1\hat{B}_1 + \hat{s}_2\hat{B}_2 > 0,$$

with $\hat{B}_1, \hat{B}_2$ given in (3.9). Therefore, it is necessary to impose assumption (3.24).

Chapter 4

Decoupled AC power flow and DC power networks with CPLs

Synopsis In AC and DC power systems with constant power loads, the analysis of existence of steady states is cast as the analysis of solutions of a set of nonlinear algebraic equations of the form $f(x) = 0$, where $f : \mathbb{R}^n \to \mathbb{R}^n$. In this chapter, the vector field f is associated to the ordinary differential equation $\dot{x} = f(x)$ and by invoking advanced concepts of dynamical systems theory and effectively exploiting some exhibited monotonicity features, the following traits are established. (i) Proof that, if there are equilibria, there is a *distinguished* one that is stable and attractive, and give conditions such that it is unique. (ii) Establishment of a simple on-line procedure to decide whether equilibria exist or not, and to compute the distinguished one. (iii) Proof that the method is also applicable for the case when the parameters of the system are not exactly known. It is shown how the proposed tool can be applied to the analysis of voltage regularity in AC power systems, and to the study of existence of steady states of multi-terminal high-voltage DC systems and DC microgrids.

4.1 Introduction

This chapter explores a methodological approach to determine the existence and stability of the equilibria in diverse power systems problems. The specific problems are enlisted as

P1 Analysis of voltage regularity[1] in AC power systems with "light" active power load. The study of this important property, also called "static (or long-term) voltage stability" [56, Chapter 14] or "loadability limit" [119, Chapter 7], is standard in the power systems community.

P2 Study of existence of steady states of two emerging power system concepts, namely multi-terminal high-voltage (MT-HV) DC networks [120, 50] and DC microgrids [37, 33].

P3 In addition, if stationary voltage solutions exist, the proposed method also allows to identify the solution with the highest voltage magnitudes, which is the desired operating condition in these applications.

[1] Prof David Hill is graciously acknowledged for suggesting this, most appropriate, terminology.

In these three examples, the key problem is the study of a nonlinear algebraic equation $f(x) = 0$, with $f : \mathbb{R}^n \to \mathbb{R}^n$, where only solutions x with positive components are of interest. The approach adopted in the chapter is to associate to $f(x)$ the ordinary differential equation (ODE) $\dot{x} = f(x)$, which is shown to be well-defined on the positive orthant of $\mathbb{R}^n$, and to apply to it tools of dynamical systems [43]—in particular, monotone systems [114]—to study existence and stability of its equilibria, which are the solutions of the primal algebraic equation.

The main contributions of this chapter are the proofs of the following properties of the ODE.

C1 If there are no equilibria then, in all the solutions of the ODE, one or more components converge to zero in finite time.

C2 If equilibria exist, there is a distinguished equilibrium, say $\bar{x}_{\texttt{max}}$, among them that dominates component-wise all the other ones. This equilibrium $\bar{x}_{\texttt{max}}$ is stable and attracts all trajectories that start in a certain well-defined domain. Moreover, physically-interpretable conditions on the problem data that ensure $\bar{x}_{\texttt{max}}$ is the only stable equilibrium, are provided.

C3 By solving a system of n convex algebraic inequalities in n positive unknowns, a set of initial conditions are explicitly identified. These initial conditions posses the following properties. (i) All trajectories starting there monotonically decay in all components. (ii) Either some component converges to zero in a finite time for all those trajectories or, for all of them, all components remain separated from zero on the infinite time horizon. Moreover, in the latter case, the trajectory is forward complete and converges to $\bar{x}_{\texttt{max}}$. An additional outcome of this analysis is the generation of an estimate for the domain of attraction of asymptotically stable equilibia.

C4 Proof that the method is applicable even if the parameters of $f(x)$ are unknown, and only upper and lower bounds for them are available.

In [34], the authors propose conditions for the solvability of affinely parameterized quadratic equations that contain, as a particular case, the kind of nonlinear equations studied in the present chapter. Nonetheless, a standing assumption in that paper is that *a solution exists*, and the focus is to derive conditions under which the solutions belong to a certain pre-specified set. Conversely, in this chapter the existence of solutions is not taken for granted; instead the conditions under which they exist (or not) are given. Additionally, the identification of the dominant equilibrium $\bar{x}_{\texttt{max}}$ and the analysis of its regularity properties—from the viewpoint of reactive power flow analysis—is carried out thanks to the stability identification of the ODE's equilibria; the latter central *analytical* aspect reported in this chapter cannot be addressed with the tools used in [34]. More recently, in [123], analytical conditions for the existence of solutions of the (full) *power flow* equations are given.[2] However, by invoking the standard "decoupling" assumption, only the problem of reactive power flow is addressed in the present chapter. Finally, in [1], the authors propose a *numerical method* to solve the load flow equations, which is by now

[2]Recall the preliminaries on power systems in Chapter 2.

standard and implemented in many commercial software packages, such as *DigSilent PowerFactory*. Nevertheless, as already mentioned, this problem is beyond the scope of this chapter.

The remainder of the chapter is organized as follows. Section 4.2 describes the ODE $\dot{x} = f(x)$ of interest and gives the main theoretical results pertaining to it, with some practical extensions given in Section 4.3. In Section 4.4 these results are illustrated with three canonical power systems examples. Section 4.5 presents some numerical simulation results. The chapter is wrapped-up with a brief summary in Section 4.6. To enhance readability, all proofs of the technical results are given in a technical appendix at the end of the chapter.

4.2 Analysis of the ODE of Interest

As indicated in the introduction, one of the main interests of the chapter is the analysis of voltage regularity of steady solutions of AC power systems (under the common decoupling assumption [56]), and on the study of the existence of steady states of MT-HVDC networks as well as DC microgrids—the three of them with CPLs. In Section 4.3, it is shown that these studies boil down to the analysis of solutions of the following algebraic equations in $\bar{x} \in \mathcal{K}_+^n$[3]

$$a_{i1}\bar{x}_1 + a_{i2}\bar{x}_2 + \cdots + a_{in}\bar{x}_n + \frac{b_i}{\bar{x}_i} = w_i, \quad i \in \{1, \ldots, n\}, \tag{4.1}$$

where $a_{ij} \in \mathbb{R}$, $w_i \in \mathbb{R}$ and $b_i \in \mathbb{R}$. These equations can be written in compact form as

$$A\bar{x} + \operatorname{stack}\left(\frac{b_i}{\bar{x}_i}\right) - w = 0. \tag{4.2}$$

In the chapter, the following assumption is adopted.

Assumption 4.1. The matrix $A = A^\top$ is positive definite, its off-diagonal elements are non-positive and $b_i \neq 0$ for all i.

To study the solutions of (4.2), the following ODE is considered.

$$\dot{x} = f(x) := -Ax - \operatorname{stack}\left(\frac{b_i}{x_i}\right) + w. \tag{4.3}$$

The main interest of the chapter is in studying the existence, and stability, of the equilibria of (4.3). In particular, the answers to the following questions are provided.

Q1 When do equilibria exist? Is it possible to offer a simple test to establish their existence?

Q2 If there are equilibria, is there a distinguished element among them?

Q3 Is this equilibrium stable and/or attractive?

Q4 If it is attractive, can its domain of attraction be estimated?

[3]Recall from the preliminaries that $\mathcal{K}_+^n$ denotes the positive orthant of $\mathbb{R}^n$.

Q5 Is it possible to propose a simple procedure to compute this special equilibrium using the system data (A, b, w)?

Q6 Are there other stable equilibria?

Instrumental to answer to the queries Q1-Q6 is the fact that the system (4.3) is monotone. That is, for any two solutions $x_a(\cdot), x_b(\cdot)$ of (4.3), defined on a common interval $[0, T]$, the inequality $x_a(0) \leq x_b(0)$ implies that $x_a(t) \leq x_b(t)\ \forall t \in [0, T]$. This can be verified by noticing that equation (4.3) satisfies the necessary and sufficient condition for monotonicity [114, Proposition 1.1 and Remark 1.1, Ch. III]

$$\frac{\partial f_i(x)}{\partial x_j} \geq 0,\ \forall i \neq j,\ \forall x \in \mathcal{K}_+^n. \tag{4.4}$$

In the sequel, $x(t, x_0)$ denotes the solution of (4.3) with initial conditions $x(0) = x_0 > 0$, and use the following.

Definition 4.1. An equilibrium $\bar{x} > 0$ of (4.3) is said to be attractive from above if for any $x_0 \geq \bar{x}$, the solution $x(t, x_0)$ is defined on $[0, \infty)$ and converges to $\bar{x}$ as $t \to \infty$. The equilibrium is said to be hyperbolic if the Jacobian matrix $\nabla f(\bar{x})$ has no eigenvalue with zero real part [43].

Remark 4.1. Along the lines of the standard Kron reduction, the findings of the chapter can be extended to the case where some of the coefficients b_i are equal to zero.[4]

The proof of this remark is given in Appendix 4.A.

4.2.1 The simplest example

To gain an understanding of some key traits of possible results, it is instructive to start with the simplest case $n = 1$. Then, $x \in \mathbb{R}$ and (4.3) is the scalar equation

$$\dot{x} = -ax - \frac{b}{x} + w, \tag{4.5}$$

and $a > 0, b \neq 0$. Feasible behaviors of the system are exhaustively described in Figure 4.1.

The following can be inferred from this figure.

B1 The system either has no equilibria, or it has finitely many equilibria, or it has a single equilibrium.

B2 If the system has equilibria, the rightmost of them is attractive from above.

B3 Non-hyperbolic equilibria may be attractive from above but unstable; moreover, there may be no other equilibria.

B4 Hyperbolic and attractive from above equilibria are stable.

B5 If $b > 0$, globally attractive equilibria do not exist.

It is shown next that several of the traits occurring in the scalar case are inherited by the n-th order ODE (4.3).

[4] An anonymous reviewer is acknowledged for indicating this.

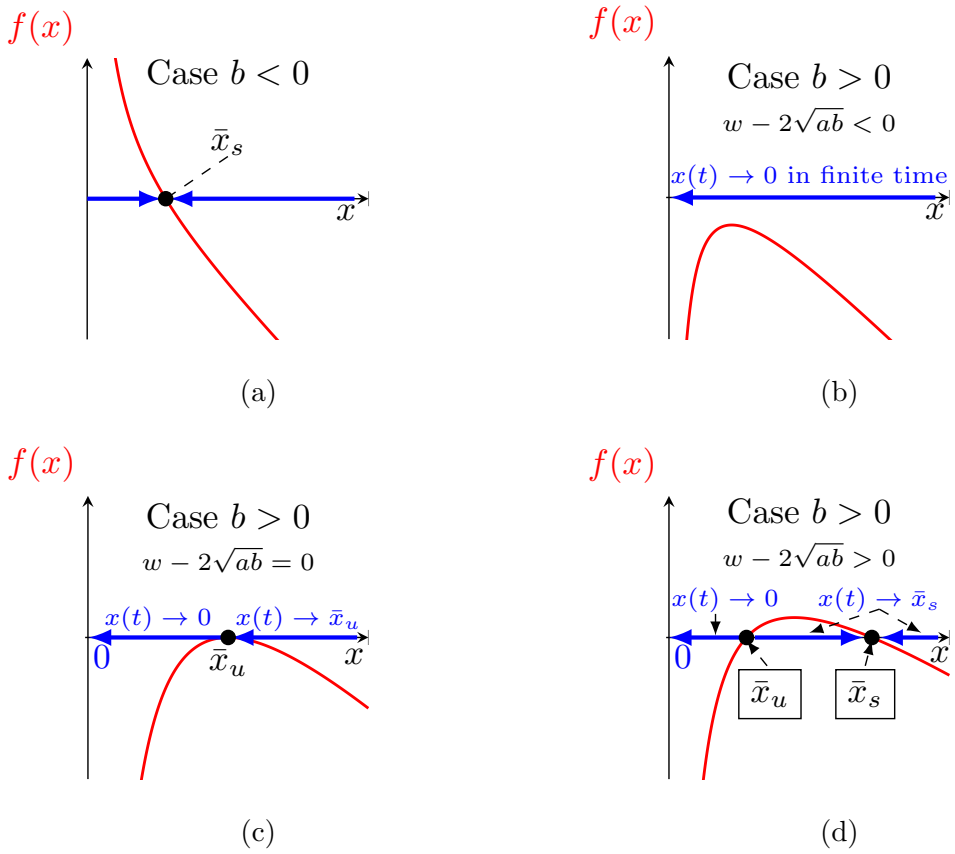

Figure 4.1: Feasible behaviors of the one-dimensional system (4.5): (a) A unique globally attractive equilibrium $\bar{x}_s$; (b) No equilibria, all solutions converge to zero in a finite time t_f; (c) Unique unstable equilibrium $\bar{x}_u$, which is attractive from above, whereas any solution starting on the left diverges from $\bar{x}_u$ and converges to 0 in a finite time; (d) Two equilibria, the smallest of which $\bar{x}_u$ is unstable, whereas the larger one $\bar{x}_s$ is stable and attractive from above.

4.2.2 An extra assumption

The situation described in item B3 above may happen in the general case —*e.g.*, considering a diagonal matrix A. However, some evidence suggesting that this situation "almost never" occurs is now given. This forms a ground to treat the opposite situation as "typical", "regular", and "prevalent" and to pay special attention to it.

To be specific, a case where item B3 is impossible is identified.

Assumption 4.2. There are no non-hyperbolic equilibria of the system (4.3). In other words, the following set identity holds

$$\left\{ x \in \mathcal{K}_+^n \;\middle|\; \begin{array}{c} \det\left[A - \operatorname{diag}\left(\frac{b_i}{x_i^2}\right)\right] = 0, \\ w = Ax + \operatorname{stack}\left(\frac{b_i}{x_i}\right) \end{array} \right\} = \emptyset. \tag{4.6}$$

The lemma below proves that Assumption 4.2 is almost surely true.

Lemma 4.1. For any given A and $b_i \neq 0$, the set of all $w \in \mathbb{R}^n$ for which Assumption 4.2 does not hold has zero Lebesgue measure and is nowhere dense.

Proof. See Appendix 4.A at the end of the chapter. □□□

4.2.3 Main results on the system (4.3)

The first claim contains a qualitative analysis of the system.

Proposition 4.1. Consider the system (4.3) verifying Assumption 4.1. One and only one of the following two mutually exclusive statements holds.

S1 There are no equilibria $\bar{x}$, either stable or unstable, and any solution $x(\cdot)$ is defined only on a finite time interval $[0, t_f) \subset [0, \infty)$, since there exists at least one coordinate x_i such that $x_i(t) \to 0, \dot{x}_i(t) \to -\infty$ as $t \to t_f$. Such a coordinate is necessarily associated with $b_i > 0$.[5]

S2 Equilibria $\bar{x}^k$ do exist. One of them $\bar{x}_{\mathtt{max}} > 0$ verifies $\bar{x}_{\mathtt{max}} \geq \bar{x}^k$, $\forall k$, and is attractive from above.

Suppose that Assumption 4.2 is also met. Then in the case S2 there are finitely many equilibria and $\bar{x}_{\mathtt{max}}$ is locally asymptotically stable. If in addition all b_i's are of the same sign, then there are no other stable equilibria apart from $\bar{x}_{\mathtt{max}}$.

Proof. See Appendix 4.D at the end of the chapter. □□□

Lemma 4.1 allows to claim that the traits described in the last two sentences of Proposition 4.1 occur almost surely.

A constructive test to identify which of the cases S1 or S2 holds, as well as a method to find $\bar{x}_{\mathtt{max}}$ in the case S2, are presented. To this end, the following concept is introduced.

[5] This implies that the case in claim S1 does not occur if $b_j < 0$, $\forall\, j$.

Definition 4.2. A solution $x(\cdot)$ of the ODE (4.3) is said to be *distinguished* if its initial condition lives in the set

$$\mathcal{E} := \left\{ x \in \mathcal{K}_+^n \mid Ax > \operatorname{stack}\left(\langle w_i \rangle + \frac{\langle -b_i \rangle}{x_i} \right) \right\}.^6 \tag{4.7}$$

If $b_i > 0$ for all i, then the set (4.7) reduces to the (convex open polyhedral) cone $\left\{ x \in \mathcal{K}_+^n \mid Ax > \operatorname{stack}\left(\langle w_i \rangle \right) \right\}$.

Proposition 4.2. Consider the system (4.3) verifying Assumption 4.1.

I The set $\mathcal{E}$ is non-empty, consequently there are distinguished solutions.

II All such solutions strictly decay, in the sense that $\dot{x}(t) < 0$, for all t in the domain of definition of $x(\cdot)$.

III One and only one of the following two mutually exclusive statements holds simultaneously for all distinguished solutions $x(\cdot)$:

i For a finite time $t_f \in (0, \infty)$, some coordinate $x_i(\cdot)$ approaches zero, that is,

$$\lim_{t \to t_f} x_i(t) = 0, \tag{4.8}$$

and the solution $x(\cdot)$ is defined only on a finite time interval $[0, t_f)$.

ii There is no coordinate approaching zero, the solution is defined on $[0, \infty)$, and the following limit exists and verifies

$$\lim_{t \to \infty} x(t) > 0. \tag{4.9}$$

This limit is the same for all distinguished solutions.

IV If the case III.i holds for a distinguished solution, the situation S1 from Proposition 4.1 occurs.

V If the case III.ii holds for a distinguished solution, the situation S2 from Proposition 4.1 occurs, and the dominant equilibrium $\bar{x}_{\mathtt{max}}$ is equal to the limit (4.9).

Proof. See Appendix 4.D at the end of the chapter. □□□

Remark 4.2 (Additional properties of (4.3))**.**

P1 In III.i, there may be several components x_i with the described property, but not all of them necessarily possess it.

P2 The claim S1 in Proposition 4.1 and IV in Proposition 4.2 yield that (4.8) is necessarily associated with $b_i > 0$ and $\dot{x}_i(t) \to -\infty$ as $t \to t_f$.

P3 Regarding the claim S2 in Proposition 4.1 the basin of attraction of the equilibrium $\bar{x}_{\mathtt{max}}$ contains all states $x \geq \bar{x}_{\mathtt{max}}$. Under Assumption 4.2, this basin is open.

[6] The operator $\langle \cdot \rangle$ denotes the clipping function $\langle a \rangle := \max\{a, 0\}$.

P4 The linear programming problem of finding elements in the set

$$\left\{x \in \mathcal{K}_+^n \mid Ax > 0\right\}$$

has been widely studied in the literature [28, 100, 11]. There is a whole variety of computationally efficient methods to solve this problem, including the Fourier-Motzkin elimination, the simplex method, interior-point/barrier-like approaches, and many others; for a recent survey, the reader is referred to [35].

4.3 A Numerical Procedure and a Robustness Analysis

With the aim of extending the realm of application of the previous results, this section addresses the issues of numerical computation and robustness of the claims. Additionally, explicit answers to the questions raised at the beginning of Section 4.2 are given.

4.3.1 A numerical procedure to verify Propositions 4.1 and 4.2

Proposition 4.2 suggests a computational procedure to verify whether the system has equilibria and, if they do exist, to find the dominant one $\bar{x}_{\texttt{max}}$ among them. Specifically, it suffices to find an element of the set $\mathcal{E}$ defined in (4.7), to launch the solution of the differential equation (4.3) from this vector, and to check whether—as the solution decays—there is a coordinate approaching zero or, conversely, all of them remain separated from zero. In the last case, the solution has a limit, which is precisely the dominant equilibrium of the system.

The statement I of Proposition 4.2 ensures that the first step of this algorithm, *i.e.*, generating an element of the set $\mathcal{E}$ defined in (4.7), is feasible. Technically, this step consists in solving a system of feasible convex inequalities given by

$$\langle w_i \rangle + \frac{\langle -b_i \rangle}{x_i} - \sum_{j=1}^{n} a_{ij} x_j < 0, \quad x_i > 0, \qquad \forall i.$$

This problem falls within the area of convex programming and so there is an armamentarium of effective tools to solve it. Nevertheless, this problem can be further simplified through transition from nonlinear convex inequalities to linear ones, modulo closed-form solution of finitely many scalar quadratic equations. The basis for this is given by the following lemma, whose proof is given in Appendix 4.B.

Lemma 4.2. Pick any vector $z > 0$ such that $Az > 0$.[7] Then, the scaled vector $x := \mu z$ verifies $x \in \mathcal{E}$, provided that

$$\mu > \frac{\langle w_i \rangle + \sqrt{\langle w_i \rangle^2 + 4(Az)_i \frac{\langle -b_i \rangle}{z_i}}}{2(Az)_i}, \ \forall i. \tag{4.10}$$

[7] In Appendix 4.B it is shown that, under Assumption 4.1, this system of linear inequalities is feasible.

For any i with $b_i > 0$, relation (4.10) simplifies into

$$\mu > \frac{\langle w_i \rangle}{(Az)_i}.$$

4.3.2 Robustness *vis-à-vis* uncertain parameters

The proposition below extends the results of Proposition 4.1 to the case where the parameters $\mathfrak{C} := (A, \{b_i\}_i, w)$ of the system (4.2) are not known, but only their component-wise bounds are available, *i.e.*,

$$A^+ \leq A \leq A^-, \quad b_i^+ \leq b_i \leq b_i^-, \quad w^- \leq w \leq w^+. \tag{4.11}$$

To streamline the presentation of the proposition, define the bounding sets $\mathfrak{C}^\pm := (A^\pm, \{b_i^\pm\}_i, w^\pm)$.

Proposition 4.3. Suppose that $\mathfrak{C}$ verifies Assumption 4.1, and (4.11) holds. Then, the following statements are true.

i If the case of claim S1 from Proposition 4.1 holds for $\mathfrak{C}^+$, this case also holds for both $\mathfrak{C}$ and $\mathfrak{C}^-$.

ii If the case S2 from Proposition 4.1 hold for $\mathfrak{C}^-$, this case also holds for both $\mathfrak{C}$ and $\mathfrak{C}^+$.

iii In the situation ii, the dominant equilibria $\bar{x}^-_{\mathtt{max}}$, $\bar{x}_{\mathtt{max}}$, $\bar{x}^+_{\mathtt{max}}$ related to $\mathfrak{C}^-, \mathfrak{C}, \mathfrak{C}^+$, respectively, are such that

$$\bar{x}^-_{\mathtt{max}} \leq \bar{x}_{\mathtt{max}} \leq \bar{x}^+_{\mathtt{max}}. \tag{4.12}$$

Moreover, $x^+_{\mathtt{max}} \to x^-_{\mathtt{max}}$ as $A^+ \to A^-, b_i^+ \to b_i^-, w^+ \to w^-$.

Proof. See Appendix 4.D at the end of the chapter. □□□

Proposition 4.3 can be used to estimate the distance from the initial state $x \in \mathcal{E}$ of the employed distinguished solution to the dominant equilibrium $\bar{x}_{\mathtt{max}}$. This can be done picking $\mathfrak{C}^-$ and noting that, due to (4.12) and II in Proposition 4.2, the distance of interest does not exceed $\|x - \bar{x}^-_{\mathtt{max}}\|$. Certainly, $\mathfrak{C}^-$'s with easily computable $\bar{x}^-_{\mathtt{max}}$ are of especial interest. An example is obtained via "zeroing" all off-diagonal elements of A in $\mathfrak{C}$ if for any i either $b_i < 0$ or $b_i > 0$ and $w_i \geq 2\sqrt{a_{ii} b_i}$. Then

$$x^-_{\mathtt{max}} = \mathrm{stack}\Big(\frac{w_i + \sqrt{w_i^2 - 4a_{ii}b_i}}{2a_{ii}}\Big).$$

Thanks to S2 in Proposition 4.1 and (4.12), $\bar{x}^-_{\mathtt{max}}$ can be used, instead of a vector from the set (4.7), as the initial state when seeking $\bar{x}_{\mathtt{max}}$ via integration of the ODE (4.3). An example of this situation, happens when $b_i > 0\ \forall i$. Then, in (4.11), take $A^+ := A, w^+ := w$, and $b_i^+ > 0$ arbitrarily close to 0, and moreover, finally let $b_i^+ \to 0+$. Then, by using Lemma 4.3, it can be shown that integration of the ODE can be started with $A^{-1}w$ provided that $A^{-1}w > 0$.

4.3.3 Answers to the queries Q1-Q6 in Section 4.2

Now, the previous discussion of this section is put into a nutshell by giving a synopsis of the answers to Q1-Q6.
Answer to Q1

- Equilibria exist if and only if neither distinguished solution of the ODE (4.3) approaches the boundary of the positive cone $\mathcal{K}_+^n$ for a finite time.
- To check this existence criterion, it suffices to examine the behavior of an arbitrary distinguished solution.
- To accomplish the latter, a solution $x \in \mathbb{R}^n$ for a certain convex or a less conservative linear programming problem should be found and then the ODE (4.3) should be integrated from this vector x.

Answer to Q2

- There exists a distinguished equilibrium, $\bar{x}_{\mathtt{max}}$, that satisfies $\bar{x}_{\mathtt{max}} \geq \bar{x}_{\mathrm{eq}}$, for any other system's equilibrium, $\bar{x}_{\mathrm{eq}}$.

Answer to Q3

- The equilibrium $\bar{x}_{\mathtt{max}}$ is attractive from above and "almost surely" is stable and locally asymptotically stable.

Answer to Q4

- This domain covers the set (4.7); the latter set contains any vector built as is discussed in Lemma 4.2.

Answer to Q5

- It suffices to invoke the solution of the ODE (4.3) from the answer to Q1 and to compute it until it converges.

Answer to Q6

- If in (4.2), all b_i's are of the same sign and Assumption 4.2 holds, there are no other stable equilibria.

4.4 Application to Some Canonical Power Systems

In this section, the results of Section 4.2 are applied to three different problems of power systems containing constant power loads. These comprise the standard voltage stability (in a static sense) of AC power systems with "light" active power load and the study of existence of equilibria of MT-HVDC networks and DC microgrids

4.4.1 Voltage stability (in a static sense) of AC power systems

The standard static analysis of voltage stability in AC power systems assumes the dynamics is in steady state, and concentrates its attention on the algebraic equations relating the active and reactive power, with the voltages and the phase angles—the well-known power flow equations. In [121] it was first suggested to investigate the sign of the real parts of the eigenvalues of the power flow Jacobian matrix as an indicator of voltage stability. This sensitivity analysis of the voltage magnitudes with respect to changes in the active and reactive power flows is the prevailing approach to analyze voltage stability in AC networks as explained in power systems textbooks, *i.e.*, [56, Chapter 14] and [119, Chapter 7]. In this subsection it is shown how the analysis framework developed in Section 4.2 can be applied to carry out this analysis, for the particular case of power systems with "light" active power load.

Consider a high-voltage AC power network with $n \geq 1$ PQ nodes. Denote by $V_i > 0$, δ_i and Q_i the voltage magnitude, phase angle and the reactive power load demand at node i, respectively. The analysis is restricted to scenarios in which the following standard "light" active power load (also called "decoupling") assumption is satisfied [56, Chapter 14.3.3], [99, Assumption 1].

Assumption 4.3. $\delta_i - \delta_j \approx 0$ for all $i, j \in \{1, \dots, n\}$.

With Assumption 4.3, the reactive power flow at node i is given by [56, 108, 99][8]

$$Q_{\text{ZIP},i} = V_i \sum_{j=1}^{n} |B_{ij}|(V_i - V_j),$$

where $B_{ij} < 0$ if nodes i and j are connected via a power line and $B_{ij} = 0$ otherwise. The reactive power demand $Q_{\text{ZIP},i}$ at the i-th node is described by a, so-called, ZIP model, namely

$$Q_{\text{ZIP},i} := \left(\mathcal{Y}_i V_i^2 + k_i V_i + Q_i\right).$$

The term ZIP load refers to a parallel connection of a constant susceptance $\mathcal{Y}_i \in \mathbb{R}$, a constant reactive current $k_i \in \mathbb{R}$, and a constant power $Q_i \in \mathbb{R}$ load. Then, the (algebraic) reactive power balance equation is obtained as

$$\left(\mathcal{Y}_i V_i^2 + k_i V_i + Q_i\right) = V_i \sum_{j=1}^{n} |B_{ij}|(V_i - V_j),\ i \in \{1, \dots, n\}, \tag{4.13}$$

which by defining $x := \text{stack}\,(V_i) \in \mathcal{K}_+^n$, $A \in \mathbb{R}^{n \times n}$ with

$$\begin{aligned} A_{ii} &= \sum_{j=1}^{n} |B_{ij}| - \mathcal{Y}_i,\ A_{ij} = -|B_{ij}|, \\ w &= \text{stack}(k_i),\ b_i = -Q_i, \end{aligned} \tag{4.14}$$

[8]The reader is referred here to Chapter 2 for a detailed derivation of the power flow equations and particularly to the developments leading to equation (2.22) which appears by the end said chapter.

can be rewritten as (4.2). If the reasonable assumption that $\mathcal{Y}_i < 0$ for at least one node is considered, then the matrix A satisfies Assumption 4.1.

Consider the following notion of voltage stability, called voltage regularity—also referred as static (or long-term) voltage stabilty—for the system (4.2) with the parameters (4.14), which relates the analysis of Section 4.2 to standard power system practice, see [56, Chapter 14], [119, Chapter 7] and the more recent work [108].

Definition 4.3 (cf. [65, 45])**.** A positive root $\bar{x}$ of the system (4.2) is voltage-regular if the Jacobian $\nabla f(x)\big|_{x=\bar{x}}$, with $f(x)$ given in (4.3) with the parameters (4.14), is Hurwitz.

The following remarks concerning the application of the results of Section 4.2 to this particular problem are in order.

R1 The coefficients $-b_i$ are the constant reactive powers extracted or injected into the network, being positive (capacitive) in the former case, and negative (inductive) in the latter. As indicated in Section 4.2, sharper results—*i.e.*, that $\bar{x}_{\texttt{max}}$ is the only stable equilibrium, and a simpler structure of the set $\mathcal{E}$ of initial conditions for the distinguished solutions—are available if the signs of the coefficients b_i are known. Hence, the proposed conditions have a direct interpretation in terms of reactive power demand.

R2 The solution $\bar{x}_{\texttt{max}}$ of the system (4.13) represents the physically admissible steady state with the highest values of voltage magnitudes at each node, which is the usually desired high-voltage operating point.

R3 Lemma 4.5 in the Appendix implies that the Jacobian of the dynamics (4.3) evaluated at any stable equilibrium point is Hurwitz. Hence, if case V of Proposition 4.2 applies then the dominant equilibrium is voltage-regular in the sense of Definition 4.3. Consequently, Proposition 4.2 provides a constructive procedure to evaluate the existence of a unique dominant and voltage-regular solution in power systems with constant power loads.

4.4.2 Multi-terminal HVDC transmission networks with constant power devices

An MT-HVDC network with n power-controlled nodes ($\mathcal{P}$-nodes) and s voltage-controlled nodes ($\mathcal{V}$-nodes), interconnected by m resistive-inductive (RL) transmission lines, can be modeled by [92]

$$\begin{aligned} \tau \dot{I}_t &= -I_t - h(V), \\ L\dot{I} &= -RI + \mathcal{B}_{\mathcal{P}}^{\top} V + \mathcal{B}_{\mathcal{V}}^{\top} V_{\mathcal{V}}, \\ C\dot{V} &= I_t - \mathcal{B}_{\mathcal{P}} I - GV, \end{aligned} \tag{4.15}$$

where $I_t \in \mathbb{R}^n$, $V \in \mathcal{K}_+^n$, $I \in \mathbb{R}^m$ and $V_{\mathcal{V}} \in \mathbb{R}^s$. The matrices R, L, G, C, and τ are diagonal, positive definite of appropriate sizes. The physical meaning of each state variable and of every matrix of parameters is given in Table 4.1. Furthermore, $\mathcal{B} = \text{stack}\,(\mathcal{B}_{\mathcal{V}}, \mathcal{B}_{\mathcal{P}}) \in \mathbb{R}^{(s+n)\times m}$ denotes the, appropriately split, node-edge incidence

Table 4.1: Nomenclature for the model (4.15).

	State variables
I_t	$\mathcal{P}$-nodes injected currents
V	$\mathcal{P}$-nodes voltages
I	Line currents
	Parameters
L	Line inductances
C	$\mathcal{P}$-nodes shunt capacitances
R	Line resistances
G	$\mathcal{P}$-nodes shunt conductances
τ	Converter time constants
$V_{\mathcal{V}}$	$\mathcal{V}$-nodes voltages

matrix of the network.[9] The open-loop current injection at the power terminals is described by

$$h(V) = \text{stack}\left(\frac{P_i}{V_i}\right),$$

where $P_i \in \mathbb{R}$ denotes the power setpoint.[10] See also [132] for a systematic model procedure of HVDC systems using the port-Hamiltonian framework.

By simple algebraic computations, it can be shown that (4.15) admits an equilibrium if and only if the algebraic equations

$$0_n = -h(\bar{V}) - \left(\mathcal{B}_{\mathcal{P}} R^{-1} \mathcal{B}_{\mathcal{P}}^{\top} + G\right) \bar{V} - \mathcal{B}_{\mathcal{P}} R^{-1} \mathcal{B}_{\mathcal{V}}^{\top} V_{\mathcal{V}}, \tag{4.16}$$

have real solutions for $\bar{V} \in \mathcal{K}_+^n$. Notice that (4.16) is equivalent to the right hand side of (4.3) if $x := \bar{V}$ and

$$A := \mathcal{B}_{\mathcal{P}} R^{-1} \mathcal{B}_{\mathcal{P}}^{\top} + G,\ b_i := P_i,\ w := -\mathcal{B}_{\mathcal{P}} R^{-1} \mathcal{B}_{\mathcal{V}}^{\top} V_{\mathcal{V}}.$$

Given that $\mathcal{B}_{\mathcal{P}}$ is an incidence matrix, R and G are diagonal positive definite matrices, then, the term $\mathcal{B}_{\mathcal{P}} R^{-1} \mathcal{B}_{\mathcal{P}}^{\top}$ is a Laplacian matrix and thus it is positive semidefinite. Consequently, $A = A^{\top}$ is positive definite and Assumption 4.1 is satisfied and the results of Section 4.2 can be used to analyze the existence of equilibria of the dynamical system (4.15). This, through the computation of the solutions of $\dot{x} = f(x)$, taking f as the right hand side of (4.16).

As in Remark R1 of the previous example, the coefficients $-b_i$ are the powers extracted or injected into the network, being negative in the former case and positive in the latter; the observation of Remark R2 is also applicable in this example.

4.4.3 DC microgrids with constant power loads

A model of a DC microgrid, with $n \geq 1$ converter-based distributed generation units, interconnected by $m \geq 1$ resistive-inductive (RL) transmission lines, can be

[9] Recall the preliminaries on graph theory and on power systems reported in Chapter 2.

[10] The first equation in (4.15) represents the simplified converter dynamics, see [92, Section II, equation (18)] and [92, Figure 4]. The converter usually has a PI current control, see the equations (27) and (28) of [92]. For simplicity, the analysis of this chapter is restricted to to study equilibria of the network without the PI. Nonetheless, the presented methodology applies also to the closed-loop scenario.

Table 4.2: Nomenclature for the model (4.17).

	State variables
I_t	Generated currents
V	Load and bus voltages
I	Line currents
	Parameters
L_t	Filter inductances
L	Line inductances
C	Shunt capacitances
R_t	Filter resistances
R	Line resistances
	External variables
u	Control input (converter voltage)
I_{ZIP}	$\mathcal{Y}_i$: Constant impedance k_i: Constant current P_i: Constant power

written as [26]

$$\begin{aligned} L_t\dot{I}_t &= -R_tI_t - V + u, \\ C_t\dot{V} &= I_t + \mathcal{B}I - I_{\text{ZIP}}(V), \\ L\dot{I} &= -\mathcal{B}^\top V - RI, \end{aligned} \tag{4.17}$$

where $I_t \in \mathbb{R}^n$, $V \in \mathcal{K}^n_+$, $u \in \mathcal{K}^n_+$ and $I \in \mathbb{R}^m$ as well as R_t, R, L_t, L and C_t are diagonal, positive definite matrices of appropriate size; the physical meaning of each term appears in Table 4.2. Denote by $\mathcal{B} \in \mathbb{R}^{n\times m}$, the node-edge incidence matrix of the network. The load demand is described by a ZIP model, *i.e.,*

$$I_{\text{ZIP}}(V) = \mathcal{Y}V + k + \text{stack}\left(\tfrac{P_i}{V_i}\right),$$

where $\mathcal{Y} \in \mathbb{R}^{n\times n}$ is a diagonal positive semi-definite matrix, $k \in \mathbb{R}^n$ is a constant vector, and $P_i \in \mathbb{R}$.

Some simple calculations show that, for a given $u = \bar{u}$ constant, the dynamical system (4.17) admits a real steady state if and only if, the algebraic equations

$$0_n = R_t^{-1}\left(\bar{u} - \bar{V}\right) - \mathcal{B}R^{-1}\mathcal{B}^\top\bar{V} - I_{\text{ZIP}}(\bar{V}), \tag{4.18}$$

have real solutions for $\bar{V} \in \mathcal{K}^n_+$. Defining $x := \bar{V}$ and

$$A := R_t^{-1} + \mathcal{Y} + \mathcal{B}R^{-1}\mathcal{B}^\top,\ b_i := P_i,\ w := R_t^{-1}\bar{u} - k.$$

the system (4.18) can be written in the form (4.2). Similarly as for the MT-HVDC model, it can be shown that A is a positive definite matrix and, hence, satisfies the conditions in Assumption 4.1. Therefore, the results of Section 4.2 can be applied to study the solutions of the steady state equation (4.18).

Once again, Remarks R1 and R2 of Subsection 4.4.1 are also applicable here.

4.5 Numerical simulations

In this section, some numerical simulations that illustrate the results reported in Section 4.2 are presented.

4.5.1 An RLC circuit with constant power loads

The electrical network shown in Fig. 4.2 has been used in [9] as a benchmark example to study the existence of its equilibria. In steady state, this network is described by the system of quadratic equations

$$\begin{aligned} z &= -Yv + u, \\ v_i z_i &= P_i > 0,\ i = 1, 2, \end{aligned} \tag{4.19}$$

where z_i is the current through the inductor L_i, v_i is the voltage across the capacitor C_i, P_i is the power of the $i-$th CPL, and

$$Y = \begin{bmatrix} \frac{1}{r_2} + \frac{1}{r_1} & -\frac{1}{r_2} \\ -\frac{1}{r_2} & \frac{1}{r_2} \end{bmatrix},\ u = \begin{bmatrix} \frac{E}{r_1} \\ 0 \end{bmatrix}.$$

Define

$$x := \begin{bmatrix} v_1 \\ v_2 \end{bmatrix},\ A := Y,\ b_i = P_i,\ w := u,$$

then, the algebraic system (4.19) can be equivalently written in the form of (4.2), and hence its solvability can be studied through the computation of distinguished solutions, $x(t, x_0)$, of the ODE (4.3).

To analyze the existence of steady states using Proposition 4.2, first it is necessary to identify the set $\mathcal{E}$,[11] which for this example is given by

$$\mathcal{E} = \left\{ x \in \mathcal{K}_+^n \ : \quad \left(\frac{1}{r_2} + \frac{1}{r_1}\right) x_1 - \frac{1}{r_2} x_2 > \frac{E}{r_1},\ -\frac{1}{r_2} x_1 + \frac{1}{r_2} x_2 > 0 \right\},$$

or in a simpler form by

$$\mathcal{E} = \left\{ x \in \mathcal{K}_+^n \ : \quad E < x_1 < x_2 < \frac{(r_1 + r_2)}{r_1} x_1 - \frac{r_2 E}{r_1} \right\}.$$

This set is illustrated in Fig. 4.3a for the parameters' values of Table 4.3; a distinguished solution of the ODE $\dot{x} = f(x)$ is also plotted.

The method is tested in three steps: first, an initial condition

$$x_0 = (25.01, 25.77),$$

which belongs to the set $\mathcal{E}$ is taken; then, two different values for CPLs' powers are fixed, which are codified by the vector b; and finally, for each of these values of b, the associated distinguished solution is computed and its behavior, observed.

Fix $b = (500, 450)$. The plot of the associated distinguished solution is shown in Fig. 4.3c; notice that none of its components is approaching to zero having then the case III.ii of Proposition 4.2: the network admits equilibria. Furthermore, $x(t, x_0)$ asymptotically converges to $\bar{x}_{\texttt{max}} = (22.24, 20.95)$. The latter equilibrium is the only ODE's stable equilibrium, fact which is established from Proposition 4.1 by observing that $b_i > 0$ for all i.

The described procedure is repeated now fixing $b = (3000, 1000)$. The plot of the associated distinguished solution is shown in Fig. 4.3d; its second component,

[11] See equation (4.7).

Table 4.3: Simulation Parameters of the multi-port network of Fig. 4.2.

E (V)	r_1 (Ω)	L_1(µH)	C_1(mF)
24	0.04	78	2
	r_2 (Ω)	L_2(µH)	C_2(mF)
	0.06	98	1

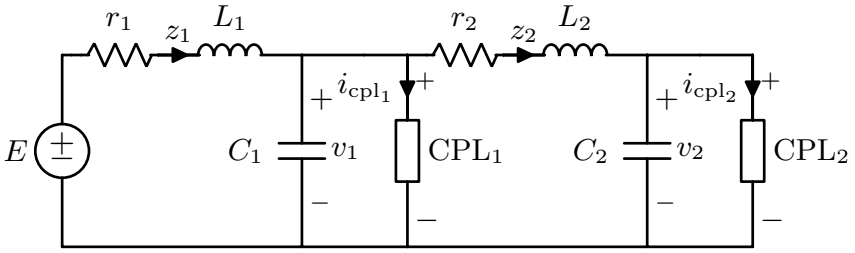

Figure 4.2: DC Linear RLC circuit with two CPLS

denoted by $x_2(t)$, converges to zero in finite time, hence, falling in the scenario III.i of Proposition 4.2: the network has no equilibria.

A graphical comparison that clearly illustrates the radically different behavior between the former and the latter distinguished solutions is shown in Fig. 4.3e.

Finally, the consistency of the method with respect to the *analytical* necessary and sufficient condition for existence of equilibria presented in [9, Proposition 1 and 3] is underscored: the shadowed region shown in Fig. 4.3b, which represents the values of b for which equilibria exist, can be obtained using this condition.

4.5.2 An HVDC transmission system

This subsection carries out a numerical evaluation of the existence (and approximation) of equilibrium points for the particular HVDC system presented as an example in [92, Fig. 5]. The network, whose associated graph is shown in Fig. 4.4, consists in four nodes $\mathcal{N} = \{\mathcal{V}_1, \mathcal{P}_1, \mathcal{P}_2, \mathcal{P}_3\}$, where $\mathcal{V}_1$ is a voltage controlled node, with voltage $V_{\mathcal{V}}^{(1)} = E$, and $\mathcal{P}_1$, $\mathcal{P}_2$ and $\mathcal{P}_3$ are power-controlled nodes, with power P_1, P_2, and P_3, respectively. The network edges, representing the RL transmission lines, are $\mathbf{c} = \{c_1, c_2, ..., c_5\}$, with each c_i having an associated pair of parameters (r_i, L_i). An incidence matrix $\mathcal{B} = \text{stack}\,(\mathcal{B}_{\mathcal{V}}, \mathcal{B}_{\mathcal{P}})$ is defined, where

$$\mathcal{B}_{\mathcal{V}} = \begin{bmatrix} -1 & -1 & -1 & 0 & 0 \end{bmatrix},$$
$$\mathcal{B}_{\mathcal{P}} = \begin{bmatrix} 0 & 0 & 1 & 0 & 1 \\ 1 & 0 & 0 & -1 & 0 \\ 0 & 1 & 0 & 1 & -1 \end{bmatrix}.$$

Table 4.4: Numerical parameters associated with the edges for the network in Fig. 4.4.

Transmission line	e_1	e_2	e_3	e_4	e_5
r_i (Ω)	0.9576	1.4365	1.9153	1.9153	0.9576

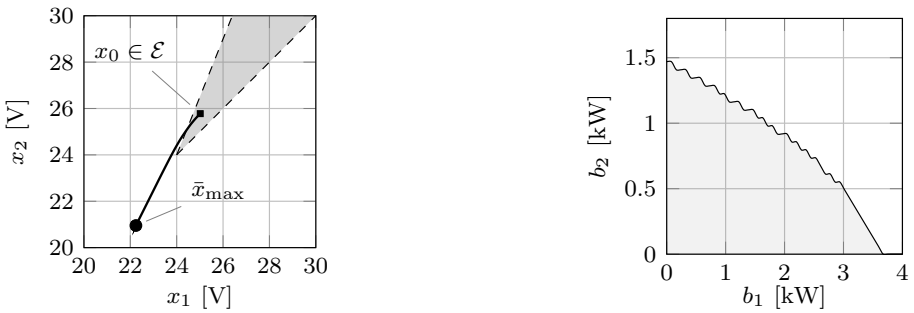

(a)

(b)

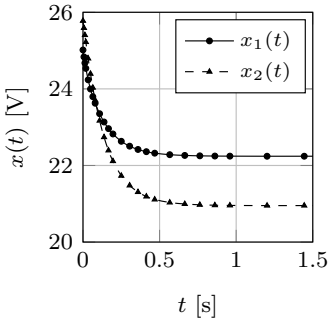

(c)

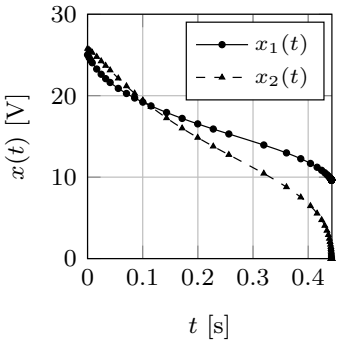

(d)

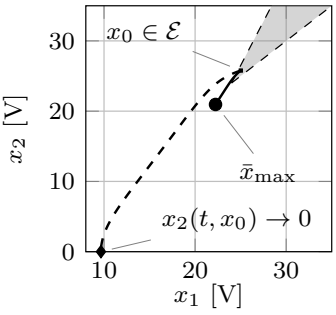

(e)

Figure 4.3: Simulation results for the RLC circuit of Fig. 4.2: (a) plot of a portion of the set $\mathcal{E}$ and a distinguished solution converging to $\bar{x}_{\texttt{max}}$. (b) Set of positive values (shadowed region) for (b_1, b_2) for which the network admits an equilibrium. (c) Distinguished solution $x(t, x_0)$, with $b = (500, 450)$, converging to the equilibrium point $\bar{x}_{\texttt{max}}$. (d) Distinguished solution $x(t, x_0)$, taking $b = (3000, 1000)$, with one of its components converging to zero in finite time: the system has no equilibrium points. (e) Phase-space plot of the distinguished solution $x(t, x_0)$ for two different values of b: one feasible and another one infeasible. Convergence to $\bar{x}_{\texttt{max}}$ is observed in the former (solid curve), and convergence of the second component to zero is visualized in the latter (dashed curve).

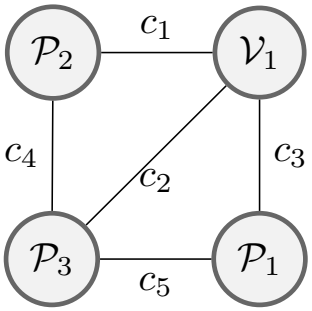

Figure 4.4: Associated graph for the HVDC network studied in [92, Section V].

Then, the elements of the algebraic system (4.16), which is codified by $f(x) = 0$, with $x = \bar{V}$, are given by

$$A = \begin{bmatrix} \gamma_1 + \frac{1}{r_3} + \frac{1}{r_5} & 0 & -\frac{1}{r_5} \\ 0 & \gamma_2 + \frac{1}{r_1} + \frac{1}{r_4} & -\frac{1}{r_4} \\ -\frac{1}{r_5} & -\frac{1}{r_4} & \gamma_3 + \frac{1}{r_2} + \frac{1}{r_4} + \frac{1}{r_5} \end{bmatrix},$$

$$b = \text{stack}(P_i), \;\; w = \text{stack}\left(\frac{E}{r_3}, \frac{E}{r_1}, \frac{E}{r_2}\right),$$

where r_i and γ_i are the diagonal elements of the matrices R and G, respectively.

Taking the numerical values shown in Tables 4.5 and 4.4, and through Lemma 4.2, an initial condition $x_0 \in \mathcal{E}$ is computed as

$$x_0 = 10^5 \cdot \text{stack}(6.66, 4.66, 5.99).$$

The particular solution $x(t, x_0)$ of $\dot{x} = f(x)$ is shown in Fig. 4.5. Clearly, none of its components converges to zero. Then, by Proposition 4.2, it is established that the limit of this solution is the dominant equilibrium point, $\bar{x}_{\texttt{max}}$, of the system; its numerical value is given by

$$\bar{x}_{\texttt{max}} = 10^5 \cdot \text{stack}(4.0054, 3.9991, 4.0043).$$

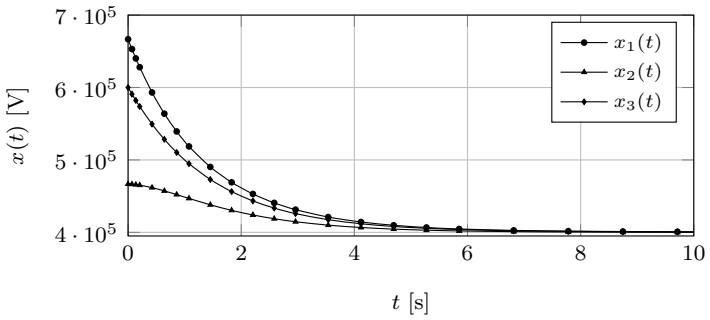

Figure 4.5: Distinguished solution $x(t, x_0)$ converging to an equilibrium point. Once again, from Proposition 4.2 it is established that $x(t, x_0) \to \bar{x}_{\texttt{max}}$ as $t \to \infty$.

Table 4.5: Numerical parameters associated with the nodes for the network in Fig. 4.4.

Power converter	$\mathcal{V}_1$	$\mathcal{P}_1$	$\mathcal{P}_2$	$\mathcal{P}_3$
$V_{\mathcal{V}}^{(i)}$ (kV)	400	-	-	-
P_i (MW)	-	-160	140	-180
γ_i (µS)	-	0.02290	0.02290	0.3435

4.6 Summary

A systematic methodology to analyze the behavior the ODE (4.3) is presented in the chapter. Exploiting the fact that this ODE describes a monotone dynamical system, all possible scenarios for existence of its equilibria and, under minor extra assumptions, for their stability and uniqueness, have been described. It has been proven that if equilibria exist, then, there is a distinguished one, denoted by $\bar{x}_{\texttt{max}}$, which dominates—component-wise—all the other ones and attracts all the ODE trajectories starting from a well-defined domain. It has been further provided an algorithm to establish whether solutions of the ODE will converge to $\bar{x}_{\texttt{max}}$ or not and shown that the procedure is applicable even in the case when the system parameters are only known to live in a polytope.

These results have been applied to study the voltage regularity of "lightly" loaded AC power systems and to give conditions for existence of equilibria in DC microgrids and MT-HVDC networks—all of them containing CPLs.

Finally, it has been demonstrated though supporting numerical experiments on two benchmark power system models that the methodology performs very satisfactorily for realistic power system parameterizations.

Technical Appendices of the Chapter

4.A Proofs of Remark 4.1 and Lemma 4.1

Proof of Remark 4.1: Suppose that system (4.2) meets Assumption 4.1 except for the claim $b_i \neq 0 \ \forall i$. It is shown next that this system can be reduced to an equivalent one that has the same structure of (4.2), of a lower order, and that satisfies Assumption 4.1 in full, including the claim $b_i \neq 0 \ \forall i$.

To this end, it suffices to eliminate every variable x_k with $b_k = 0$ by using (4.1): $x_k = a_{kk}^{-1}[w_k - \sum_{j\neq k} a_{kj}x_j]$. This shapes any remaining equation (4.1) (with $i \neq k$) into

$$\sum_{j\neq k} \big[a_{ij} - a_{ik}a_{kj}/a_{kk}\big]x_j + b_i/x_i = w_i - w_k a_{ik}/a_{kk} \quad i \neq k.$$

In the left-hand side, the matrix A_r of the linear part is symmetric and its off-diagonal elements $a_{ij} - a_{ik}a_{kj}/a_{kk} \leq 0 \ \forall i \neq j, i, j \neq k$ since $a_{kk} > 0$ for the positive definite matrix A. Meanwhile, a symmetric matrix $\mathcal{A}$ is positive definite if and only if $-\mathcal{A}$ is Hurwitz. By [18, Theorem 9.5], this is also equivalent to the fact that the equation $\mathcal{A}z = b$ has a unique root $z \geq 0$ whenever $b \geq 0$. The equation $A_r z = b$ is equivalent to the system $\sum_{j=1}^{n} a_{ij}x_j = b_i$ if $i \neq k$ and 0 otherwise. Since this system

has a unique nonnegative solution x, and dropping x_k in x results in the solution z, it is seen that A_r is positive definite.

Consecutively eliminating all x_i with $b_i = 0$, an equivalent system (4.2), that meets Assumption 4.1 in full, is obtained. □□□

Proof of Lemma 4.1: The set $\Pi := \left\{z \in \mathbb{R}^n : \det\left[A - \operatorname{diag}(z_i)\right] = 0\right\}$ is closed and for any i and given z_j's with $j \neq i$, its section

$$\{z_i \in \mathbb{R} : \operatorname{stack}(z_1, \ldots, z_n) \in \Pi\}$$

has no more than n elements. So the measure of Π is zero by the Fubini theorem. The function $x \in \mathcal{K}^n_+ \mapsto g(x) := \operatorname{stack}\left(b_i x_i^{-2}\right)$ diffeomorphically maps $\mathcal{K}^n_+$ onto an open subset of $\mathbb{R}^n$. Hence the inverse image $\Pi_\downarrow := g^{-1}(\Pi)$ is closed, has the zero measure and, due to these two properties, is nowhere dense.

Let C be the set of all critical points of the semi-algebraic map [25] $x \in \mathcal{K}^n_+ \mapsto h(x) := Ax + \operatorname{stack}\left(b_i x_i^{-2}\right) \in \mathbb{R}^n$, *i.e.*, points x such that the Jacobian matrix $\nabla h(x)$ is singular. By the extended Sard theorem [58], the set of critical values $h(C)$ has the zero measure and is nowhere dense. Meanwhile, the restriction $h_{\mathcal{K}^n_+ \setminus C}$ is a local diffeomorphism and so the image $h(\Pi_\downarrow \setminus C)$ is nowhere dense and has the zero Lebesgue measure. It remains to note that the set of w's for which Assumption 4.2 does not hold lies in $h(\Pi_\downarrow \setminus C) \cup h(C)$. □□□

4.B Proof of Lemma 4.2

Consider first the following lemma and its proof.

Lemma 4.3. The following system of inequalities is feasible

$$Az > 0, \qquad z > 0. \tag{4.20}$$

Proof. Suppose that the system (4.20) is infeasible. Then two open convex cones $A\mathcal{K}^n_+$ and $\mathcal{K}^n_+$ are disjoint and so can be separated by a hyperplane: there exists

$$\tau \in \mathbb{R}^n, \qquad \tau \neq 0 \tag{4.21}$$

such that

$$\tau^\top x \geq 0 \quad \forall x \in \mathcal{K}^n_+, \qquad \tau^\top x \leq 0 \quad \forall x \in A\mathcal{K}^n_+.$$

By continuity argument, these inequalities extend on the closures of the concerned sets:

$$\begin{aligned} &\tau^\top x \geq 0 \quad \forall x \in \overline{\mathcal{K}}^n_+ = \{x : x_i \geq 0\}, \\ &\tau^\top x \leq 0 \quad \forall x \in \overline{A\mathcal{K}^n_+} \supset A\overline{\mathcal{K}}^n_+. \end{aligned}$$

Here the first relation implies that $\tau \in \overline{\mathcal{K}}^n_+ \Rightarrow A\tau \in A\overline{\mathcal{K}}^n_+$ and so $\tau^\top A\tau \leq 0$ by the second one. Since A is positive definite by Assumption 4.1, the last inequality yields that $\tau = 0$, in violation of the second relation from (4.21). This contradiction completes the proof. □□□

Based on any solution z of (4.20), a solution of (4.7) can be built in the form $x := \mu z$ by picking $\mu > 0$ so that for all i,

$$\mu(Az)_i > \langle w_i\rangle + \frac{\langle -b_i\rangle}{\mu z_i} \Leftrightarrow \mu^2(Az)_i - \mu\langle w_i\rangle - \frac{\langle -b_i\rangle}{z_i} > 0$$
$$\Leftrightarrow \mu > \frac{\langle w_i\rangle + \sqrt{\langle w_i\rangle^2 + 4(Az)_i\frac{\langle -b_i\rangle}{z_i}}}{2(Az)_i}.$$

Since such a choice of μ is feasible, the proof of Lemma 4.2 is hence completed.

4.C Claims underlying Propositions 4.1 and 4.2

This section, considering a C^1-map $g : \mathcal{K}^n_+ \to \mathbb{R}^n$, provides a general study of the ODE

$$\dot{x} = g(x), \qquad x \in \mathcal{K}^n_+, \tag{4.22}$$

under the following.

Assumption 4.4. For any $x \in \mathcal{K}^n_+$, the off-diagonal elements of the Jacobian matrix $\nabla g(x)$ are nonnegative.

Assumption 4.5. For any $x \in \mathcal{K}^n_+$, the Jacobian matrix $\nabla g(x)$ is symmetric.

For the convenience of the reader, some facts that are instrumental in the presented study are recalled. The first group of them reflects that the system (4.22) is *monotone*.[12]

Proposition 4.4. Let Assumption 4.4 hold and let the order $\succ$ in $\mathbb{R}^n$ be either $\geq$ or $>$. For any solutions $x_1(t), x_2(t), x(t)$ of (4.22) defined on $[0,\tau], \tau > 0$, the following relations hold

$$x_2(0) \succ x_1(0) \Rightarrow x_2(t) \succ x_1(t)\ \forall t \in [0,\tau], \tag{4.23}$$

$$\begin{array}{l} \dot{x}(0) \prec 0 \Rightarrow \dot{x}(t) \prec 0\ \forall t \in [0,\tau], \\ \dot{x}(0) \succ 0 \Rightarrow \dot{x}(t) \succ 0\ \forall t \in [0,\tau]; \end{array} \tag{4.24}$$

$$(x_+ > 0\ \wedge\ g(x_+) > 0) \Rightarrow \quad \text{the domain } \Upsilon_+ := \{x : x \succ x_+\} \text{ is positively invariant.} \tag{4.25}$$

Proof. Relation (4.23) is given by [114, Prop. 1.1 and Rem. 1.1, Ch. 3], whereas (4.24) is due to [114, Prop. 2.1, Ch. 3]. To prove (4.25), consider the maximal solution $x_\dagger(t), t \in [0,\theta)$ of (4.22) starting from $x_\dagger(0) = x_+$. Since $\dot{x}_\dagger(0) = g(x_+)>0$, (4.24) guarantees that $x_\dagger(\cdot)$ constantly increases $\dot{x}_\dagger(t)>0\ \forall t \in [0,\theta)$ and so $x_\dagger(t)>x_+\ \forall t \in (0,\theta)$. Now let a solution $x(t), t \in [0,\tau], \tau \in (0,\infty)$ start in Υ_+. Then $x(0) \succ x_\dagger(0)$ and by (4.23), $x(t) \succ x_\dagger(t)>x_+$ if $t > 0$. So $x(t) \in \Upsilon_+$ for any $t \in [0,\tau] \cap [0,\theta)$. It remains to show that $\tau < \theta$ if $\theta < \infty$.

Suppose to the contrary that $\tau \geq \theta$. Letting $t \to \theta-$, it is seen that $\|x_\dagger(t)\| \to \infty$ by [43, Theorem 3.1, Ch. II] since $x_\dagger(t) \succ x_+ > 0$. So $x(t) \succ x_\dagger(t) \Rightarrow \|x(t)\| \to \infty$. However, $\|x(t)\| \to \|x(\tau)\| < \infty$. This contradiction completes the proof. □□□

[12] See [114] for a definition.

Let $x(t,a), t \in [0, \tau_a)$ stand for the maximal solution of (4.22) that starts at $t = 0$ with $a > 0$. The distance $\inf_{x' \in A} \|x - x'\|$ from point $x \in \mathbb{R}^n$ to a set $A \subset \mathbb{R}^n$ is denoted by $\mathbf{dist}(x, A)$.

Corollary 4.1. Whenever $0 < a_1 \leq a \leq a_2$, it follows that $\tau_a \geq \min\{\tau_{a_1}, \tau_{a_2}\}$.

The following lemma is a trivial corollary of [18, Theorem 9.5].[13]

Lemma 4.4. A nonsingular matrix $A = A^\top$ with nonnegative off-diagonal elements is Hurwitz if

$$Ah > 0 \Rightarrow h \leq 0. \tag{4.26}$$

Lemma 4.5. Let Assumptions 4.4 and 4.5 hold. Suppose that a solution $x(t), t \in [0, \infty)$ of (4.22) decays $\dot{x}(t) < 0 \ \forall t$ and converges to $\bar{x} > 0$ as $t \to \infty$. Then $\bar{x}$ is an equilibrium of the ODE (4.22). If this equilibrium is hyperbolic, it is locally asymptotically stable.

Proof. The first claim is given by [114, Prop. 2.1, Ch. 3]. By Lemma 4.4, it suffices to show that $A := \nabla g(\bar{x})$ meets (4.26) to prove the second claim. Suppose to the contrary that $Ah > 0$ and $h_i > 0$ for some i and $h \in \mathbb{R}^n$. For $x^0_\varepsilon := \bar{x} + \varepsilon h$ and small enough $\varepsilon > 0$, it follows that $g(x^0_\varepsilon) = g(\bar{x}) + \varepsilon Ah + o(\varepsilon) = \varepsilon Ah + o(\varepsilon) > 0, x^0_\varepsilon > 0$, $x^0_{\varepsilon,i} > \bar{x}_i$, and $x(0) \in \Upsilon_+ = \{x : x > x^0_\varepsilon\}$. Since the set Υ_+ is positively invariant by (4.25), $x(t) \in \Upsilon_+ \Rightarrow x_i(t) > x_{\varepsilon,i} > \bar{x}_i$, in violation of $x(t) \to \bar{x}$ as $t \to \infty$. This contradiction completes the proof. □□□

For any $x' \leq x'' \in \mathbb{R}^n$, it is denoted by $\uparrow x', x'' \uparrow := \{x \in \mathbb{R}^n : x' \leq x \leq x''\}$.

Lemma 4.6. Suppose that Assumption 4.4 holds and $\bar{x} > 0$ is a locally asymptotically stable equilibrium. Its domain of attraction $\mathcal{A}(\bar{x}) \subset \mathcal{K}^n_+$ is open and

$$a', a'' \in \mathcal{A}(\bar{x}) \wedge a' \leq a'' \Rightarrow \uparrow a', a'' \uparrow \subset \mathcal{A}(\bar{x}). \tag{4.27}$$

Proof. Let $B(r, x)$ stand for the open ball with a radius of $r > 0$ centered at x. For any $a \in \mathcal{A}(\bar{x})$, it follows that $\tau_a = \infty$ and $x(t,a) \to \bar{x}$ as $t \to \infty$, whereas $B(2\varepsilon, \bar{x}) \subset \mathcal{A}(\bar{x})$ for a sufficiently small $\varepsilon > 0$ since $\bar{x}$ is locally asymptotically stable. Clearly, there is $\theta > 0$ such that $x(\theta, a) \in B(\varepsilon, \bar{x})$. By [43, Theorem 2.1, Ch. V], there exists $\delta > 0$ such that whenever $\|a^\dagger - a\| < \delta$, the solution $x(\cdot, a^\dagger)$ is defined at least on $[0, \theta]$ and $\|x(\theta, a^\dagger) - x(\theta, a)\| < \varepsilon$. It follows that $x(\theta, a^\dagger) \in B(2\varepsilon, \bar{x})$ and so $x(\cdot, a^\dagger)$ is in fact defined on $[0, \infty)$ and converges to $\bar{x}$ as $t \to \infty$. Thus, it is seen that $\|a^\dagger - a\| < \delta \Rightarrow a^\dagger \in \mathcal{A}(\bar{x})$, *i.e.*, the set $\mathcal{A}(\bar{x})$ is open.

Let $a \in \uparrow a', a'' \uparrow$. By Corollary 4.1 and (4.23), $\tau_a = \infty$ and $x(t, a') \leq x(t, a) \leq x(t, a'') \ \forall t \geq 0$. Letting $t \to \infty$ shows that $x(t, a) \to \bar{x}$ and so $a \in \mathcal{A}(\bar{x})$. □□□

Lemma 4.7. Let $\overline{x}_- \leq \overline{x}_+$ and let $D \subset \Xi := \uparrow \overline{x}_-, \overline{x}_+ \uparrow$ be an open (in Ξ) set such that

i) $\uparrow x', x'' \uparrow \subset D \ \forall x', x'' \in D$.

[13] An anonymous reviewer is acknowledged for indicating this.

ii) either $\overline{x}_- \in D$ or $\overline{x}_+ \in D$.

iii) $D \neq \Xi$.

Then there exists a continuous map $M : \Xi \to \Xi$ such that $M[\Xi] \subset \Xi_- := \Xi \setminus D$ and $M[x] = x \quad \forall x \in \Xi_-$.[14]

Proof. Let $\overline{x}_+ \in D$ for the definiteness; then $\overline{x}_- \notin D$ by i) and iii). It can be assumed that $0 = \overline{x}_- < \overline{x}_+$. Denote by $\chi_x(\theta) := \max\{x - \theta\zeta; 0\}$, where $\zeta := \mathrm{stack}(1, \dots, 1)$ and the max is meant component-wise. Then, $\Theta(x) := \big\{\theta \geq 0 : \chi_x(\theta) \in D\big\} = [0, \tau(x)), \quad x \in D$, where $0 < \tau(x) < \infty$. For $x \notin D$, put $\tau(x) := 0$. It is shown first that the function $\tau(\cdot)$ is continuous on Ξ. To this end, it suffices to prove that $\tau(\bar{x}) = \tau_*$ whenever

$$\bar{x} = \lim_{k\to\infty} x^k, \quad x^k \in \Xi, \quad \text{and} \quad \tau_* = \lim_{k\to\infty} \tau(x^k).$$

Passing to a subsequence ensures that either $x^k \notin D \ \forall k$ or $x^k \in D \ \forall k$. In the first case, $\bar{x} \notin D$ since D is open. Then $\tau(\bar{x}) = 0 = \tau(x^k) = \tau_*$. Let $x^k \in D \ \forall k$. Since $\chi_{x^k}[\tau(x^k)] \notin D$ and D is open, letting $k \to \infty$ yields $\chi_{\bar{x}}[\tau_*] \notin D \Rightarrow \tau(\bar{x}) \leq \tau_*$. So the claim holds if $\tau_* = 0$. If $\tau_* > 0$, pick $0 < \theta < \tau_*$. Then $\theta < \tau(x^k)$ for $k \approx \infty$, *i.e.*, $\chi_{x^k}(\theta) \in D$. Let x_i^ν be the i-th component of $x^\nu \in \mathbb{R}^p$. Then

$$\tau_k' := \max\big\{\tau \geq 0 : \chi_{\bar{x}}(\tau) \geq \chi_{x^k}(\theta)\big\} = \max_{i:x_i^k \geq \theta} \big[\bar{x}_i - x_i^k + \theta\big].$$

Here the second max is over a nonempty set since $\chi_{x^k}(\theta) \in D \not\ni 0$. Thus $\tau_k' \to \theta$ as $k \to \infty$. By i), $\chi_{\bar{x}}(\tau_k') \in D$ and so $\tau(\bar{x}) \geq \tau_k' \xRightarrow{k\to\infty} \tau(\bar{x}) \geq \theta \ \forall \theta < \tau_* \Rightarrow \tau(\bar{x}) \geq \tau_* \Rightarrow \tau(\bar{x}) = \tau_*$. Thus the function $\tau(\cdot)$ is continuous indeed. The needed map M is given by $M(x) := \chi_x[\tau(x)]$. □□□

Lemma 4.8. Let Assumption 4.4 hold and $0 < \overline{x}_- \leq \overline{x}_+, \overline{x}_- \neq \overline{x}_+$ be two locally asymptotically stable equilibria. Then there exists a third equilibrium $\bar{x}$ in between them $\overline{x}_- \leq \bar{x} \leq \overline{x}_+, \bar{x} \neq \overline{x}_-, \overline{x}_+$.

Proof. Denote by $\Xi := [\overline{x}_-, \overline{x}_+]$, like in Lemma 4.7. By Lemma 4.6, the set $D_\pm := \mathcal{A}(\overline{x}_\pm) \cap \Xi$ meets the assumptions of Lemma 4.7, which associates $D_\pm$ with a map $M_\pm$. Since the sets $D_\pm$ are open and disjoint, they do not cover the connected set Ξ. So the set $\Xi_\blacklozenge := \Xi \setminus (D_- \cup D_+)$ of all fixed points of the map $M = M_- \circ M_+$ is non-empty and compact. For all $a \in \Xi$, the solution $x(\cdot, a)$ is defined on $[0, \infty)$ by Corollary 4.1 and $x(t, a) \in \Xi$ by (4.23). So the flow $\{\Phi_t(a) := x(t, a)\}_{t\geq 0}$ is well defined on Ξ, acts from Ξ into Ξ, and is continuous by [43, Theorem 2.1, Ch. V]. The sets $D_\pm$ are positively and negatively invariant with respect to it:

$$\begin{aligned} a \in & D_\pm \Rightarrow \Phi_t(a) \in D_\pm \ \forall t \geq 0, \\ a \in & \Xi \wedge \big[\exists t \geq 0 : \Phi_t(a) \in D_\pm\big] \Rightarrow a \in D_\pm. \end{aligned}$$

It follows that $\Xi_\blacklozenge$ is positively invariant with respect to this flow. By the Brouwer fixed point theorem, the continuous map $\Phi_t \circ M : \Xi \to \Xi_\blacklozenge \subset \Xi$ has a fixed point

[14] In brief, this lemma says that Ξ_- is a retract of the convex set Ξ.

$a_t = \Phi_t \circ M(a_t) \in \Xi$. Since $M(a_t) \in \Xi_\blacklozenge$ and $\Phi_t(\Xi_\blacklozenge) \subset \Xi_\blacklozenge$, it is seen that $a_t \in \Xi_\blacklozenge$ and so $M(a_t) = a_t$ and $a_t = \Phi_t(a_t)$.

Since $\Xi_\blacklozenge$ is compact, there exists a sequence $\{t_k > 0\}_{k=1}^{\infty}$ such that $t_k \to 0$ and $a_{t_k} \to \bar{x}$ as $k \to \infty$ for some point $\bar{x} \in \Xi_\blacklozenge$. Since $\overline{x}_\pm \notin \Xi_\blacklozenge$, it follows that $\bar{x} \neq \overline{x}_\pm$; meanwhile $\bar{x} \in \Xi_\blacklozenge \subset \Xi \Rightarrow \overline{x}_- \leq \bar{x} \leq \overline{x}_+$. Furthermore,

$$0 = \frac{\Phi_{t_k}(a_{t_k}) - a_{t_k}}{t_k} = t_k^{-1} \int_0^{t_k} g[x(t, a_{t_k})]\, dt \xrightarrow{k\to\infty} g(\bar{x}).$$

Thus, it is seen that $g(\bar{x}) = 0$, *i.e.*, $\bar{x}$ is an equilibrium. □□□

4.D Proofs of Propositions 4.1, 4.2, and 4.3

The system (4.3) under Assumption 4.1 is studied next.

Lemma 4.9. Suppose that y belongs to the set (4.7). There exists $\theta \in (0,1)$ such that the domain $\Xi_-(\theta) := \{x : 0 < x \leq \theta y\}$ is globally absorbing, *i.e.*, the following statements hold:

i This domain is positively invariant: if a solution starts in $\Xi_-(\theta)$, it does not leave $\Xi_-(\theta)$;

ii Any solution defined on $[0, \infty)$ eventually enters $\Xi_-(\theta)$ and then never leaves this set.

Proof. Thanks to (4.7), there exists $\delta > 0$ such that

$$Ay > \operatorname{stack}\left(\langle w_i\rangle + \frac{\langle -b_i\rangle}{y_i} + 3\delta\right). \tag{4.28}$$

The value $\theta \in (0,1)$ is picked so close to 1 that for any i, the following holds.

$$[\theta - 1]\langle w_i\rangle + \delta\theta \geq 0, \quad [\theta - \theta^{-1}]\langle -b_i\rangle y_i^{-1} + \delta\theta \geq 0. \tag{4.29}$$

Let $x(\cdot)$ be a solution of (4.3). By the Danskin theorem [27], the function $\varrho(t) := \max_{i\in\{1,\dots,n\}} x_i(t)/y_i$ is absolutely continuous and for almost all t, the following equation holds

$$\begin{aligned} \dot{\varrho}(t) &= \max_{i\in I(t)} \dot{x}_i(t)/y_i, \quad \text{where} \\ I(t) &:= \{i : x_i(t)/y_i = \varrho(t)\}. \end{aligned} \tag{4.30}$$

If $i \in I(t)$ and j, it follows that $x_i(t) = y_i\varrho(t), x_j(t) \leq y_j\varrho(t)$, and

$$\begin{aligned} \dot{x}_i(t) &\overset{(4.3)}{=} -a_{ii}x_i(t) + \sum_{j\neq i} \underbrace{[\ -a_{i,j}\ ]}_{\geq 0 \text{ by Asm. 4.1}} x_j(t) - \frac{b_i}{x_i(t)} + w_i \\ &\leq -\varrho(t)\left(a_{ii}y_i + \sum_{j\neq i} a_{i,j}y_j\right) - \varrho(t)^{-1}\frac{b_i}{y_i} + w_i \\ &\overset{(4.28)}{\leq} -\varrho(t)\left[\langle w_i\rangle + \frac{\langle -b_i\rangle}{y_i} + 3\delta\right] + \varrho(t)^{-1}\frac{\langle -b_i\rangle}{y_i} + \langle w_i\rangle \\ &= -\delta\varrho(t) - \{[\varrho(t) - 1]\langle w_i\rangle + \delta\varrho(t)\} \\ &\qquad - \left\{[\varrho(t) - \varrho(t)^{-1}]\frac{\langle -b_i\rangle}{y_i} + \delta\varrho(t)\right\}. \end{aligned} \tag{4.31}$$

Hence whenever $\varrho(t) \geq \theta \in (0,1)$,

$$\dot{x}_i(t) \leq -\delta\varrho(t) - \{[\theta-1]\langle w_i\rangle_+ + \delta\theta\} \\ - \left\{[\theta-\theta^{-1}]\frac{\langle b_i\rangle_-}{y_i} + \delta\theta\right\} \overset{(4.29)}{\leq} -\delta\varrho(t).$$

So (4.30) implies that $\varrho(t) > \theta \Rightarrow \dot{\varrho}(t) \leq -\delta\varrho(t) \leq -\delta\theta$.[15] Claims (i) and (ii) are immediate from this entailment. □□□

Lemma 4.10. Claim II of Proposition 4.2 holds.

Proof. This is immediate from (4.24) since for any distinguished solution $x(\cdot)$ and $y := x(0)$,

$$\dot{x}(0) \overset{(4.3)}{=} -Ay + \mathrm{stack}\left(-\frac{b_i}{y_i} + w_i\right) \\ \leq -Ay + \mathrm{stack}\left(\frac{\langle -b_i\rangle}{y_i} + \langle w_i\rangle\right) \overset{(4.7)}{<} 0.$$

□□□

Lemma 4.11. Suppose that a solution $x(\cdot)$ of (4.3) cannot be extended from $[0,\tau)$ with $\tau < \infty$ to the right. Then there is i such that $b_i > 0$ and $x_i(t) \to 0, \dot{x}_i(t) \to -\infty$ as $t \to \tau_-$.

Proof. By Lemma 4.2, there is a solution $y > 0$ for (4.7). Via multiplying y by a large enough factor, it is ensured that $y > x(0)$. Let $x_\uparrow(\cdot)$ be the distinguished solution starting with $x_\uparrow(0) = y$. By Lemma 4.10, $x_\uparrow(t) \leq y$ for $t \geq 0$, and $x(t) \leq x_\uparrow(t)$ on the intersection of the domains of definitions of $x(\cdot)$ and $x_\uparrow$ by (4.23). Then by [43, Theorem 3.1, Ch. II], $x(t)$ converges to the boundary of $\mathcal{K}_+^n$ as $t \to \tau_-$ and is bounded, *i.e.,*

$$\min_i x_i(t) \to 0 \text{ as } t \to \tau_-, \quad c := \sup_{t\in[0,\tau)} \|x(t)\| < \infty. \tag{4.32}$$

Putting $W := \max_i \left[|w_i| + c\sum_j |a_{ij}|\right]$, it is seen that

$$\dot{x}_i(t) \overset{(4.31)}{=} -\sum_j a_{i,j}x_j(t) - \frac{b_i}{x_i(t)} + w_i \\ \in \left[-W - \frac{b_i}{x_i(t)}, W - \frac{b_i}{x_i(t)}\right],$$

$$b_i < 0 \wedge x_i(t) \leq \frac{|b_i|}{2W} \Rightarrow \dot{x}_i(t) \geq W > 0, \tag{4.33}$$

$$b_i > 0 \wedge x_i(t) \leq \frac{|b_i|}{2W} \Rightarrow \dot{x}_i(t) \leq -\frac{b_i}{2x_i(t)} < 0 \\ \Rightarrow x_i^2(\theta) \leq x_i^2(t) - b_i(\theta - t)\ \forall \theta \in [t,\tau). \tag{4.34}$$

[15] In fact, this holds for almost all t such that the premises are true.

Due to (4.33), $x_i(t)$ is separated from zero if $b_i < 0$. So by (4.32), there exists i such that $b_i > 0$ and for any $\varepsilon > 0$, arbitrarily small left vicinity $(\tau_- \delta, \tau), \delta \approx 0$ of τ contains points t with $x_i(t) < \varepsilon$. Then for $\varepsilon < \frac{|b_i|}{2W}$, formula (4.34) guarantees that $x_i(t') < \varepsilon \; \forall t' \in (t, \tau)$. Overall, it is seen that $x_i(t) \to 0$ as $t \to \tau_-$; then $\dot{x}_i(t) \to -\infty$ as $t \to \tau_-$ by (4.34). □□□

Lemma 4.12. Suppose that Assumption 4.2 holds. Then the following claims hold true.

i) Stable equilibria of (4.3) (if exist) are locally asymptotically stable.

ii) Let $0 < x^- \le x^0 \le x^+$ be equilibria of (4.3). If $x^\pm$ are stable and all b_i's are of the same sign, x^0 is also stable.

Proof. By Assumption 4.2 and (4.3), the Jacobian matrix

$$\begin{gathered} \nabla f(x) = A(k) := -A + \operatorname{diag}(k_i), \\ k := k(x) := \operatorname{stack}\left(b_i x_i^{-2}\right) \end{gathered} \tag{4.35}$$

has no eigenvalues with the zero real part at any equilibrium x. So for any stable equilibrium x, the matrix (4.35) is Hurwitz and so x is locally asymptotically stable. Since $A(k)^\top = A(k)$ by Assumption 4.1, $A(k)$ is Hurwitz if and only if the following quadratic form in $h \in \mathbb{R}^n$ is negative definite

$$Q_x(h) := -h^\top A h + \sum_{i=1}^n k_i(x) h_i^2.$$

Thus both forms $Q_{x^\pm}$ are negative definite. Meanwhile, $k_i(x^0) \le k_i(x^-) \; \forall i$ if $b_i > 0 \;\; \forall i$, whereas $k_i(x^0) \le k_i(x^+) \; \forall i$ if $b_i < 0 \; \forall i$. In any case, Q_{x^0} is upper estimated by a negative definite quadratic form (either Q_{x^-} or Q_{x^+}) and so is negative definite as well. □□□

Corollary 4.2. Suppose that Assumption 4.2 holds, $0 < x^{(0)} \le x^{(1)}$ are stable equilibria of (4.3) and all b_i's are of the same sign. Then $x^{(0)} = x^{(1)}$.

Proof. Suppose to the contrary that $x^{(0)} \ne x^{(1)}$. By Lemma 4.8 and (i) of Lemma 4.12, there exists one more equilibrium $x^{(1/2)}$ in between $x^{(0)}$ and $x^{(1)}$, *i.e.*, $x^{(0)} \le x^{(1/2)} \le x^{(1)}$ and $x^{(1/2)} \ne x^{(0)}, x^{(1)}$. By (ii) of Lemma 4.12, this newcoming equilibrium $x^{(1/2)}$ is stable. This allows to repeat the foregoing arguments first for $x^{(0)}$ and $x^{(1/2)}$ and second for $x^{(1/2)}$ and $x^{(1)}$. As a result, it is seen that there exist two more stable equilibria $x^{(1/4)} \in \uparrow x^{(0)}, x^{(1/2)} \uparrow$ and $x^{(3/4)} \in \uparrow x^{(1/2)}, x^{(1)} \uparrow$ that differ from all previously introduced equilibria. This allows to repeat the foregoing arguments once more to show that there exist stable equilibria $x^{(1/8)}, x^{(3/8)}, x^{(5/8)}, x^{(7/8)}$ such that $x^{(i/8)} \le x^{(j/8)} \; \forall 0 \le i \le j \le 8$ and $x^{(i/8)} \ne x^{(j/8)} \; \forall 0 \le i, j \le 8, i \ne j$. By continuing likewise, a stable equilibrium $x^{(r)}$ is assigned to any number $r \in [0, 1]$ whose representation in the base-2 numeral system is finite (*i.e.*, number representable in the form $r = j2^{-k}$ for some $k = 1, 2, \ldots$ and $j = 0, \ldots, 2^k$) and ensure that these

equilibria are pairwise distinct and depend on r monotonically: $x^{(r)} \leq x^{(\varrho)}$ whenever $0 \leq r \leq \varrho \leq 1$.

Since all they lie in the compact set $\uparrow x^{(0)}, x^{(1)} \uparrow$, there is a sequence $\{r_k\}_{k=1}^{\infty}$ of pairwise distinct numbers r's for which $\exists \bar{x} = \lim_{k\to\infty} x^{(r_k)}$. Then $\bar{x} \in \uparrow x^{(0)}, x^{(1)} \uparrow$ and so $\bar{x} > 0$ and $f(\bar{x}) = \lim_{k\to\infty} f[x^{(r_k)}] = 0$, *i.e.*, $\bar{x}$ is an equilibrium. Then the Jacobian matrix $\nabla f(\bar{x})$ is nonsingular, as was remarked just after (4.35). However, this implies that in a sufficiently small vicinity V of $\bar{x}$, the equation $f(x) = 0$ has no roots apart from $\bar{x}$ in violation of $x^{(r_k)} \in V\ \forall k \approx \infty$ and $x^{(r_k)} \neq x^{(r_l)}\ \forall k \neq l$. The contradiction obtained completes the proof. □□□

Proof of Proposition 4.2: Claim I is given by Lemma 4.2.

Claim II is justified by Lemma 4.10.

For Claim III, let $x(t), t \in [0, t_f)$ be a distinguished solution. If $t_f < \infty$, then III.i of Proposition 4.2 holds by Lemma 4.11. Suppose that $t_f = \infty$. Then the limit $\bar{x}$ from (4.9) exists due to Claim II, and $\bar{x} \geq 0$. It is shown next that in fact $\bar{x} > 0$.

Suppose to the contrary that $\bar{x}_i = 0$ for some i. Then $x_i(t) \to 0$ as $t \to \infty$, (4.33) means that $b_i > 0$, and (4.34) (where $\tau = \infty$ now) implies that $\|x(\theta)\|^2$ assumes negative values for large enough θ. This assures that $\bar{x} > 0$ and so (4.9) does hold. By Lemma 4.5, $\bar{x}$ is an equilibrium.

Now suppose that III.i holds for a distinguished solution $x_\dagger(\cdot)$. Suppose that there is another distinguished solution $x(\cdot)$ for which III.i is not true. Then $x(\cdot)$ is defined on $[0, \infty)$ by Lemma 4.11 and also $\exists \bar{x} = \lim_{t\to\infty} x(t) > 0$ by the foregoing. By (ii) of Lemma 4.9 (with $y := x_\dagger(0)$), $x(\sigma) \leq \theta x_\dagger(0) \leq x_\dagger(0)$ for large enough σ. By applying (4.23) to $x_1(t) := x(t + \sigma)$ and $x_2(t) = x_\dagger(t)$, is follows that $x(t + \sigma) \leq x_\dagger(t)$ and so $x_i(t)$ goes to zero in a finite time, in violation of $\bar{x} > 0$ and II. This contradiction proves that III.i holds simultaneously for all distinguished solutions.

Since III.i and III.ii are mutually exclusive and complementary, it is noticed that either III.i holds for all distinguished solutions, or III.ii holds for all of them.

Let III.ii hold. As it has been shown in the paragraph prior to the previous paragraph, $x(t+\sigma) \leq x_\dagger(t)$ for any two distinguished solutions $x(\cdot)$ and $x_\dagger(\cdot)$. Hence $\lim_{t\to\infty} x(t) \leq \lim_{t\to\infty} x_\dagger(t)$. By flipping $x(\cdot)$ and $x_\dagger(\cdot)$ here, it is appreciated that these limits coincide, *i.e.,* the limit (4.9) is the same for all distinguished solutions.

Claim IV follows from Lemmata 4.9 and 4.11 since any equilibrium is related to a constant solution defined on $[0, \infty)$.

To establish Claim V, suppose that III.ii holds. Let $\bar{x}_{\mathtt{max}}$ stand for the limit (4.9). By (4.9) and Lemma 4.5, $\bar{x}_{\mathtt{max}}$ is an equilibrium. Consider a solution $x(\cdot)$ defined on $[0, \infty)$ and a distinguished solution $x_\dagger(\cdot)$. By retracing the above arguments based on (ii) of Lemma 4.9, is is observed that $x(\varsigma + t) \leq x_\dagger(t)\ \forall t \geq 0$ for some $\varsigma \geq 0$. By considering here a constant solution $x(\cdot)$ and letting $t \to \infty$, it follows that $\bar{x}_{\mathtt{max}}$ dominates any other equilibrium.

Let $x(0) \geq \bar{x}_{\mathtt{max}}$. By (4.23), $x(t) \geq \bar{x}_{\mathtt{max}}$ on the domain Δ of definition of $x(\cdot)$ and so $\Delta = [0, \infty)$ by Lemma 4.11. Thus, it is observed that $x_{\mathtt{max}} \leq x(\varsigma+t) \leq x_\dagger(t)\ \forall t \geq$

0 for some $\varsigma \geq 0$. It follows that $x(t) \to x_{\max}$ as $t \to \infty$, *i.e.,* the equilibrium $x_{\max}$ is attractive from above by Definition 4.1. □□□

Proof of Proposition 4.1: This proposition is immediate from Proposition 4.2, except for the concluding claims that refer to Assumption 4.2.

Let this assumption and S2 in Proposition 4.1 hold. Then $\bar{x}_{\max}$ is locally asymptotically stable by Lemma 4.5 and Claims II, V in Proposition 4.2. The last sentence of Proposition 4.1 is given by Corollary 4.2. It remains to show that there exist only finitely many equilibria $\bar{x}^k$.

Suppose the contrary. Since all equilibria lie in the compact set $\{x : 0 \leq x \leq \bar{x}_{\max}\}$, there exists an infinite sequence $\{\bar{x}^{k_s}\}_{s=1}^{\infty}$ of pairwise different equilibria that converges $\bar{x}^{k_s} \to \bar{x}$ as $t \to \infty$ to a point $\bar{x} \geq 0$. The estimates (4.33), (4.34) applied to any equilibrium solution $x(\cdot)$ assure that $x_i \geq |b_i|/(2W)$ on it, where $W := \max_i \left[|w_i| + c\sum_j |a_{ij}|\right]$ and c is any upper bound on $\|x(t)\|$. For the solutions related to the convergent and so bounded sequence $\{\bar{x}^{k_s}\}_{s=1}^{\infty}$, this bound can be chosen common. As a result, it is inferred that $\bar{x} > 0$ and so $f(\bar{x}) = \lim_{s\to\infty} f[x^{k_s}] = 0$, *i.e.*, $\bar{x}$ is an equilibrium. Then the Jacobian matrix $\nabla f(\bar{x})$ is nonsingular, as was remarked just after (4.35). This implies that in a sufficiently small vicinity V of $\bar{x}$, the equation $f(x) = 0$ has no roots apart from $\bar{x}$, in violation of $x^{k_s} \in V\ \forall s \approx \infty$ and $x^{k_s} \neq x^{k_r}\ \forall s \neq r$. This contradiction completes the proof. □□□

Proof of Proposition 4.3: Let $f^-(\cdot), f(\cdot), f^+(\cdot)$ be defined by (4.3) for $\mathfrak{C}^-$, $\mathfrak{C}$, $\mathfrak{C}^+$, respectively. Retracing the proof of Lemma 4.2 demonstrates existence of $a \in \mathcal{K}_+^n$ such that

$$A^+ a > \mathrm{stack}\Big(\max\{\langle w_i^-\rangle; \langle w_i\rangle\langle w_i^+\rangle\} + \frac{\max\{\langle -b_i^-\rangle; \langle -b_i\rangle\langle -b_i^+\rangle\}}{a_i}\Big).$$

By Definition 4.2, the solutions of $\dot{x} = f(x)$ and $\dot{x}^{\pm} = f^{\pm}(x^{\pm})$ that start with a are distinguished for the respective ODEs (4.3). Here $f^-(x) \leq f(x) \leq f^+(x)\ \forall x \in \mathcal{K}_+^n$ due to (4.11). So by [115, Theorem 8.1, Ch. II],

$$x^-(t) \leq x(t) \leq x^+(t),$$

where each inequality holds whenever its both sides are defined for the concerned t. So the claims i-iii are immediate from III-V in Proposition 4.2.

Now let $A^+ \to A^-, b_i^+ \to b_i^-, w^+ \to w^-$. For the left hand sides of these relations, there exist respective constant upper bounds $\hat{A}^+, \hat{b}_i^+, \hat{w}^+$ that satisfy Assumption 4.1. Let $\hat{x}_{\max}$ be the dominant equilibrium related to these bounds. By (4.12), $x_{\max}^- \leq x_{\max}^+ \leq \hat{x}_{\max}^+$ and so the variety of $x_{\max}^+$'s is bounded. For any limit point $\bar{x}$ of $x_{\max}^+$'s, it holds that $0 < x_{\max}^- \leq \bar{x}$ and $\bar{x}$ is the equilibrium of the $\mathfrak{C}^-$-related system by the continuity argument. So $x_{\max}^- = \bar{x}$ by the definition of the dominant equilibrium. Thus all limit points of $x_{\max}^+$'s are the same and equal $x_{\max}^-$. Hence $x_{\max}^+ \to x_{\max}^-$. □□□

Chapter 5

Power-Controlled Hamiltonian Systems: Application to Power Systems with CPLs

Synopsis This chapter explores a type of port-Hamiltonian system in which the controller or disturbance acts directly on the system's power balance equation—a scenario that appears in many practical applications. A suitable framework is provided to model these systems and to investigate their shifted passivity properties, based on which a stability analysis is carried out. The applicability of the results is illustrated with the stability analysis of electrical circuits with constant power loads.

5.1 Introduction

In recent years, port-Hamiltonian (pH) modeling of physical systems has gained extensive attention. pH systems theory provides a systematic framework for modeling and analysis of physical systems and processes [93, 70, 84, 82, 95]. Typically, the external inputs (controls or disturbances) in pH systems act on the flow variables—that is on the derivative of the energy storing coordinates. However, in some cases of practical interest, the external inputs act on the systems *power* balance equation, either as a control variable, or as power that is extracted from (or injected to) the system. These kind of systems are referred as *Power-controlled Hamiltonian* (P_wH) systems. P_wH systems cannot be modeled with constant control input matrices, which is the scenario considered in [49]. Consequently, to analyze its passivity properties, the development of new mathematical tools is required.

The objectives of the chapter are to propose a suitable framework to model P_wH systems and to develop analytical tools to infer stability properties of their—intrinsically non-zero—equilibrium points. The latter objective is achieved by identifying a class of P_wH systems that are shifted passive [93]. Following [49], a shifted storage function is used to address this issue. This shifted function is closely related to the notion of availability function used in thermodynamics [2, 51], and is associated with the Bregman divergence of the Hamiltonian with respect to an equilibrium of the system for constant non-zero input [17]. Therefore, the shifted Hamiltonian is used as a candidate Lyapunov function, which is based on the physical energy of the system, and, unlike the Brayton-Moser potential, is trivially computed. Two immediate corollaries of the shifted passivity property are: (i) that the shifted equi-

librium can be stabilized with simple PI controllers [49]; (ii) that in the uncontrolled case, when a constant input power or load is imposed, stability of this equilibrium can be established. This chapter focuses on the latter issue, that was first studied in the standard pH systems framework in [70]. Furthermore, the framework proposed in the chapter allows to give an analytic characterization of an estimate of the ROA in the case of a quadratic Hamiltonian and a positive definite dissipation matrix.

The remainder of this chapter is organized as follows. The proposed model for P_wH systems is introduced in Section 5.2. The main result, that is, the derivation of conditions for their shifted passivity, is provided in Section 5.3. The stability analysis is given in Section 5.4. The utility of the main result is illustrated in Section 5.5 with its application to electrical systems with CPLs, and in Section 5.6 with the application to synchronous generators. Finally, some concluding remarks are provided in Section 5.7.

5.2 Model

Consider the pH system driven by the *flow* $f \in \mathbb{R}^m$ [93]

$$\begin{aligned} \dot{x} &= (J-R)\nabla H(x) + Bf \\ e &= B^\top \nabla H(x) \ , \end{aligned}$$

where $x \in \mathbb{R}^n$ is the state vector (with $n \geq m$), $e \in \mathbb{R}^m$ is the *effort*, H is the system Hamiltonian (energy) function, and the $n \times n$ *constant* matrices $J = -J^\top$ and $R \geq 0$, are the structure and the dissipation matrices, respectively. The pH system satisfies the power-balance

$$\dot{H} = -\nabla H^\top(x) R \nabla H(x) + e^\top f \ .$$

Now consider the scenario where the external signals u_i act *directly* on the power balance equation of the system. Define the *control power input* $u \in \mathbb{R}^m$ as the element-wise product of effort and flow, *i.e.*, $u := \mathrm{diag}\,(e)\mathrm{diag}\,(f)1_m$. Hence, $f = \mathrm{diag}\,(e)^{-1}u$. Without loss of generality, by re-arranging the actuated and the non-actuated states, the constant matrix B is defined as

$$B := \begin{bmatrix} I_m \\ 0_{(n-m)\times m} \end{bmatrix} \ . \tag{5.1}$$

Accordingly, the vector ∇H is decomposed into

$$\nabla H = \begin{bmatrix} \mathfrak{G}_u(x) \\ \mathfrak{G}_0(x) \end{bmatrix} \ ,$$

where $\mathfrak{G}_u(x) \in \mathbb{R}^m$ is associated with the actuated states. It follows that

$$\begin{aligned} Bf = B\mathrm{diag}\,(e)^{-1}u &= B\mathrm{diag}\left(B^\top \nabla H(x)\right)^{-1}u \\ &= B\mathrm{diag}\left(\mathfrak{G}_u(x)\right)^{-1}u \\ &= G(x)u \ , \end{aligned}$$

where the *power input matrix* $G(x) \in \mathbb{R}^{n\times m}$ is defined as

$$G(x) := \begin{bmatrix} \mathrm{diag}\left(\mathfrak{G}_u(x)\right)^{-1} \\ 0_{(n-m)\times m} \end{bmatrix} . \tag{5.2}$$

The input matrix $G(x)$ is well-defined in the set Ω^+ characterized as

$$\Omega^+ := \{x \in \mathbb{R}^n \ : \ \text{diag}\,(\mathfrak{G}_u(x)) > 0\}.$$

Then the dynamics of the Power-controlled Hamiltonian (P_wH) system is given by

$$\dot{x} = (J - R)\nabla H(x) + G(x)u \ , \quad x \in \Omega^+ \ , \tag{5.3}$$

with the first m components of x corresponding to the *power* controlled states. Then it is easy to see that the power balance equation takes the form

$$\dot{H} = -\nabla H^\top(x)\, R\, \nabla H(x) + \ 1_m^\top u \ ,$$

implying that the natural output corresponding to the input u is given as the constant vector 1_m, in accordance with the fact that the total supplied power is $1_m^\top u$. The natural operating points for P_wH systems are non-zero equilibria corresponding to non-zero constant inputs u. Therefore, it is convenient to describe the system dynamics using the shifted model. Towards this end, the following steady-state relation is identified.

$$\mathcal{E} := \{(x, u) \in \mathbb{R}^n \times \mathbb{R}^m : \ \ (J - R)\nabla H(x) + G(x)u = 0\},$$

Following [49], the shifted Hamiltonian is defined as

$$\mathcal{H}(x) := H(x) - (x - \bar{x})^\top \nabla \bar{H} - \bar{H} \ , \tag{5.4}$$

which is, in fact, the Bregman divergence of the Hamiltonian with respect to $\bar{x}$ [17]. This function, as shown below, is instrumental to obtain a suitable representation of the shifted dynamics.

Lemma 5.1. Fix $(\bar{x}, \bar{u}) \in \mathcal{E}$, then the system (5.3), with the input matrix G as defined in (5.2), can be rewritten as

$$\dot{x} = \Big[J - \big(R + Z(x)\big)\Big]\nabla \mathcal{H}(x) + G(x)(u - \bar{u}) \ , \tag{5.5}$$

where

$$Z(x) := \bar{G}\text{diag}\,(\bar{u})G^\top(x) \ . \tag{5.6}$$

Proof. Subtracting the steady-state equation from (5.3) gives

$$\dot{x} = (J - R)\big(\nabla H(x) - \nabla \bar{H}\big) + G(x)u - \bar{G}\bar{u} \ \ .$$

Notice that

$$\nabla \mathcal{H}(x) = \nabla H(x) - \nabla \bar{H}, \tag{5.7}$$

it follows that

$$\begin{aligned}
\dot{x} =& (J - R)\, \nabla \mathcal{H}(x) + G(x)u - \bar{G}\bar{u} \\
& \qquad - G(x)\bar{u} + G(x)\bar{u} \\
=& (J - R)\, \nabla \mathcal{H}(x) + G(x)(u - \bar{u}) \\
& + \Big(G(x) - \bar{G}\Big)\bar{u}
\end{aligned}$$

Observe that

$$\begin{aligned}\Big(G(x)-\bar{G}\Big)\bar{u} &= -\Big(\mathrm{diag}\left(\nabla H(x)\right)-\mathrm{diag}\left(\nabla\bar{H}\right)\Big)\bar{G}G^{\top}(x)B\bar{u}\\ &= -\bar{G}\mathrm{diag}\left(\bar{u}\right)G^{\top}(x)\big(\nabla H(x)-\nabla\bar{H}\big)\\ &= -Z(x)\nabla\mathcal{H}\ ,\end{aligned}$$

where B is given in (5.1) and the fact that for all $a, b \in \mathbb{R}^n$, it holds that $\mathrm{diag}\,(a)b = \mathrm{diag}\,(b)a$ has been used. Hence

$$\dot{x} = \Big(J-\big(R+Z(x)\big)\Big)\nabla\mathcal{H}(x)+G(x)(u-\bar{u})\ ,$$

as claimed.

□□□

The natural output of the shifted model (5.5) is defined as

$$y = G^{\top}(x)\nabla\mathcal{H}(x)\ . \tag{5.8}$$

The next section investigates the conditions under which the system (5.5), with output (5.8), satisfies the following notion of shifted passivity; this concept is studied for general and pH systems in [93].

Definition 5.1. Consider the system (5.5) with output (5.8). Let $(\bar{x},\bar{u}) \in \mathcal{E}$ and define $\bar{y} = G^{\top}(\bar{x})\nabla\mathcal{H}(\bar{x})$. Then, the system is *shifted passive* if the mapping $(u-\bar{u}) \mapsto (y-\bar{y})$ is passive, *i.e.*, if there exists a function $\mathcal{S} : \mathbb{R}^n \to \mathbb{R}$, $\mathcal{S}(x) \geq 0\ \forall x$, such that, along trajectories of (5.5), satisfies

$$\dot{\mathcal{S}} = (\nabla\mathcal{S})^{\top}\dot{x} \leq (u-\bar{u})^{\top}(y-\bar{y}), \tag{5.9}$$

for all $(x,u) \in \mathbb{R}^n \times \mathbb{R}^m$.[1]

5.3 Main Result: Shifted Passivity

This section explores the passivity properties of the mapping $u-\bar{u} \mapsto y-\bar{y}$ defined by the $\mathrm{P_wH}$ model (5.5), (5.8)—where $\bar{y}$ is the value of the output y at an equilibrium point.

To establish the shifted passivity property, the trajectories are further restricted to be inside the set

$$\bar{\Omega}_{\mathrm{p}} := \{x \in \Omega^{+}\ :\ R+Z(x) \geq 0\}\ , \tag{5.10}$$

that is the closure of the open set

$$\Omega_{\mathrm{p}} := \{x \in \Omega^{+}\ :\ R+Z(x) > 0\}\ . \tag{5.11}$$

Assumption 5.1. The set $\bar{\Omega}_{\mathrm{p}}$ defined in (5.10) is non-empty.

[1]This concept is also defined in Chapter 2, however, it is included here to enhance readability.

Theorem 5.1. Consider the system (5.3), (5.8), where Assumption 5.1 holds. Fix $(\bar{x}, \bar{u}) \in \mathcal{E}$, and the corresponding output $\bar{y}$. For all trajectories $x \in \bar{\Omega}_p$, it holds that

$$\dot{\mathcal{H}} \leq (y - \bar{y})^\top (u - \bar{u}) \ . \tag{5.12}$$

Moreover, if H is convex, the system is shifted passive [93], *i.e.*, the mapping $(u - \bar{u}) \mapsto (y - \bar{y})$ is passive.

Proof. Using Lemma 5.1, the system can be written as in (5.5). Therefore,

$$\dot{\mathcal{H}} = -\nabla\mathcal{H}^\top \big(R + Z(x)\big) \nabla\mathcal{H} + y^\top (u - \bar{u}) \ .$$

Notice that $\bar{y} = 0$. Indeed, using (5.7) in (5.8), y can be written as

$$y = G^\top(x) \left(\nabla H(x) - \nabla \bar{H}\right) \ ,$$

and hence $\bar{y} = 0$. The proof of (5.12) is completed restricting the trajectories to satisfy $x \in \bar{\Omega}_\mathrm{p}$. To establish the passivity claim, notice that since H is convex, $\mathcal{H}(x)$ has a minimum at $\bar{x}$, and hence is non-negative. □□□

Remark 5.1. In case the control input includes only power *sources*, *i.e.*,

$$\mathrm{diag}\,(\bar{u}) \geq 0,$$

it can be seen from (5.6) and the fact that $x \in \Omega^+$, that $Z(x) \geq 0$, and hence $\bar{\Omega}_\mathrm{p} = \Omega^+$. In this case, Assumption 5.1 is trivially satisfied.
Therefore, throughout this chapter, the cases where at least one control input element is acting as a power load, *i.e.*, $\mathrm{diag}\,(\bar{u}) \ngeq 0$, is investigated. Although, in this case, Assumption 5.1 might be restrictive, it is shown that it is satisfied for both of the numerical case studies. Furthermore, a suitable control design, and in particular PI controllers, can guarantee $\bar{\Omega}_\mathrm{p}$ to be non-empty. As the focus of the chapter is on modeling and stability of the uncontrolled system, the control design is not pursued here.

Remark 5.2. Theorem 5.1 holds also for systems with an additional constant input, *i.e.*,

$$\dot{x} = (J - R)\nabla H(x) + G(x)u + \bar{u}_c \ ,$$

since the constant input $\bar{u}_c \in \mathbb{R}^n$ disappears in the shifted model (5.5).

5.4 Stability Analysis for Constant Inputs

Consider the system (5.3) with a constant input $u = \bar{u}$. Then the dynamics reads as

$$\dot{x} = (J - R)\nabla H(x) + G(x)\bar{u} \ . \tag{5.13}$$

In this section is investigated the local stability of the equilibria of the system (5.13), that is, points $\bar{x}$ such that $(\bar{x}, \bar{u}) \in \mathcal{E}$. Then, an estimate of their region of attraction (ROA) is provided. To establish these results, Assumption 5.1 is strengthened as follows.

Assumption 5.2. The set Ω_p defined in (5.11) is non-empty.

Naturally, only equilibrium points $\bar{x} \in \Omega_p$ are considered.

5.4.1 Local stability

Using the result of Theorem 5.1, consider the following corollary:

Corollary 5.1. Consider the system (5.13) satisfying Assumption 5.2, and having a point $\bar{x} \in \Omega_p$ such that $(\bar{x}, \bar{u}) \in \mathcal{E}$ and $\nabla^2 H(\bar{x}) > 0$. Then, the equilibrium $x = \bar{x}$ of the system (5.13) is asymptotically stable.

Proof. Since $R + Z(\bar{x}) > 0$ and $\nabla^2 H(\bar{x}) > 0$, there exists a ball $\mathcal{B}(\bar{x})$, centered in $\bar{x}$, such that $\mathcal{H}(x) > 0$ and $R + Z(x) > 0$ for all $x \in \mathcal{B}(\bar{x})$, $x \neq \bar{x}$. Moreover, $\mathcal{H}$ satisfies

$$\dot{\mathcal{H}} = -\nabla\mathcal{H}^\top \big(R + Z(x)\big) \nabla\mathcal{H} < 0, \quad \forall x \in \mathcal{B}(\bar{x}),\ x \neq \bar{x},$$

making it a strict Lyapunov function. This completes the proof. □□□

Remark 5.3. The physical interpretation of Assumption 5.2 is that the system should have a non-zero damping on all states. Apparently this assumption is restrictive in many cases, however, it can be relaxed to Assumption 5.1 if a *detectability* condition is satisfied, guaranteeing asymptotic stability by the use of LaSalle's Invariance principle; see [95, Chapter 8].

5.4.2 Characterizing an estimate of the ROA

As is well-known, all bounded level sets of Lyapunov functions are invariant sets. However, the proof of asymptotic stability is restricted to the domain Ω_p. Consequently, to provide an estimate of the ROA of $\bar{x}$ it is necessary to find a constant k such that the corresponding sublevel set of $\mathcal{H}$

$$\mathcal{L}_k := \{x \in \mathbb{R}^n :\ \mathcal{H}(x) < k,\ k > 0\}, \tag{5.14}$$

is bounded and is contained in Ω_p. To solve this, otherwise daunting task, two additional assumptions are made on the system.

Assumption 5.3. The dissipation matrix is positive definite, that is, $R > 0$.

Given this assumption, it is possible to construct a set—defined in terms of lower bounds on the elements of ∇H—that is strictly contained in Ω_p.

Lemma 5.2. Take Assumption 5.3 as true. Then the set Ω_Γ defined as

$$\Omega_\Gamma := \left\{ x \in \Omega^+ :\ \mathrm{diag}\left(\mathfrak{G}_u(x)\right) > -\frac{\mathrm{diag}\left(\bar{\mathfrak{G}}_u\right)^{-1}\mathrm{diag}\left(\bar{u}\right)}{\lambda_m\{R\}} \right\}, \tag{5.15}$$

is contained in Ω_p.

Proof. For all $x \in \Omega_\Gamma$ it holds that

$$\lambda_m\{R\} I_m + \mathrm{diag}\left(\bar{\mathfrak{G}}_u\right)^{-1}\mathrm{diag}\left(\bar{u}\right)\mathrm{diag}\left(\mathfrak{G}_u(x)\right)^{-1} > 0$$

Recall from (5.1) that $B = \begin{bmatrix} I_m & 0_{m\times(n-m)} \end{bmatrix}^\top$. Then

$$\lambda_m\{R\} + B\mathrm{diag}\left(\bar{\mathfrak{G}}_u\right)^{-1}\mathrm{diag}\left(\bar{u}\right)\mathrm{diag}\left(\mathfrak{G}_u(x)\right)^{-1}B^\top > 0\ ,$$

where the fact that $\lambda_m\{R\} > 0$ is used. Hence

$$\lambda_m\{R\} I_n + \bar{G}\mathrm{diag}\left(\bar{u}\right)G^\top(x) > 0\ ,$$

The proof is completed by noticing that the second left-hand term above is $Z(x)$, and by recalling that $R \geq \lambda_m\{R\} I_n$. □□□

A second assumption is on the Hamiltonian.

Assumption 5.4. The Hamiltonian is quadratic of the form

$$H(x) = \frac{1}{2}x^\top \mathcal{M} x, \quad \mathcal{M} > 0. \tag{5.16}$$

In this case, the shifted Hamiltonian (5.4) reduces to

$$\mathcal{H}(x) = \frac{1}{2}(x - \bar{x})^\top \mathcal{M}(x - \bar{x}). \tag{5.17}$$

Moreover, all the sublevel sets $\mathcal{L}_k$, given in (5.14), are *bounded*. Therefore, in view of Lemma 5.2, it is necessary to find a constant $k_c > 0$ such that $\mathcal{L}_{k_c} \subset \Omega_\Gamma$, and this sublevel set provides an estimate of the ROA of $\bar{x}$.

Theorem 5.2. Consider the system (5.13) with Assumptions 5.3 and 5.4 satisfied. Assume that $\bar{x} \in \Omega_\Gamma$ where Ω_Γ is given by (5.15). Define

$$k_c := \frac{1}{2\lambda_M\{\mathcal{M}\}} \min_{i=1,\dots,m} \left\{ \left(\gamma_i - (\mathcal{M}\bar{x})_i\right)^2 \right\} ,$$

with

$$\gamma_i := \max\{0, -\frac{\bar{u}_i}{\lambda_m\{R\}\bar{\mathfrak{G}}_{u_i}}\},$$

where $(\mathcal{M}\bar{x})_i$ and $\bar{\mathfrak{G}}_{u_i}$ are the i-th element of the vectors $\mathcal{M}\bar{x}$ and $\bar{\mathfrak{G}}_u$. Then, an estimate of the ROA of the equilibrium $\bar{x}$ is the sublevel set $\mathcal{L}_{k_c}$ of the shifted Hamiltonian function $\mathcal{H}(x)$ defined in (5.17).

Proof. From (5.17),

$$\mathcal{H}(x) = \frac{1}{2}(\mathcal{M}x - \mathcal{M}\bar{x})^\top \mathcal{M}^{-1}(\mathcal{M}x - \mathcal{M}\bar{x}).$$

Hence,

$$\mathcal{H}(x) \geq \frac{|\mathcal{M}x - \mathcal{M}\bar{x}|^2}{2\lambda_M\{\mathcal{M}\}}$$

with $|\cdot|$ the Euclidean norm. This bound, together with $\mathcal{H}(x) < k_c$, ensures that for all $i \in \{1, \cdots, m\}$,

$$((\mathcal{M}x)_i - (\mathcal{M}\bar{x})_i)^2 < (\gamma_i - (\mathcal{M}\bar{x})_i)^2.$$

Notice that since $\bar{x} \in \Omega_\Gamma$, it follows that $(\mathcal{M}\bar{x})_i > \gamma_i$. Hence $\gamma_i - (\mathcal{M}\bar{x})_i < 0$. Consequently,

$$\gamma_i - (\mathcal{M}\bar{x})_i < (\mathcal{M}x)_i - (\mathcal{M}\bar{x})_i < -\gamma_i + (\mathcal{M}\bar{x})_i \, .$$

The left hand side of the inequality above guarantees $(\mathcal{M}x)_i > \gamma_i$. Therefore, using Lemma 5.2, it follows that $R + Z(x) > 0$. The proof is completed by noticing that the latter ensures $\mathcal{H}(x)$ is a strict Lyapunov function of the system. □□□

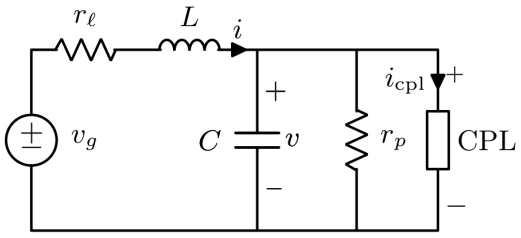

Figure 5.1: Single-Port DC circuit connected to a CPL.

5.5 Application to DC Networks with Constant Power Loads (CPL)

In this section the proposed method is applied to study the stability of equilibria of single-port and multi-port DC networks with CPLs.

5.5.1 Single-port system

A schematic representation of a DC network with a single CPL is shown in Figure 5.1. Observe that the combination of the resistive load r_p and the CPL, acts as a ZIP load connected to the capacitor C. In view of Remark 5.2, the current sink is omitted for brevity.

Define the state vector $x = \text{col}(q, \varphi)$, where q is the capacitor's electric charge and φ is the inductor's magnetic flux. Then the system can be modeled by

$$\dot{x} = (J - R)\nabla H(x) + G(x)u + u_c \,, \quad x \in \Omega^+ \,, \tag{5.18}$$

with $H = \frac{1}{2}x^\top \mathcal{M} x$ and

$$\mathcal{M} = \begin{bmatrix} \frac{1}{C} & 0 \\ 0 & \frac{1}{L} \end{bmatrix}, \; J = \begin{bmatrix} 0 & 1 \\ -1 & 0 \end{bmatrix}, \; R \; = \begin{bmatrix} \frac{1}{r_p} & 0 \\ 0 & r_\ell \end{bmatrix} \,, \tag{5.19}$$

and $u_c = \text{col}(0, v_g)$, $u = -P$, where $P > 0$ is the power extracted by the CPL. The input matrix is

$$G(q, \varphi) = \begin{bmatrix} \frac{C}{q} \\ 0 \end{bmatrix},$$

which is well defined in the set

$$\Omega^+ = \{(q, \varphi) \in \mathbb{R}^2 \,|\, q > 0\}.$$

Notice that the power balance equation takes the form

$$\dot{H} = \underbrace{-\nabla H^T R \nabla H}_{\textit{dissipated power}} + \underbrace{\nabla H^T u_c}_{\textit{external power}} + \underbrace{\nabla H^T G u}_{=-P} \,.$$

The equilibria of the system (5.18), (5.19) are computed in the following lemma.

Lemma 5.3. The system (5.18)-(5.19) admits two equilibria given by

$$\bar{q}_{\rm s} = Cr_p\frac{v_g+\sqrt{\Delta}}{(r_\ell+r_p)},\ \bar{\varphi}_{\rm s} = L\frac{r_pv_g-\sqrt{\Delta}}{r_\ell(r_\ell+r_p)}$$

and

$$\bar{q}_{\rm u} = Cr_p\frac{v_g-\sqrt{\Delta}}{(r_\ell+r_p)},\ \bar{\varphi}_{\rm u} = L\frac{r_pv_g+\sqrt{\Delta}}{r_\ell(r_\ell+r_p)},$$

where

$$\Delta := v_g^2 - 4\frac{r_\ell(r_p+r_\ell)}{r_p}P.$$

The equilibrium points are real if and only if $\Delta \geq 0$ or equivalently

$$P \leq P^{\rm e}_{\rm max},\quad P^{\rm e}_{\rm max} := \frac{r_pv_g^2}{4r_\ell(r_\ell+r_p)}\ . \tag{5.20}$$

Through straightforward computations, it can be shown that the Jacobian of the vector field in the right hand side of (5.18) has a positive eigenvalue at the equilibrium point $(\bar{q}_{\rm u},\bar{\varphi}_{\rm u})$, and hence this equilibrium is unstable. Furthermore, it can be shown that for small values of the load power, the Jacobian is negative definite at the equilibrium point $(\bar{q}_{\rm s},\bar{\varphi}_{\rm s})$.

Considering the results of Lemma 5.3, the equilibrium $(\bar{q}_{\rm s},\bar{\varphi}_{\rm s})$ is proposed as the candidate for nonlinear stability analysis. To use the results of Corollary 5.1, compute

$$R+Z(q,\varphi) = \begin{bmatrix} \frac{1}{r_p}-\frac{C^2P}{\bar{q}_{\rm s}q} & 0 \\ 0 & r_\ell \end{bmatrix}. \tag{5.21}$$

Next, observe that $R+Z(\bar{q}_{\rm s},\bar{\varphi}_{\rm s})>0$ if and only if

$$P < P^{\rm s}_{\rm max},\quad P^{\rm s}_{\rm max} := \frac{r_pv_g^2}{(r_p+2r_\ell)^2}\ . \tag{5.22}$$

Hence, according to Corollary 5.1, if the condition (5.22) is satisfied, then the equilibrium $(\bar{q}_{\rm s},\bar{\varphi}_{\rm s})$ is asymptotically stable. Notice that if $P<\min\{P^{\rm e}_{\rm max},P^{\rm s}_{\rm max}\}$, then the existence of the asymptotically stable equilibrium point $(\bar{q}_{\rm s},\bar{\varphi}_{\rm s})$ is guaranteed.

Remark 5.4. Let $\bar{v} := \frac{\bar{q}_{\rm s}}{C}$ denote the voltage of the CPL at the equilibrium $(\bar{q}_{\rm s},\bar{\varphi}_{\rm s})$. Then the physical equivalent of the term $-\frac{C^2P}{\bar{q}_{\rm s}q}$ in (5.21), is the inverse of a nonlinear negative resistor with the resistance

$$r_{\rm CPL}(v) := \Big(\frac{C^2P}{\bar{q}_{\rm s}q}\Big)^{-1} = \frac{\bar{v}}{P}v\ .$$

This resistor is in parallel with r_p, *i.e.*,

$$R+Z(q,\varphi) = \begin{bmatrix} \frac{1}{r_{\rm eq}} & 0 \\ 0 & r_\ell \end{bmatrix},$$

where $r_{\rm eq}(v) := \big(\frac{1}{r_p}-\frac{1}{r_{\rm CPL}(v)}\big)^{-1}$ is the equivalent resistor. Interestingly, the physical interpretation of the condition (5.22) is that the equivalent resistance is positive (and thus a passive element) at the equilibrium point, *i.e.*, $r_{\rm eq}(\bar{v})>0$.

As the dissipation matrix R is diagonal, and the Hamiltonian of the states are decoupled, the largest k in (5.14)—and hence the largest $\mathcal{L}_k$ contained in $\Omega_{\rm p}$—can be constructed explicitly.

To streamline the presentation of the result, consider the constants

$$\eta_i := -\frac{\bar{u}_i}{R_{ii}\bar{\mathfrak{G}}_{u_i}}, \tag{5.23}$$

and the constant vectors

$$\ell^i := \text{col}(\bar{x}_1, \bar{x}_2, \cdots, \bar{x}_{i-1}, \frac{\eta_i}{\mathcal{M}_{ii}}, \bar{x}_{i+1}, \cdots, \bar{x}_n) \ . \tag{5.24}$$

Corollary 5.2. Consider the system (5.13) with the quadratic Hamiltonian (5.16) with *diagonal* $R > 0$ and $\mathcal{M} > 0$. Assume that $\bar{x} \in \Omega_{\rm p}$. Define

$$k_d := \min_{i=1,\ldots,m} \left\{\mathcal{H}(\ell^i)\right\},$$

with (5.23) and (5.24). Then, an estimate of the ROA of the equilibrium $\bar{x}$ is the sublevel set $\mathcal{L}_{k_d}$ of the shifted Hamiltonian function $\mathcal{H}(x)$ defined in (5.17).

Proof. The proof follows analogously to the proof of Theorem 5.2, and hence is omitted. □□□

Remark 5.5. Notice that the set $\mathcal{L}_k$ in the case considered in the corollary is the ellipsoid

$$\sum_{i=1}^{n} \left(\frac{x_i - \bar{x}_i}{\sqrt{\frac{2k}{\mathcal{M}_{ii}}}} \right)^2 < 1 \ . \tag{5.25}$$

Now, using Corollary 5.2, an estimate of the ROA of $(\bar{q}_{\rm s}, \bar{\varphi}_{\rm s})$ can be derived. Bearing in mind that the dissipation matrix R is diagonal, and using Lemma 5.2, $\Omega_{\rm p}$ is computed as

$$\Omega_{\rm p} = \{(q, \varphi) \in \mathbb{R}^2 \ : \ \ q > q_{\min}\},$$

where

$$q_{\min} := Pr_p \frac{C^2}{\bar{q}_{\rm s}} = \frac{P}{P^{\rm s}_{\max}} \bar{q}_{\rm s} > 0 \ . \tag{5.26}$$

Remark 5.6. The interpretation of (5.26) is that the closer the load power to $P^{\rm s}_{\max}$ is, the smaller the ROA is. According to (5.22), this means that, with a fixed $\bar{q}_s$, larger resistances r_ℓ and r_p result in a larger ROA. Hence, in the proposed method, small parasitic elements provide a small region of attraction in the absence of the load resistance and the voltage source output resistance.

Now assume that (5.22) holds. Using Corollary 5.2, the set $\mathcal{L}_{k_d}$ with

$$k_d = \mathcal{H}(q_{\min}, \bar{\varphi}_{\rm s}) \ ,$$

is an estimate of the ROA. Furthermore, using (5.25), this set can be written as the oval

$$\left(\frac{q - \bar{q}_{\rm s}}{\sqrt{2Ck_d}} \right)^2 + \left(\frac{\varphi - \bar{\varphi}_{\rm s}}{\sqrt{2Lk_d}} \right)^2 < 1 \ . \tag{5.27}$$

Table 5.1: Simulation Parameters of the Single-Port CPL

v_g(V)	r_ℓ (Ω)	r_p(Ω)	L(µH)	C(mF)	P(kW)
24	0.04	0.1	78	2	1

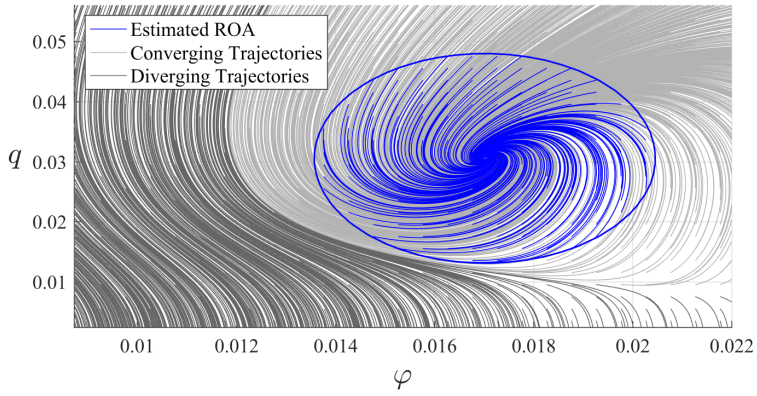

Figure 5.2: Phase plane of the system (5.18)-(5.19) with the parameters given in Table 5.1.

This set guarantees $q > q_{\min}$ for all solutions starting within the oval.

The results are evaluated by a numerical example of the network shown in Figure 5.1, with the parameters given in Table 5.1. The maximal power for existence of the equilibrium and its local stability is computed as $P^{\mathrm{e}}_{\max} = 2.57\,\mathrm{kW}$ and $P^{\mathrm{s}}_{\max} = 2.33\,\mathrm{kW}$, respectively. Notice that the CPL satisfies the conditions (5.20) and (5.22), since

$$P < P^{\mathrm{s}}_{\max} < P^{\mathrm{e}}_{\max}.$$

Figure 5.2 shows the phase plane of the system (5.18)-(5.19). The estimate of the ROA (the oval (5.27)) is shown in blue, and all other converging solutions are shown in light gray. It is evident that the proposed method provides an appropriate estimate of the ROA, as the solutions just beneath this region (in dark gray), diverge from the equilibrium.

5.5.2 Multi-port networks

The stability of a complete multi-port DC network with CPLs can be investigated in a similar fashion. It is assumed that the capacitors and the inductors are not ideal, *i.e.*, it is considered that all the inductors have a resistance in series and the capacitors posses a resistor in parallel. Moreover, it is assumed that the constant power loads are connected to a capacitor in parallel. This feature amounts to the capacitive effect of the input filters for this type of loads; see [10, 20, 22]. Let $i_{\mathrm{M}} \in \mathbb{R}^l$ represent the currents through the inductors, and $v_{\mathrm{C}} \in \mathbb{R}^c$ denote the voltages across the capacitors, where l and c are the number of inductors and capacitors, respectively. With a little abuse of notation, define the state vector $x = \mathrm{col}(q, \varphi) \in \mathbb{R}^{c+l}$ and the control vector $u = -P \in \mathbb{R}^c$, where $q \in \mathbb{R}^c$ denotes the electric charge of the capacitors, and $\varphi \in \mathbb{R}^l$ denotes the magnetic flux of the inductors. Then the network dynamics of a multi-port network admits a port-Hamiltonian representation

given by

$$\dot{x} = (J - R)\nabla H(x) + G(x)u + u_c,$$

with $H = \frac{1}{2}x^\top \mathcal{M} x$ and

$$\mathcal{M} = \begin{bmatrix} \mathcal{C}^{-1} & 0 \\ 0 & \mathcal{L}^{-1} \end{bmatrix},\ J = \begin{bmatrix} 0 & -\Gamma^\top \\ \Gamma & 0 \end{bmatrix},\ R = \begin{bmatrix} \mathcal{Y} & 0 \\ 0 & \mathcal{Z} \end{bmatrix},$$

where $\mathcal{C} > 0 \in \mathbb{R}^{c\times c}$ and $\mathcal{L} > 0 \in \mathbb{R}^{l\times l}$ are matrices associated with the magnitude of capacitors and inductors (and mutual inductances), $\mathcal{Y} \in \mathbb{R}^{c\times c}$ and $\mathcal{Z} \in \mathbb{R}^{l\times l}$ are positive definite matrices associated with the resistances, and $\Gamma \in \mathbb{R}^{l\times c}$ is the matrix associated with the network topology. The vector $u_c \in \mathbb{R}^{c+l}$ is constant and its components are linear combinations of the voltages and currents of the sources in the network. Similar to the case of the single-port *RLC* circuit with a CPL, and using Theorem 5.2, an ellipsoid can be computed here as an estimate of the ROA.

5.6 Application to a Synchronous Generator Connected to a CPL

In this section, the results are applied to the case of a synchronous generator connected to a CPL. This system can be modeled by[2]

$$\dot{p} = (J - R)\nabla H(p) + G(p)\, u + u_c, \tag{5.28}$$

with

$$\begin{aligned} &p = M\omega,\ J = 0,\ R = D_m + D_d,\ G(p) = \frac{M}{p} = \omega^{-1}, \\ &H = \frac{1}{2M}p^2,\ u = -P_e,\ u_c = \tau_{\mathrm{m}} + D_d\omega^*, \end{aligned} \tag{5.29}$$

where $p > 0$ is the angular momentum, $M > 0$ is the total moment of inertia of the turbine and generator rotor, $\omega \in \mathbb{R}_+$ is the rotor shaft velocity, $\omega^* > 0$ is the angular velocity associated with the nominal frequency of 50 Hz, $D_m > 0$ is the damping coefficient of the mechanical losses, $D_d > 0$ is the damping-torque coefficient of the damper windings, $\tau_{\mathrm{m}} > 0$ is the constant mechanical torque (physical input), and P_e is the constant power load.

Let

$$\Delta := (D_d\omega^* + \tau_m)^2 - 4(D_d + D_m)P_e\ ,$$

and assume that $\Delta > 0$, *i.e.*,

$$P_e < \frac{(D_d\omega^* + \tau_m)^2}{4(D_d + D_m)}.$$

Then, the dynamics (5.28), (5.29) has the following two equilibria

$$\bar{\omega}_{\mathrm{s}} = \frac{D_d\omega^* + \tau_m + \sqrt{\Delta}}{2(D_d + D_m)}, \quad \bar{\omega}_{\mathrm{u}} = \frac{D_d\omega^* + \tau_m - \sqrt{\Delta}}{2(D_d + D_m)}\ .$$

[2]This model is called the *improved swing equation* in [130, 76]. An inverter with a capacitive inertia can be modeled by similar dynamics; see [77].

Table 5.2: Simulation Parameters of the Synchronous Generator (p.u.)

M	D_m	D_d	P_e	τ_m
0.2	10^{-6}	10^{-4}	3	0.0027

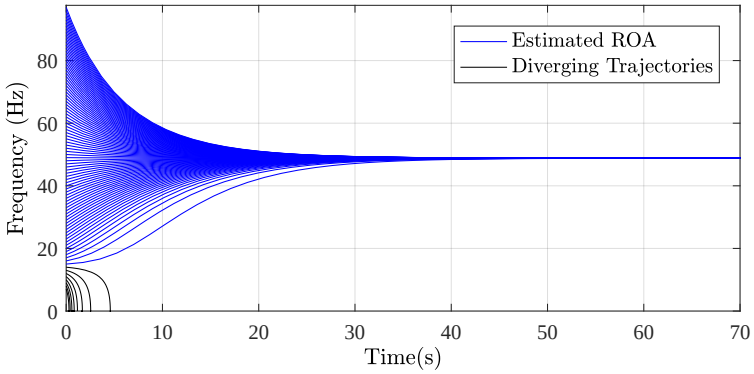

Figure 5.3: Solutions of the system (5.28),(5.29) with different initial conditions.

Moreover,

$$R + Z(\omega) = D_d + D_m - \frac{P_e}{\bar{\omega}_{\mathrm{s}}\omega} .$$

The equilibrium point $\omega = \bar{\omega}_{\mathrm{s}}$ is asymptotically stable since

$$R + Z(\bar{\omega}_{\mathrm{s}}) = \frac{\tau_m + D_d\omega^*}{\bar{\omega}_{\mathrm{s}}} > 0.$$

Through straightforward computations, it can be shown that the set Ω_{p} in (5.11) can be written as

$$\Omega_{\mathrm{p}} = \{\omega \in \mathbb{R}_+ \ : \ \omega > \bar{\omega}_{\mathrm{u}}\} . \tag{5.30}$$

In this set, the shifted Hamiltonian $\mathcal{H} = \frac{1}{2}M(\omega - \bar{\omega}_{\mathrm{s}})^2$ is strictly decreasing. Therefore the solutions tend to the equilibrium $\bar{\omega}_{\mathrm{s}}$ and move away from the point $\bar{\omega}_{\mathrm{u}}$ when time increases. Consequently the set Ω_{p} in (5.30) is forward invariant, and represents an estimate of the ROA.

Figure 5.3 shows the trajectories of a number of solutions of the system (5.28)-(5.29), with the parameters given by Table 5.2, and with different initial conditions. It is clear that the proposed method successfully identifies a very precise estimate of the ROA (blue), as all the solutions starting from outside the ROA estimate (black) diverge from the equilibrium. The result, which is derived from the systematic approach proposed in the chapter, shows an improvement over the results of [76], as both derived ROAs have the same lower bound, while here, the estimate has no upper bound.

Interestingly, it can be shown that any solution that does not start in Ω_p, diverges from the stable equilibrium ω_{s}. Therefore, here, the set Ω_p is not only an estimate, but is the exact region of attraction.

5.7 Summary

This chapter has explored a class of pH systems in which the control input (or disturbance) acts on the power of the system. These systems have been referred here as Power-controlled Hamiltonian (P_wH) systems. First, a model for such systems was proposed, and second, a condition for shifted passivity was derived. Using these results, the stability of equilibria was investigated. Furthermore, an estimate of the region of attraction was derived for P_wH systems with quadratic Hamiltonian.

The proposed modeling procedure and stability analysis were illustrated with two cases of practical interest: A DC circuit and a synchronous generator, both connected to constant power loads. The validity and utility of the proposed method was confirmed by numerical simulations of these case studies.

Part III

STABILIZATION: AN ADAPTIVE CONTROL APPROACH

Chapter 6

Voltage Control of a Buck-Boost Converter

Synopsis This chapter addresses the problem of regulating the output voltage of a DC-DC buck-boost converter that supplies electric energy to a constant power load. The model of the network is a nonlinear, second order dynamical system that is shown to be non-minimum phase with respect to both states. Moreover, to design a high-performance controller, the knowledge of the extracted load power, which is difficult to measure in industrial applications, is required. In this chapter, an adaptive interconnection and damping assignment passivity-based control—that incorporates the immersion and invariance parameter estimator for the load power—is proposed to stabilize the system around a desired equilibrium. Some detailed simulations are provided to validate the transient behavior of the proposed controller and compare it with the performance of a classical proportional-derivative scheme.

6.1 Introduction

The DC-DC buck-boost power converter is increasingly utilized in power distribution systems since it can step up or down the voltage between the source and load, providing flexibility in choosing the voltage rating of the DC source [125, 116, 124]. Although the control of these converters in the face of classical loads is well-understood, this is not the case when constant power loads (CPLs) are considered. This scenario significantly differs from the classical one and poses a new challenge to control theorist, see [9, 71, 38, 53, 80, 128] for further discussion on the topic and [110] for a recent literature review. It should be underscored that the typical application of this device requires large variations of the operating point—therefore, the dynamic description of its behavior cannot be captured by a linearized model, requiring instead a nonlinear one.

To address the voltage regulation of a buck-boost converter with a CPL, several techniques have been proposed in the power electronics literature, but without a nonlinear stability analysis. In [88], the active-damping approach is utilized to address the negative impedance instability problem raised by the CPL. The main idea of this method is that a virtual resistance is considered in the original circuit to increase the system damping. However, the stability result is obtained by applying small-signal analysis, which is valid only in a small neighborhood of the operating point. A new nonlinear feedback controller, which is called “Loop Cancellation”, has

been proposed to stabilize the buck-boost converter by "canceling the destabilizing behavior caused by CPL" [89]. The control problem turns into the design of a controller for the linear system by using loop cancellation method. However, the construction is based on feedback linearization [47] that, as is well-known, is highly non-robust. A sliding mode controller is designed in [111] for this problem. However, for the considered nonlinear system, the stability result is obtained by adopting the linear system theory. In addition, as it is widely acknowledged, the drawbacks of this method are that the proposed control law suffers from chattering and its relay action injects a high switching gain. The deleterious effect of these factors is illustrated in experiments shown in [111], which exhibit a very poor performance.

Aware of the need to deal with the intrinsic nonlinearities of power converters some authors of this community have applied passivity-based controllers (PBCs), which is a natural candidate in these applications. Unfortunately, in many of these reports the theoretical requirements of the PBC methodology are not rigorously respected. For instance, in [60], the well-known standard PBC [83] is used for the buck-boost with a CPL. Unfortunately, the given result is theoretically incorrect due to the fact that the authors fail to validate the stability of the zero dynamics of the system with respect to the controlled output that, as explained in [83], is an essential step for the stability analysis and, as shown in this chapter, it turns out to be violated.

An additional drawback of the existing results is that all of them require the knowledge of the power extracted by the CPL, which is difficult to measure in industrial applications. Designing an estimator for the power is a hard task because the original system is nonlinear and the only available measurements are the inductor current and the output voltage.

In this chapter, the well-known interconnection and damping assignment (IDA) PBC, first reported in [82] and reviewed in [81], is applied to stabilize the buck-boost converter with a CPL. The main contributions are enlisted as follows.

1) Derivation of an IDA-PBC that ensures the desired operating point is a (locally) asymptotically stable equilibrium with a guaranteed region of attraction.

2) Design of an estimator of the load's power, which is based on the Immersion and Invariance (I&I) technique[8] and has guaranteed stability properties, to make the IDA-PBC adaptive.

3) Proof that the zero dynamics of the system, with respect to both states, is unstable—limiting the achievable performance of classical PD controllers to "low-gain tunings".

The rest of the chapter is organized as follows. Section 6.2 contains the model of the system and the analysis of its zero dynamics with respect to its two states. Section 6.3 proposes the IDA-PBC assuming that the power extraction of the load is known. To make the latter scheme adaptive, in Section 6.4 an on-line power estimator is designed and some simulations, carried out in MATLAB, are provided in Section 6.5. The chapter is wrapped-up with some concluding remarks in Section 6.6. To enhance readability, the derivation of the IDA-PBC, that is conceptually simple but computationally involved, is given in a Technical Appendix at the end of the chapter.

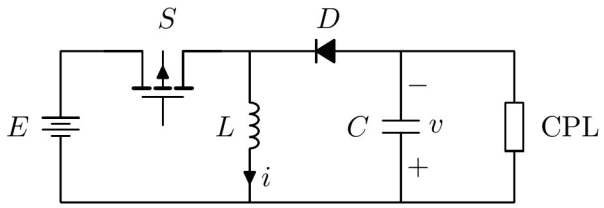

Figure 6.1: Circuit representation of the DC-DC buck-boost converter with a CPL

6.2 System Model, Problem Formation and Zero Dynamics Analysis

In this section, the average model[1] of the buck-boost converter supplying electric energy to a CPL is presented and an analysis of its zero dynamics is carried out.

6.2.1 Model of buck-boost converter with a CPL

The topology of a buck-boost converter supplying electric energy to a CPL is shown in Fig. 6.1. Under the standard assumption that it operates in continuous conduction mode, the average model is given by

$$\begin{aligned} L\frac{di}{dt} &= -(1-u)v + uE, \\ C\frac{dv}{dt} &= (1-u)i - \frac{P}{v}, \end{aligned} \tag{6.1}$$

where $i > 0$ is the current through the inductor L, $v > 0$ the voltage across the capacitor C, $P \geq 0$ the power extracted by the CPL, $E > 0$ is the input voltage and $u \in [0, 1]$ is the converter's duty ratio, which is the control signal.

Some simple calculations show that the assignable equilibrium set is given by

$$\mathcal{E} := \left\{ (i, v) \in \mathbb{R}^2 : \; i - P\left(\frac{1}{v} + \frac{1}{E}\right) = 0, \; v > 0 \right\}. \tag{6.2}$$

6.2.2 Control problem formulation

Consider the system (6.1) verifying the following conditions.

Assumption 6.1. The power load P is *unknown* but the parameters L, C and E are known and fixed.

Assumption 6.2. The state (i, v) is available for measurement.

Fix a *desired output voltage* $v_\star > 0$ and compute the associated assignable equilibrium point $(i_\star, v_\star) \in \mathcal{E}$. Design a static state-feedback control law with the following features.

(F1) $(i_\star, v_\star)$ is an asymptotically stable equilibrium of the closed-loop, with a well-defined region of attraction.

[1] The reader is referred to the introduction of [112] for a detailed explanation on average models of power converters in general.

(F2) It is possible to define a subset Ω, in the positive orthant of $\mathbb{R}^2$, which is *positively-invariant* and inside the region of attraction of the equilibrium. That is, a set inside the positive orthant verifying

$$[(i(0), v(0)) \in \Omega \;\Rightarrow\; (i(t), v(t)) \in \Omega, \forall t \geq 0]$$
$$\lim_{t\to\infty} (i(t), v(t)) = (i_\star, v_\star).$$

To simplify the notation, and without loss of generality, a normalized model of the system is to be used. This normalized form is obtained through the change of coordinates

$$\begin{aligned} x_1 &:= \frac{1}{E}\sqrt{\frac{L}{C}}i \\ x_2 &:= \frac{1}{E}v, \end{aligned} \tag{6.3}$$

and doing the *time scale* change $\tau = \frac{t}{\sqrt{LC}}$ that yields the model

$$\begin{aligned} \dot{x}_1 &= -(1-u)x_2 + u \\ \dot{x}_2 &= (1-u)x_1 - \frac{D}{x_2} \end{aligned} \tag{6.4}$$

where

$$D := \frac{P}{E^2}\sqrt{\frac{L}{C}}.$$

Also, $\dot{(\cdot)}$ denotes $\frac{d}{d\tau}(\cdot)$ and all signals are expressed in the new time scale τ. The assignable equilibrium set $\mathcal{E}$ in the coordinates x is given by

$$\mathcal{E}_x := \left\{ x \in \mathbb{R}^2 :\; x_1 - \frac{D}{x_2} - D = 0,\; x_2 > 0 \right\} \tag{6.5}$$

Notice that, under Assumptions 6.1 and 6.2, the control problem is translated into the design of a state feedback for the system (6.4), with unknown D, such that a given $x_\star \in \mathcal{E}_x$ is asymptotically stable.

It is important to recall that the signal of interest is the output voltage v, therefore, for the fixed $x_{2\star} > 0$, the $x_{1\star} > 0$ is defined via

$$x_{1\star} = \frac{D}{x_{2\star}} + D. \tag{6.6}$$

Remark 6.1. As indicated by Assumption 6.1, the value for the input voltage E is assumed to be known and fixed. A non-trivial extension of the present work would imply the relaxation of this assumption. It is worth mentioning that this problem has been addressed in [64] and [113] but for the case of *standard impedance loads*.

6.2.3 Stability analysis of the systems zero dynamics

The design of a stabilizing controller for (6.4) is complicated by the fact that, as shown in the proposition below, its zero dynamics with respect to both states is *unstable*. This means that, if the controller injects high gain, the closed-loop system

will be *unstable*—as it stems from the fact that the poles will move towards the unstable zeros. This situation hampers the design of high performance PD controllers, which require high proportional gains to speed up the transients. See Section 6.5 for an illustration of this fact.

Proposition 6.1. Consider the system (6.4) and an assignable equilibrium $x_\star \in \mathcal{E}_x$. The zero dynamics with respect to the outputs $x_1 - x_{1\star}$ or $x_2 - x_{2\star}$ are unstable.

Proof Fixing $x_1 = x_{1\star}$ and using the first equation in (6.4), it follows that

$$u = \frac{x_2}{x_2 + 1},$$

which substituted in the second equation of (6.4) yields the zero dynamics

$$\dot{x}_2 = \frac{D}{x_{2\star} x_2 (x_2 + 1)}(x_2 - x_{2\star}) =: s(x_2). \tag{6.7}$$

The slope of $s(x_2)$ evaluated at $x_2 = x_{2\star}$ gives

$$s'(x_2)|_{x_2 = x_{2\star}} = \frac{D}{x_{2\star}^2 (1 + x_{2\star})}.$$

Since $x_{2\star} > 0$, this is a positive number proving that the equilibrium $x_{2\star}$ of the dynamics (6.7) is unstable—as claimed by the proposition.

Analogously, by fixing $x_2 = x_{2\star}$ and using the second equation of (6.4) the expression

$$u = 1 - \frac{D}{x_1 x_{2\star}}, \tag{6.8}$$

is obtained, which substituted in the first equation of (6.4) yields

$$\dot{x}_1 = 1 - \frac{x_{1\star} - D}{x_1} =: w(x_1). \tag{6.9}$$

Proceeding as done for the case above, it follows that

$$w'(x_1)|_{x_1 = x_{1\star}} = \frac{x_{1\star} - D}{x_{1\star}^2}.$$

The proof is completed noting from (6.5) that $x_{1\star} = D(1 + \frac{1}{x_{2\star}}) > D$ and the slope is, again, positive. □□□

The proof that the zero dynamics of (6.4) with respect to $x_1 - x_{1\star}$ is unstable invalidates the stability claim made in Section IV of [60]. In that paper, a standard PBC is designed fixing $x_1 = x_{1\star}$. It is well-known [83] that this kind of controller implements an inversion of the systems zero dynamics, therefore the controller will be unstable if the zero dynamics is unstable, which is the case of the PBC of [60].

6.3 IDA-PBC design

In this section, the IDA-PBC approach is proposed to stabilize the buck-boost converter feeding a CPL by assuming that the power of the load, D, is known. This condition is later relaxed in Proposition 6.4, where an estimator of D is added to the IDA-PBC.

To make this chapter self-contained the main result of the IDA-PBC methodology and its proof are presented next. For more details on IDA-PBC the reader is referred to [81].

Proposition 6.2. Consider the nonlinear system

$$\dot{x} = f(x) + g(x)u \tag{6.10}$$

with state $x \in \mathbb{R}^n$ and control $u \in \mathbb{R}^m$ and a desired operating point

$$x_\star \in \{x \in \mathbb{R}^n : \ g^\perp(x)f(x) = 0\},$$

where $g^\perp(x)$ is a full rank left annihilator of $g(x)$. Fix the target dynamics as

$$\dot{x} = F_d(x)\nabla H_d(x), \tag{6.11}$$

where $\nabla H_d(x) := \left(\frac{\partial H_d(x)}{\partial x}\right)^\top$ with the function $H_d(x)$ a solution of the PDE

$$g^\perp(x)\left[f(x) - F_d(x)\nabla H_d(x)\right] = 0, \tag{6.12}$$

verifying

$$x_\star = \arg\min\{H_d(x)\}, \tag{6.13}$$

and the matrix $F_d(x)$ is such that

$$F_d^\top(x) + F_d(x) < 0, \ \forall x. \tag{6.14}$$

Then, the system (6.10) in closed-loop with

$$u(x) := [g^\top(x)g(x)]^{-1}g^\top(x)[F_d(x)\nabla H_d(x) - f(x)] \tag{6.15}$$

has an asymptotically stable equilibrium at $x_\star$ with *strict Lyapunov function* $H_d(x)$.

Proof From the fact that the $n \times n$ matrix $\begin{bmatrix} g^\top(x) \\ g^\perp(x) \end{bmatrix}$ is full rank, the following equivalence holds.

$$f(x) + g(x)\bar{u}(x) = F_d(x)\nabla H_d(x) \ \Leftrightarrow \ (6.12), \ (6.15).$$

Hence, the closed-loop is given by (6.11). Now, (6.13) ensures $H_d(x)$ is positive definite (with respect to $x_\star$). Computing the derivative of $H_d(x)$ along the trajectories of (6.11) and invoking (6.14) it follows that

$$\dot{H}_d = (\nabla H_d(x))^\top F_d(x)\nabla H_d(x) < 0, \ \forall x \neq x_\star$$

and, therefore, $H_d(x)$ is a strict Lyapunov function for the closed-loop system, completing the proof. □□□

The next proposition is a direct application of IDA-PBC that provides a solution to considered problem.

Proposition 6.3. Consider the system (6.4) under Assumption 6.2. Further assume that D is *known* and satisfies the bounds

$$0 < D < \frac{x_{2\star}^2}{\sqrt{2}\sqrt{1+x_{2\star}}}. \tag{6.16}$$

Fix $x_{2\star} > 0$ and compute $x_{1\star} > 0$ from equation (6.6). Define the IDA-PBC

$$u = \frac{1}{u_0}(u_1 + u_2), \tag{6.17}$$

where

$$\begin{aligned} u_0 &= -x_1 \left(x_2+1\right)^2 \left(2x_1^2+x_2^2\right)^2, \\ u_1 &= \left(2x_1^2+x_2^2\right)\left(x_1x_2\left(2x_1^2+x_2^2\right)\left(k_1\left(2x_2+1\right)\left(2\left(k_2+x_1^2\right)+x_2^2\right)\right.\right. \\ &\quad \left.\left. -x_2-2\right) - D\left(x_2+1\right)\left(-2x_1^2+x_2^2+x_2\right)\right), \\ u_2 &= \sqrt{2}Dx_1x_2\sqrt{2x_1^2+x_2^2}\left(2x_2+1\right)\operatorname{arctanh}\left(\frac{x_1}{\sqrt{x_1^2+\frac{x_2^2}{2}}}\right), \end{aligned} \tag{6.18}$$

k_1 is a tuning gain satisfying

$$k_1 > \max\{-\frac{a_0}{\left(\frac{4D^2(x_{2\star}+1)^2}{x_{2\star}^2}\right)},\ -\frac{b_0}{\left(\frac{x_{2\star}^4-2D^2(x_{2\star}+1)}{x_{2\star}^3}\right)}\}, \tag{6.19}$$

with the constants a_0 and b_0 defined in Appendix 6.E, and k_2 is a constant defined in Appendix 6.F.

Then, the following claims hold true.

P1: $x_\star$ is an asymptotically stable equilibrium of the closed-loop system, with Lyapunov function

$$\begin{aligned} H_d(x) = &-\frac{1}{2}\left(x_2+\sqrt{2}D\arctan\left(\tfrac{\sqrt{2}x_1}{x_2}\right)\right) - \\ &-\frac{D\operatorname{arctanh}\left(\frac{x_1}{\sqrt{x_1^2+\frac{x_2^2}{2}}}\right)}{2\sqrt{x_1^2+\frac{x_2^2}{2}}} + \frac{k_1}{2}(x_1^2+\frac{x_2^2}{2}+k_2)^2. \end{aligned} \tag{6.20}$$

P2: There exists a sufficiently small positive constant c such that the sublevel set of the function $H_d(x)$

$$\Omega_x := \{x \in \mathbb{R}^2 :\ H_d(x) \le c\}, \tag{6.21}$$

is strictly contained in the positive orthant of $\mathbb{R}^2$, being hence an estimate of the region of attraction. That is, for all $x(0) \in \Omega_x$, it follows that $x(t) \subset \Omega_x, \forall t \ge 0$, and $\lim_{t\to\infty} x(t) = x_\star$.

Proof. See Appendix 6.A. □□□

6.4 Adaptive IDA-PBC Using an Immersion and Invariance Power Estimator

In this section, the case of unknown power D is considered and an estimator of this parameter, based on the I&I technique [8], is presented.

Proposition 6.4. Consider the model (6.4), under Assumptions 6.1 and 6.2, in closed-loop with an adaptive version of the control (6.17), which is defined as

$$u = \frac{1}{u_0}\left(u_1 + u_2\right)|_{D\equiv\hat{D}}, \tag{6.22}$$

where u_0, u_1 and u_2 are defined in (6.18) and $\hat{D}(t)$ is an on-line estimate of D, generated with the I&I estimator

$$\hat{D} = -\frac{1}{2}\gamma x_2^2 + D_I, \tag{6.23}$$

$$\dot{D}_I = \gamma x_1 x_2(1-u) + \frac{1}{2}\gamma^2 x_2^2 - \gamma D_I, \tag{6.24}$$

where $\gamma > 0$ is a free parameter. Then, there exists $k_1^{\min}$ such that for all $k_1 > k_1^{\min}$ the overall system has an *asymptotically stable* equilibrium at $(x, \hat{D}) = (x_\star, D)$. Moreover, *for all* initial conditions of the closed-loop system and all $D_I(0)$, then

$$\tilde{D}(t) = e^{-\gamma t}\tilde{D}(0), \tag{6.25}$$

where $\tilde{D} := \hat{D} - D$ is the parameter estimation error.

Proof. See Appendix 6.B. □□□

Remark 6.2. The experimental implementation of the proposed controller, described by eqs. (6.17) and (6.22), requires an initialisation stage that will ramp-up the output voltage to a neighbourhood of the input voltage. Nonetheless, this is a very common practice in many applications.

6.5 Simulation Results

In this section the performance of the proposed adaptive IDA-PBC is illustrated via some computer simulations. Moreover, its transient behavior is compared with the one of a PD controller that has been designed adopting the classical linearization technique.

In simulations, the boost mode and buck mode are tested under the proposed IDA-PBC, respectively. The system parameters of the boost mode are given in [60], which read as $P = 61.25$ W, $C = 500$ μF, $L = 470$ μH, $E = 10$ V, $v_\star = 40$ V. The desired equilibrium is fixed as $x_\star = (0.7423, 4)$. Additionally, the system parameters of the buck mode are chosen as $P = 6$ W, $E = 25$ V, $v_\star = 15$ V and the desired equilibrium is fixed as $x_\star = (0.01489,\ 0.6)$. For simplicity, only the scaled system (6.4) is simulated; however, depending on the context, the plots are shown either for x or for the original coordinates (i, v)—recalling that they are simply related by the scaling factors given in (6.3).

6.5.1 PD controller

To underscore the limitations of the PD controller and the difficulties related with its tuning, the local stability analysis of such a controller is presented. From (6.4), the error dynamics is obtained as

$$\begin{aligned}\dot{e}_1 &= -(1-e_u-u_\star)(e_2+x_{2\star})+e_u+u_\star,\\ \dot{e}_2 &= (1-e_u-u_\star)(e_1+x_{1\star})-\frac{D}{e_2+x_{2\star}},\end{aligned}$$

with error functions

$$e_1 := x_1 - x_{1\star},\ e_2 := x_2 - x_{2\star},\ e_u := u - u_\star,$$

and $u_\star := \frac{x_{2\star}}{1+x_{2\star}}$. A standard PD controller for the error dynamics is given by

$$e_u = k_p e_1 + k_d e_2, \tag{6.26}$$

where k_p, k_d are tuning gains. Notice that, for the computation of $x_{1\star}$, the implementation of this controller requires the knowledge of D. The Jacobian matrix of the closed-loop system, $\dot{e} = F(e)$, evaluated at the equilibrium point, is given by

$$\begin{aligned}J :&= \left[\begin{array}{cc}\nabla_{e_1}F_1(e) & \nabla_{e_2}F_1(e)\\ \nabla_{e_1}F_2(e) & \nabla_{e_2}F_2(e)\end{array}\right]\Bigg|_{e=0}\\ &= \left[\begin{array}{cc}k_p(1+x_{2\star}) & k_d+k_dx_{2\star}-\frac{1}{1+x_{2\star}}\\ \frac{1}{1+x_{2\star}}-\frac{Dk_p(1+x_{2\star})}{x_{2\star}} & -\frac{D(-1+k_dx_{2\star}(1+x_{2\star}))}{x_{2\star}^2}\end{array}\right],\end{aligned}$$

where $\nabla_{e_i}F_j(e) := \frac{\partial F_j(e)}{\partial e_i}$. The matrix J is Hurwitz if and only if its trace is negative and its determinant is positive, which are given by

$$\begin{aligned}\mathrm{tr}(J) &= k_p(1+x_{2\star}) - k_dD(\frac{1}{x_{2\star}}+1)+\frac{D}{x_{2\star}^2},\\ \det(J) &= k_p\frac{D}{x_{2\star}^2} - k_d + \frac{1}{(x_{2\star}+1)^2}.\end{aligned}$$

Defining the positive constants

$$\begin{aligned}m_1 &:= \frac{x_{2\star}}{D},\ b_1 := \frac{1}{x_{2\star}+x_{2\star}^2},\\ m_2 &:= \frac{D}{x_{2\star}^2},\ b_2 := \frac{1}{(1+x_{2\star})^2}.\end{aligned}$$

The trace-determinant stability conditions can be written as the two-sided inequality

$$m_2k_p + b_2 > k_d > m_1k_p + b_1, \tag{6.27}$$

which is a conic section in the plane $k_d - k_p$, that reveals the conflicting role of the two gains. Notice that the extracted power D enters in the first slope m_1 in the denominator, while it appears in the nominator in m_2—rendering harder the gain tuning task regarding this uncertain parameter.

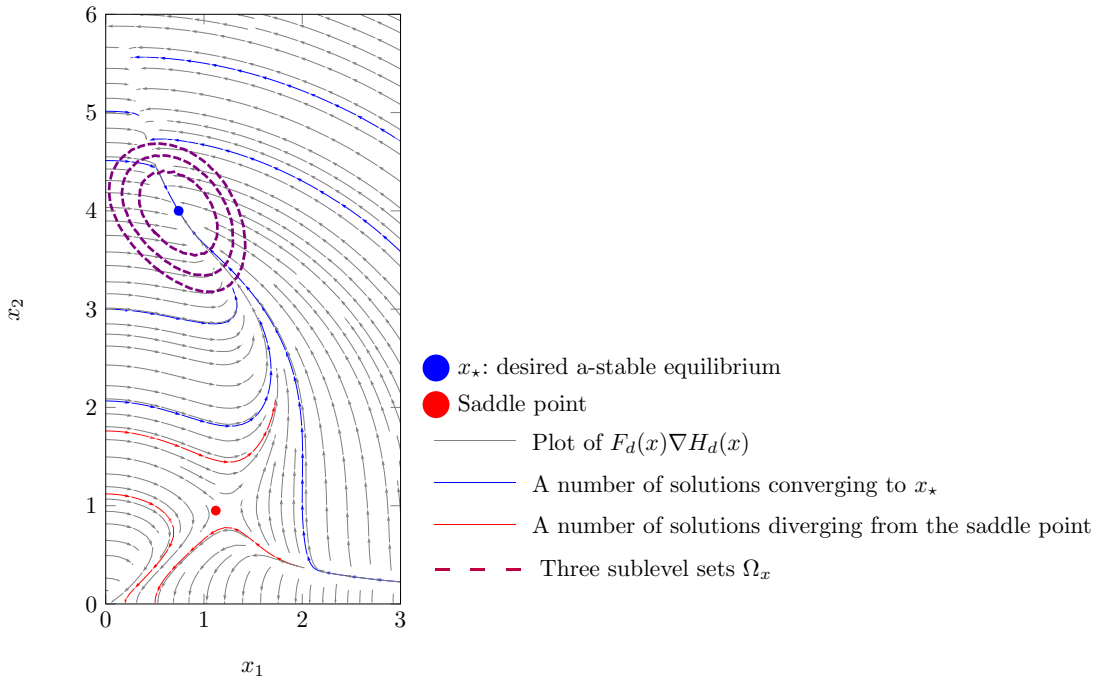

Figure 6.2: Phase plot of the system with the IDA-PBC ($k_1 = 0.01$) under boost mode, three sublevel sets Ω_x and trajectories (red) for different initial conditions.

6.5.2 IDA-PBC vs PD: Phase plots and transient response

The state-space of the closed-loop system, both with the non-adaptive IDA-PBC (6.4) and with PD controller (6.26), is a subset of the $\mathbb{R}^2$. Then, it is possible to get the global picture of the behavior of these controllers by drawing the phase plot in both cases.

Boost mode operation: In Fig. 6.2 is shown the phase plot of the closed-loop system under the designed IDA-PBC, where a particular value of the design parameter k_1 has been taken. In the same figure, some trajectories for different initial conditions are also shown and three sublevel sets Ω_x[2]—which are positively-invariant. The selected k_1 satisfy (6.19) since, for this case, $k_1 > \max\{-0.1208, \ -0.058\}$. It can be seen that the state trajectories for initial conditions starting in Ω_x remain there and converge to the desired equilibrium point, $x_\star$, marked in the plot as a blue point. Moreover, the phase portrait gives an idea of the region of attraction of this equilibrium. Clearly, the latter does not cover whole positive orthant of $\mathbb{R}^2$. Indeed, it is possible to show that the closed-loop vector field has another equilibrium in the positive orthant of $\mathbb{R}^2$ that corresponds to a saddle point, which is illustrated as a red point in the same plot.

Buck mode operation: Fig. 6.3 shows the phase plot of the system in a buck mode operation, under the proposed IDA-PBC controller. The the control parameter k_1 is chosen to satisfy inequality (6.19). It can be concluded from this and the previous figure that the designed controller has a good performance in both modes of the buck-boost converter.

[2]see equation (6.21)

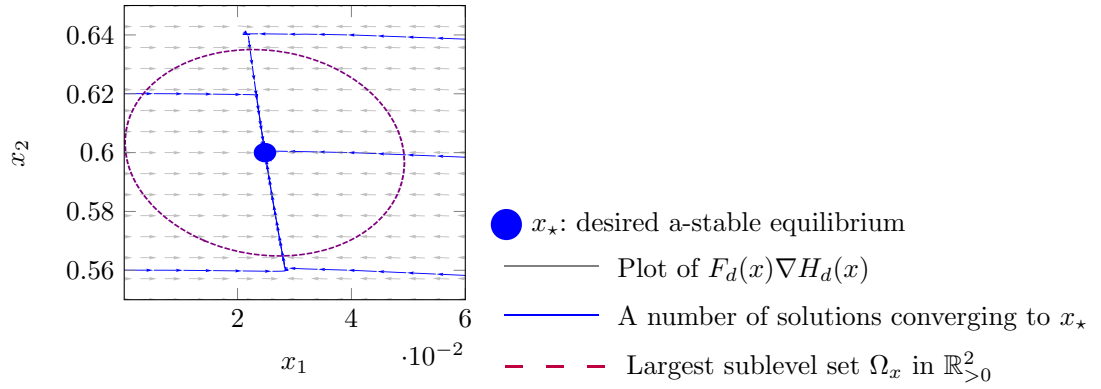

Figure 6.3: Phase portrait of the system with the IDA-PBC ($k_1 = 0.01$) under buck mode, three sublevel sets Ω_x and trajectories (red) for different initial conditions.

Buck mode (PD controller) In Fig. 6.4 is presented the phase plot of the system in closed-loop with the PD controller of equation (6.26). The controller's parameters are chosen as $k_p = -0.4, k_d = -1.5$, which satisfy the condition (6.27), numerically given in this scenario by

$$0.037k_p + 0.04 > k_d > 6.7358k_p + 0.0588.$$

Only those trajectories starting very close to the equilibrium remain in the positive orthant of $\mathbb{R}^2$ and converge to $x_\star$. Compared with Fig. 6.2, the IDA-PBC provides a much bigger region of attraction and, moreover, gives explicit estimates of it. Other values for the gains k_p and k_d have been tried yielding very similar inadmissible behaviors and are hence not reported here.

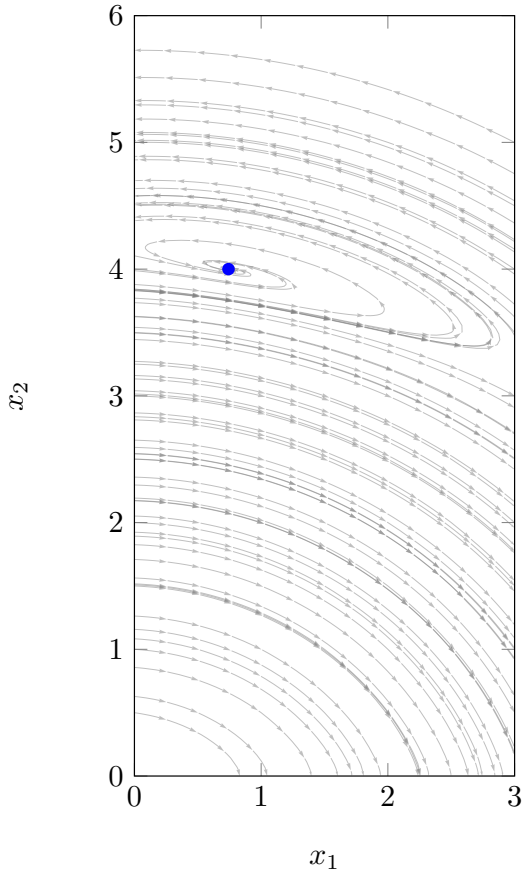

Figure 6.4: Phase portrait of the system with a PD controller.

Transient response comparison: Considering once again the boost mode, in Fig. 6.5 the transient responses of the output voltage v and the duty ratio u under the IDA-PBC and the PD controller, taking the same initial condition of $x(0) = (0.4, 3.9)$ are presented. The control gains are $k_1 = 0.01$ for the former and $k_p = -0.4, k_d = -1.5$ for the latter. It can be observed that the IDA-PBC has a faster transient performance with a smaller control signal.

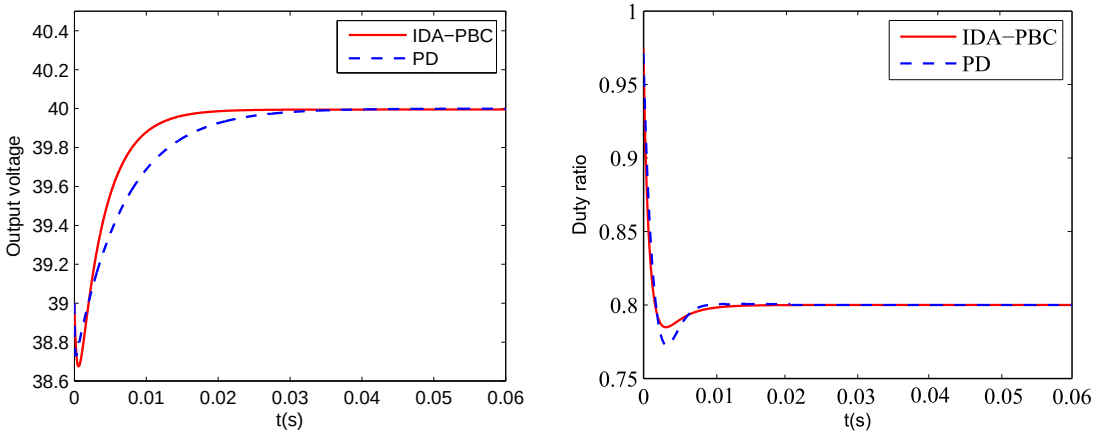

Figure 6.5: Response curves of DC-DC buck-boost converter with a CPL for the IDA-PBC and the PD controller.

6.5.3 Adaptive IDA-PBC with time-varying D

For the boost mode, Fig. 6.6 shows the profiles of the output voltage and the inductor current for the adaptive IDA-PBC—for different values of the control gain k_1 and adaptation gain $\gamma = 1$—in the face of step changes in the extracted power D. It is seen that increasing the control gain k_1 reduces the convergence time of the output voltage. It is also shown that the output voltage recovers very fast from the variations of the power D, always converging to the desired equilibrium. This is due to the fact that, as predicted by the theory, the power estimate converges—exponentially fast—to the true value independently of the control signal. It should be remarked that the PD controller becomes unstable in this scenario.

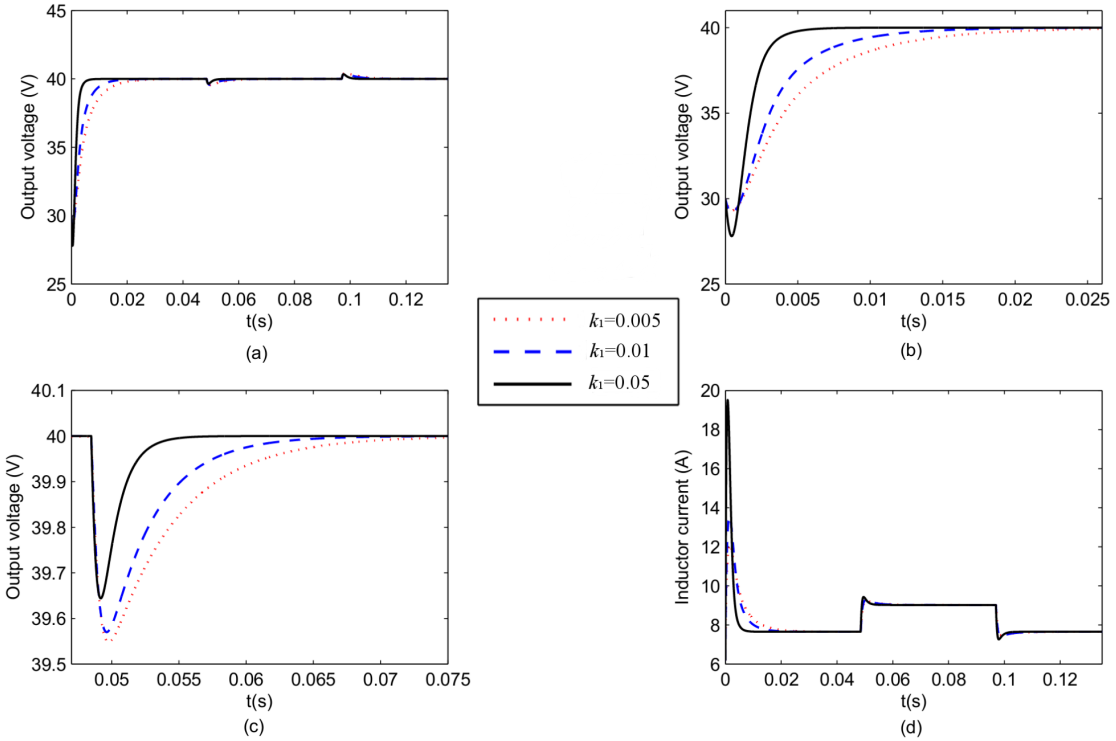

Figure 6.6: Response curves for the adaptive IDA-PBC with $\gamma = 1$ to changes in the power D: (a) output voltage—with (b) and (c) zooms for it—and (d) the inductor current.

In Fig. 6.7 the step changes in the power D and the estimate $\hat{D}$ for different values of the adaptation gain, with the initial condition $\hat{D}(0) = D(0)$, are shown. As predicted by the theory, for a larger γ, the speed of convergence of the estimator is faster. Notice, however, that in the selection of γ, there is a tradeoff between convergence speed and noise sensitivity.

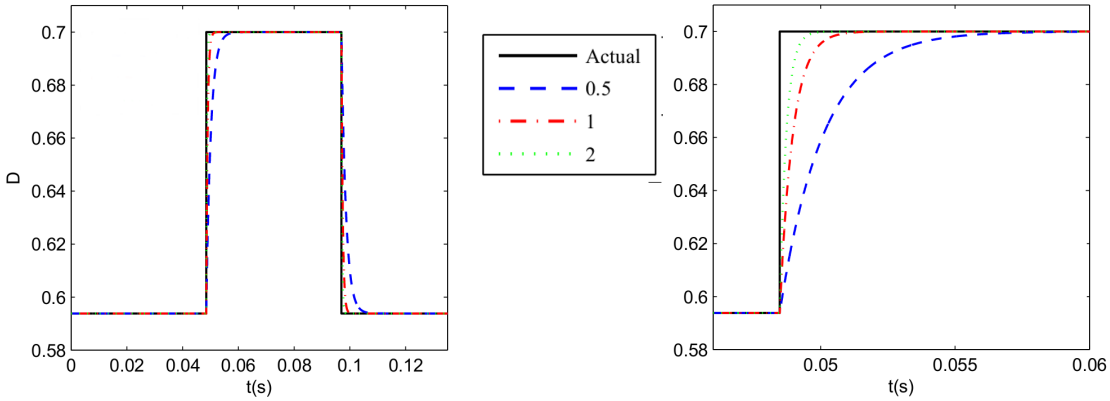

Figure 6.7: Transient performance of the estimate $\hat{D}$ under step changes of the parameter D for various adaptation gains γ and a zoom of the first step.

6.6 Summary

The challenging problem of regulation of the output voltage of a buck-boost converter supplying electric energy to a CPL with unknown power has been addressed in this chapter. First, assuming the power is known, an IDA-PBC that renders a desired equilibrium point asymptotically stable has been proposed. Subsequently, an on-line I&I estimator with global convergence property has been presented to renders the scheme adaptive, preserving the asymptotic stability property. It has also been illustrated the performance limitations of the classical PD controller stemming from the fact that, due to the presence of the CPL, the system is non-minimum phase. Some realistic simulations have been provided to confirm the effectiveness of the proposed method.

Technical Appendices of the Chapter

6.A Proof of Proposition 6.3

Proof of Claim **P1**: It is shown first that the control (6.17) can be derived using the IDA-PBC method of Proposition 6.2.

First, assign the matrix F_d as

$$F_d(x) := \begin{bmatrix} -\frac{x_2}{x_1} & -\frac{2x_2}{x_2+1} \\ \frac{2x_2}{x_2+1} & -\frac{2x_1}{(x_2+1)^2} \end{bmatrix},$$

that, for x in the positive orthant of $\mathbb{R}^2$, satisfies the condition (6.14).[3] Now, observe that the system (6.4) can be rewritten in the form (6.10), with

$$f(x) := \begin{bmatrix} -x_2 \\ x_1 - \frac{D}{x_2} \end{bmatrix}, \quad g(x) = \begin{bmatrix} x_2 + 1 \\ -x_1 \end{bmatrix}.$$

[3]It is well-known [81] that a key step for the successful application of the method is a suitable selection of this matrix, which is usually guided by the study of the solvability of the PDE (6.12). See [44] for some guidelines for its selection in this example.

The left annihilator of $g(x)$ is then $g^{\perp}(x) := [x_1 \; x_2 + 1]$. It follows that the PDE (6.12) can be written explicitly as

$$-x_2 \nabla_{x_1} H_d(x) + 2x_1 \nabla_{x_2} H_d(x) = D - x_1 + \frac{D}{x_2}. \tag{6.28}$$

Using the symbolic language Mathematica, the solution of the PDE (6.28) is computed as

$$\begin{aligned} H_d(x) = &-\frac{1}{2}\left(x_2 + \sqrt{2}D \arctan\left(\tfrac{\sqrt{2}x_1}{x_2}\right)\right) \\ &- \frac{D \operatorname{arctanh}\left(\frac{x_1}{\sqrt{x_1^2+\frac{x_2^2}{2}}}\right)}{2\sqrt{x_1^2+\frac{x_2^2}{2}}} + \Phi(x_1^2 + \frac{x_2^2}{2}), \end{aligned}$$

where $\Phi(\cdot)$ is any function with argument $\left(x_1^2 + \frac{x_2^2}{2}\right)$, which is selected as

$$\Phi(z) := \frac{k_1}{2}(z + k_2)^2,$$

with k_1 and k_2 arbitrary constants.

The existence of constants k_1 and k_2 guaranteeing that $x_\star$ is a critical point of H_d and that, furthermore, is a local minimum of it, are verified next.

Evaluate the gradient of $H_d(x)$, shown in Appendix 6.C, at the equilibrium $x_\star$[4] and substitute k_2 as presented in Appendix 6.F, which results in $\nabla H_d|_{x=x_\star} = 0$, implying that $x_\star$ is a critical point of H_d.

Now, a sufficient condition for $x_\star$ to be a local minimum of H_d, is that

$$M := \nabla^2 H_d|_{x=x_\star} > 0.$$

Being $\nabla^2 H_d$ a 2×2 real matrix,[5] the above condition is equivalent to

$$m_{11} > 0, \quad \det(M) > 0,$$

where m_{11} is the (1,1) entry of M. Regarding these expressions, the following equivalences hold.

$$\begin{aligned} m_{11} &= a_0 + k_1\left(\frac{4D^2\left(x_{2\star}+1\right)^2}{x_{2\star}^2}\right) \\ \det(M) &= b_0 + k_1\left(\frac{x_{2\star}^4 - 2D^2\left(x_{2\star}+1\right)}{x_{2\star}^3}\right), \end{aligned}$$

where a_0 and b_0 are real constants defined in Appendix 6.E. Notice that both expressions are linear with respect to k_1 and that, furthermore, the coefficients of k_1 are positive if

$$0 < D < \frac{x_{2\star}^2}{\sqrt{2}\sqrt{1+x_{2\star}}}.$$

[4] Recall equation (6.6).

[5] For completeness, the entries of $\nabla^2 H_d$ are included in Appendix 6.D.

Consequently, $M > 0$ if and only if the latter inequality on D, and

$$k_1 > \max\{-\frac{a_0}{\left(\frac{4D^2(x_{2\star}+1)^2}{x_{2\star}^2}\right)}, \; -\frac{b_0}{\left(\frac{x_{2\star}^4-2D^2(x_{2\star}+1)}{x_{2\star}^3}\right)}\}$$

$$\Rightarrow$$

$$m_{11} > 0 \;\wedge\; \det(M) > 0,$$

are satisfied simultaneously, which hold by assumption. The proof is completed showing that the IDA-PBC (6.17) results replacing the data in (6.15).

Proof of Claim **P2**: It has been shown that $H_d(x)$ has a positive definite Hessian matrix at $x_\star$, therefore it is locally *convex*. Then, for sufficiently small c, the sublevel set Ω_x defined in (6.21) is bounded and strictly contained in the positive orthant of $\mathbb{R}^2$. The proof is completed recalling that sublevel sets of strict Lyapunov functions are inside the region of attraction of the equilibrium. □□□

6.B Proof of Proposition 6.4

Computing the time-derivative of the estimation error, $\tilde{D}$, along the trajectories of (6.4), and using the expression (6.23), it follows that

$$\begin{aligned}\dot{\tilde{D}} &= -\gamma x_2 \dot{x}_2 + \dot{D}_I \\ &= -\gamma x_1 x_2 (1-u) + \gamma D + \dot{D}_I.\end{aligned}$$

Substituting (6.24) in the last equation yields

$$\begin{aligned}\dot{\tilde{D}} &= \gamma D + \frac{1}{2}\gamma^2 x_2^2 - \gamma D_I \\ &= -\gamma \tilde{D},\end{aligned}$$

from which (6.25) follows immediately.

To prove the asymptotic stability of $(x, \hat{D}) = (x_\star, D)$, the adaptive controller (6.22) is written as

$$\hat{u} := \frac{1}{u_0}\left(u_1 + u_2\right)|_{D\equiv\hat{D}}.$$

Then, the following holds

$$\hat{u} = u|_{D\ (\text{exact})} + \delta(x, \tilde{D}),$$

where $u|_{D\ (\text{exact})}$ denotes the controller (6.17). That is, the controller that assumes an exact knowledge of D is recovered, plus an additive disturbance $\delta(x, \tilde{D})$; the mapping δ can be proved to satisfy $\delta(x, 0) = 0$.

Invoking the proof of Proposition 6.3, the closed-loop system is now a cascaded system of the form

$$\begin{aligned}\dot{x} &= F_d(x)\nabla H_d(x) + g(x)\delta(x, \tilde{D}, k_1) \\ \dot{\tilde{D}} &= -\gamma \tilde{D},\end{aligned}$$

where

$$g(x) := \begin{bmatrix} x_2 + 1 \\ -x_1 \end{bmatrix},$$

is the systems input matrix. The signal $\tilde{D}(t)$ tends to zero exponentially fast for all initial conditions, and for sufficiently large k_1, *i.e.*, such that (6.19) is satisfied, the system above with $\tilde{D} = 0$ is asymptotically stable. Invoking well-known results of asymptotic stability of cascaded systems, *e.g.*, Proposition 4.1 of [101], the proof of (local) asymptotic stability is completed. □□□

6.C Explicit form of ∇H_d

$$\begin{aligned}
\nabla_{x_1} H_d &= k_1 x_1 \left(2\left(k_2 + x_1^2\right) + x_2^2\right) - \frac{D\left(x_2+1\right)}{2x_1^2 + x_2^2} \\
&\quad + \frac{\sqrt{2} D x_1 \operatorname{arctanh}\left(\frac{x_1}{\sqrt{x_1^2 + \frac{x_2^2}{2}}}\right)}{\left(2x_1^2 + x_2^2\right)^{3/2}} \\
\nabla_{x_2} H_d &= \frac{D x_1 \left(x_2+1\right)}{x_2^3 + 2x_1^2 x_2} + \frac{1}{2} k_1 x_2^3 + k_1 x_1^2 x_2 + 2 k_1 k_2 x_2 - \frac{1}{2} \\
&\quad + \frac{\sqrt{2} D x_2 \operatorname{arctanh}\left(\frac{x_1}{\sqrt{x_1^2 + \frac{x_2^2}{2}}}\right)}{\left(2x_1^2 + x_2^2\right)^{3/2}}
\end{aligned}$$

6.D Components of the Hessian matrix $\nabla^2 H_d$

$$
\begin{aligned}
\nabla^2_{x_1} H_d = {} & 4k_1 x_1^2 - \frac{6\sqrt{2}D \operatorname{arctanh}\left(\frac{x_1}{\sqrt{x_1^2+\frac{x_2^2}{2}}}\right) x_1^2}{\left(2x_1^2+x_2^2\right)^{5/2}} \\
& + \frac{\sqrt{2}D\left(\frac{1}{\sqrt{x_1^2+\frac{x_2^2}{2}}} - \frac{x_1^2}{\left(x_1^2+\frac{x_2^2}{2}\right)^{3/2}}\right) x_1}{\left(2x_1^2+x_2^2\right)^{3/2}\left(1-\frac{x_1^2}{x_1^2+\frac{x_2^2}{2}}\right)} \\
& + \frac{4D\left(x_2+1\right)x_1}{\left(2x_1^2+x_2^2\right)^2} + k_1\left(x_2^2+2\left(x_1^2+k_2\right)\right) \\
& + \frac{\sqrt{2}D \operatorname{arctanh}\left(\frac{x_1}{\sqrt{x_1^2+\frac{x_2^2}{2}}}\right)}{\left(2x_1^2+x_2^2\right)^{3/2}} \\
\nabla_{x_1 x_2} H_d = {} & -\frac{Dx_2x_1^2}{\sqrt{2}\left(x_1^2+\frac{x_2^2}{2}\right)^{3/2}\left(2x_1^2+x_2^2\right)^{3/2}\left(1-\frac{x_1^2}{x_1^2+\frac{x_2^2}{2}}\right)} + 2k_1x_2x_1 \\
& - \frac{3\sqrt{2}D \operatorname{arctanh}\left(\frac{x_1}{\sqrt{x_1^2+\frac{x_2^2}{2}}}\right) x_2x_1}{\left(2x_1^2+x_2^2\right)^{5/2}} - \frac{D}{2x_1^2+x_2^2} + \frac{2Dx_2\left(x_2+1\right)}{\left(2x_1^2+x_2^2\right)^2} \\
\nabla^2_{x_2} H_d = {} & k_1x_1^2 + \frac{Dx_1}{x_2^3+2x_1^2x_2} - \frac{D\left(x_2+1\right)\left(2x_1^2+3x_2^2\right)x_1}{\left(x_2^3+2x_1^2x_2\right)^2} \\
& - \frac{Dx_2^2x_1}{2\sqrt{2}\left(x_1^2+\frac{x_2^2}{2}\right)^{3/2}\left(2x_1^2+x_2^2\right)^{3/2}\left(1-\frac{x_1^2}{x_1^2+\frac{x_2^2}{2}}\right)} \\
& + \frac{3}{2}k_1x_2^2 + 2k_1k_2 + \frac{\frac{\sqrt{2}}{2}D \operatorname{arctanh}\left(\frac{x_1}{\sqrt{x_1^2+\frac{x_2^2}{2}}}\right)}{\left(2x_1^2+x_2^2\right)^{3/2}} \\
& - \frac{3\sqrt{2}D \operatorname{arctanh}\left(\frac{x_1}{\sqrt{x_1^2+\frac{x_2^2}{2}}}\right) x_2^2}{2\left(2x_1^2+x_2^2\right)^{5/2}}
\end{aligned}
$$

6.E Values of the constants a_0 and b_0.

$$
\begin{aligned}
a_0 &= \tfrac{x_{2s}^3}{\left(2D^2(x_{2s}+1)^2+x_{2s}^4\right)^3}\left(a_0'+a_0''\right),\\
a_0' &= \left(2D^2\left(x_{2s}+1\right)^2+x_{2s}^4\right)\left(2D^2\left(x_{2s}+1\right)\left(3x_{2s}+4\right)+x_{2s}^4\right),\\
a_0'' &= -6\sqrt{2}D^3x_{2s}\left(x_{2s}+1\right)^2\sqrt{\tfrac{2D^2(x_{2s}+1)^2+x_{2s}^4}{x_{2s}^2}}\operatorname{arctanh}\left(\frac{D\left(\frac{1}{x_{2s}}+1\right)}{\sqrt{D^2\left(\frac{1}{x_{2s}}+1\right)^2+\frac{x_{2s}^2}{2}}}\right).
\end{aligned}
$$

$$
\begin{aligned}
b_0 &= \tfrac{x_{2s}^2}{2\left(D^2(x_{2s}+1)^2+x_{2s}^4\right)^3}\left(b_0'+b_0''\right)\\
b_0' &= -4D^4\left(x_{2s}+1\right)^2\left(x_{2s}\left(x_{2s}+5\right)+5\right)-2D^2\left(3x_{2s}+4\right)x_{2s}^4\\
b_0'' &= -3\sqrt{2}Dx_{2s}\left(x_{2s}^4-2D^2\left(x_{2s}+1\right)\right)\quad\times\\
&\quad\times\sqrt{\tfrac{2D^2(x_{2s}+1)^2+x_{2s}^4}{x_{2s}^2}}\operatorname{arctanh}\left(\frac{D\left(\frac{1}{x_{2s}}+1\right)}{\sqrt{D^2\left(\frac{1}{x_{2s}}+1\right)^2+\frac{x_{2s}^2}{2}}}\right)+x_{2s}^8
\end{aligned}
$$

6.F Value of the constant k_2

$$k_2 = \frac{1}{k_2'}\left(k_2''+k_2'''\right)$$

where

$$
\begin{aligned}
k_2' &= -2k_1x_{2\star}^2\left(2D^2\left(x_{2\star}+1\right)^2+x_{2\star}^4\right)^2\\
k_2'' &= \sqrt{2}Dx_{2\star}^6\sqrt{\tfrac{2D^2(x_{2\star}+1)^2+x_{2\star}^4}{x_{2\star}^2}}\operatorname{arctanh}\left(\frac{D\left(\frac{1}{x_{2\star}}+1\right)}{\sqrt{D^2\left(\frac{1}{x_{2\star}}+1\right)^2+\frac{x_{2\star}^2}{2}}}\right)\\
k_2''' &= \left(2D^2\left(x_{2\star}+1\right)^2+x_{2\star}^4\right)\left(4D^4k_1\left(x_{2\star}+1\right)^4\right.\\
&\quad\left.+4D^2k_1\left(x_{2\star}+1\right)^2x_{2\star}^4+x_{2\star}^5\left(k_1x_{2\star}^3-1\right)\right)
\end{aligned}
$$

Chapter 7

Damping Injection on a Small-scale, DC Power System

Synopsis This chapter explores a nonlinear, adaptive controller aimed at increasing the stability margin of a direct-current (DC), small-scale, electrical network containing an *unknown* constant power load. Due to its negative incremental impedance, this load reduces the effective damping of the network, which may lead to voltage oscillations and even to voltage collapse. To overcome this drawback this chapter considers the incorporation of a controlled DC-DC power converter in parallel with the load. The design of the control law for the converter is particularly challenging due to the existence of states that are difficult to measure in a practical context, and due to the presence of unknown parameters. To tackle these obstacles, a standard input-output linearization stage, in combination with a suitably tailored adaptive observer, is proposed. The good performance of the controller is evaluated through experiments on a small-scale network.

7.1 Introduction

Various techniques have been explored for the stabilization of DC networks with CPLs—a survey may be found in [109]. These techniques are categorized into passive and active damping methods: the former are based on open-loop hardware alterations, whereas the latter imply the modification of existing—or added—control loops. In an active damping strategy the control loops can be modified at three different network's positions [109]: at the source's side, at the load's side, and at a midpoint between them. In the present chapter, the interest is in using the latter approach, which was firstly explored in [19], [129], and [55], for the stabilization of a small-scale network with a single CPL. In these references the network's stabilization is achieved by adding a *controlled* power converter in parallel with the load and then designing a suitable feedback control law for it: in [19] the converter is modeled as a simple controlled current source and a linear control law is designed to stabilize the overall network; a similar approach, but using a full model for the power converter, is used in [129]. Their stabilization result is based on the linearization of the network's dynamics. Lastly, in [55] a large signal stability analysis, but using approximate techniques, such as the Takagi-Sugeno fuzzy model, is carried out to evaluate the performance of a linear controller.

The main contribution of this chapter is described next. Following [19] and [129],

the stabilization problem for a small-scale DC network supplying electrical energy to a CPL is studied here. First, the network is augmented by placing a controlled power converter between the load and the source. Then, for the converter's controller design, instead of relying on linear-feedback techniques, this chapter proposes an adaptive observer-based nonlinear control law that provably achieves overall network's stabilization. The control design is particularly challenging due to the existence of unmeasured states—the current of the DC network—and the unknown power of the CPL. The construction of the proposed controller is based on the use of standard *input-output linearization* to which a suitably tailored *adaptive observer* is added; its good performance is evaluated via experiments on a small-scale DC network.

The stabilization problem addressed here, as well as the proposed controller topology, have previously been studied in [66], where a *full state-feedback* adaptive passivity-based control has been proposed. As discussed in Subsection 7.4.1, besides the impractical requirement of full state measurement, the approach adopted in that paper suffers from significant energy efficiency drawbacks, which renders the proposed controller design practically unfeasible. Both limitations are overcome in this chapter.

The rest of the chapter is structured as follows. In Section 7.2 the model of the system under study is presented and its stability properties are summarized. The proposed controller configuration, adopted from [19] and [129], is presented in Section 7.3. The main contributions of the chapter are developed in Section 7.4 and some preliminary realistic simulations are shown in Section 7.5. The results of two physical experimental are reported in Section 7.6 and the chapter is wrapped-up with a brief summary in Section 7.7.

7.2 Problem Formulation

7.2.1 Description of the system without the shunt damper

The electrical circuit diagram of the network under study is shown in Fig. 7.1. It represents a simplified model of a DC power system and has been used in the literature, *e.g.*, in [129], [79] and [127], to study the stability problems associated with CPLs. It is composed of a DC voltage source supplying energy to an instantaneous CPL and the transmission line is simply represented by the lossy inductor $L_1 > 0$. The CPL is assumed to be connected through the bus capacitor $C_1 > 0$. The network's dynamics are described by

$$\begin{aligned} L_1\dot{x}_1 &= -r_1 x_1 - x_2 + E, \\ C_1\dot{x}_2 &= x_1 - \frac{P}{x_2}, \end{aligned} \tag{7.1}$$

where x_1 and x_2 denote the current through L_1 and the voltage across C_1, respectively. The *constant* parameter P corresponds to the power extracted from, or injected to, the network by the CPL, being positive in the former case and negative in the latter—in the sequel, only the case $P \geq 0$ is studied. The state space for this system is defined as the set

$$\{(x_1, x_2) \in \mathbb{R}^2 : \ x_2 > 0\}.$$

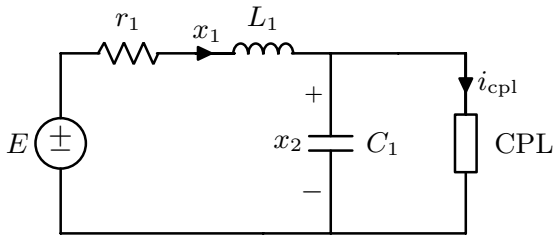

Figure 7.1: A DC source supplying power to an instantaneous CPL.

7.2.2 Equilibrium analysis

From [66], the properties of this network are enlisted as follows.

P1 The system (7.1) has two real equilibria if and only if

$$E^2 - 4Pr_1 \geq 0 \;\Leftrightarrow\; P \leq \frac{E^2}{4r_1}. \tag{7.2}$$

P2 One equilibrium corresponds to a high voltage/low current characteristic, which is stable only if

$$P \leq \frac{E^2 C_1 L_1 r_1}{(L_1 + C_1 r_1^2)^2}, \tag{7.3}$$

whenever $C_1 < \frac{L_1}{r_1^2}$.

P3 If $C_1 > \frac{4L_1}{r_1^2}$, the strict satisfaction of (7.2) is sufficient for asymptotic stability of the equilibrium in P2.

Notice that if P is negative, *i.e.,* if the load behaves as a constant power *source*, then the expressions (7.2) and (7.3) are simultaneously satisfied; consequently, this scenario poses no treat regarding voltage collapse nor network's instability, hence the focus on the case $P \geq 0$.

7.2.3 Objectives and methodology

To introduce and support the methodology used in the chapter, the following remarks are enlisted; see [66].

R1 Observe from P2 that if the capacitance C_1 is not big enough then, in order to maintain the system's stability, the power extraction from the CPL must be strictly smaller than the upper bound for existence of equilibria given in (7.3).

R2 P3 suggests a passive method to enlarge the domain of values of P for which stability is ensured. It consists in increasing the effective capacitance C_1, which can be achieved with the *open-loop* parallel interconnection of a suitable capacitor and the CPL. Some disadvantages of this approach are reviewed in [19, Section III.A].

In view of these remarks the *control objectives* are specified as follows.

O1 Regulate the voltage x_2 around a constant value.

O2 Relax the upper bound for P established in (7.3).

O3 Achieve these objectives without the knowledge of P.

Following the work of [19] and [129], to achieve these objectives a power converter is connected in parallel with the CPL and design a control strategy that stabilizes the overall network to a desired equilibrium point. The detailed description of the augmented circuit is carried out in the next section and the presentation of the control law—which is the main contribution of the chapter—is done in Section 7.4.

7.3 Augmented Circuit Model

As proposed in [19] and [129], the network of Fig. 7.1 is augmented by adding a controlled DC-DC power converter in parallel with the load, which results in the circuit shown in Fig. 7.2. The converter, which in the sequel is referred to as *shunt damper*, is composed of two complementary switches u and $(1-u)$, a lossy inductor $L_2 > 0$, a capacitor $C_2 > 0$, and a resistor $r_3 > 0$; the latter models the losses associated with the switching devices.

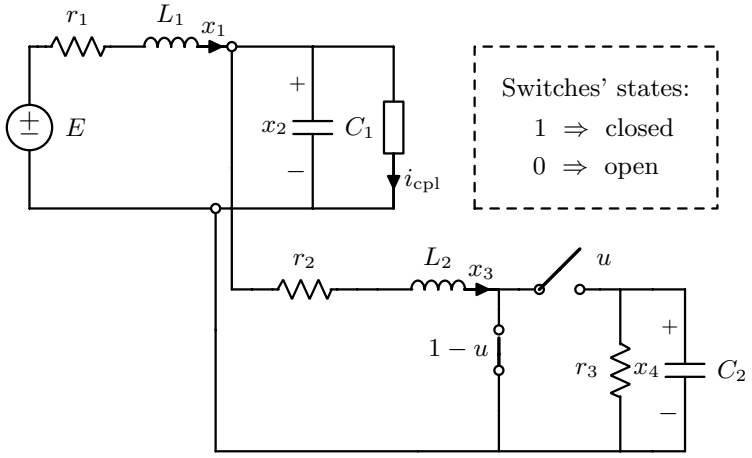

Figure 7.2: The network of Fig. 7.1 is augmented by adding a power converter in parallel with the load.

The averaged dynamic model of the augmented system is given by

$$\begin{aligned} L_1\dot{x}_1 &= -r_1x_1 - x_2 + E, \\ C_1\dot{x}_2 &= x_1 - \frac{P}{x_2} - x_3, \\ L_2\dot{x}_3 &= -r_2x_3 - ux_4 + x_2, \\ C_2\dot{x}_4 &= -\left(\tfrac{1}{r_3}\right)x_4 + ux_3, \end{aligned} \tag{7.4}$$

where x_3 is the current through L_2, x_4 is the voltage across C_2, and $u \in (0,1)$—which is the system's control variable—represents a duty cycle. The state space of

the system is given as

$$\mathcal{X} := \{x \in \mathbb{R}^4 : \ x_2 > 0, \ x_4 > 0\}.$$

It shall be underscored that x_1—being the current of a reduced model of the network—is *not measurable*, and the power P is *unknown*.

For future reference, the system (7.4) is written in an input-affine form, $\dot{x} = f(x) + g(x)u$, by defining

$$f(x) := \begin{bmatrix} -\frac{r_1}{L_1}x_1 - \frac{x_2}{L_1} + \frac{E}{L_1} \\ \frac{x_1}{C_1} - \frac{P}{C_1 x_2} - \frac{x_3}{C_1} \\ -\frac{r_2}{L_2}x_3 + \frac{x_2}{L_2} \\ -(\frac{1}{r_3})\frac{x_4}{C_2} \end{bmatrix}, \quad g(x) := \begin{bmatrix} 0 \\ 0 \\ -\frac{x_4}{L_2} \\ \frac{x_3}{C_2} \end{bmatrix}, \tag{7.5}$$

the i-th entries of which are denoted as f_i or g_i, respectively.

7.4 Main results

This section reports a nonlinear, adaptive, state-feedback controller that is such that the augmented network of Fig. 7.2 complies with the control objectives described in Subsection 7.2.3. Towards this end, first the existence of equilibria of (7.4) is analyzed and constraints, on the system's parameters, for their physical feasibility are established. Secondly, under the assumption that x_1 can be measured, and the constant parameter P is known, a full-information input-output linearization controller [48], that asymptotically stabilizes a specified equilibrium state, is presented. Finally, this controller is complemented with an observer for x_1 and an on-line estimator for P—yielding an adaptive, state-feedback controller design.

7.4.1 Existence of equilibria

A pair $(\bar{x}, \bar{u}) \in \mathcal{X} \times (0, 1)$ is an equilibrium of (7.4) if and only if it belongs to the set

$$\mathcal{E} := \{(\bar{x}, \bar{u}) \in \mathcal{X} \times \mathbb{R} : \ f(\bar{x}) + g(\bar{x})\bar{u} = 0\},$$

where the mappings f and g are given in (7.5). An important issue in the design is to ensure that the *power consumption* of the shunt damper is minimal. In order to carry-out this analysis, it is convenient to parametrize $\bar{x}$ in terms of $\bar{u}$, as follows.

Proposition 7.1. Consider the augmented circuit model (7.4). Fix $0 < \bar{u} < 1$ as a desired steady state duty cycle. Then the following conditions hold true.

C1 $(\bar{x}, \bar{u}) \in \mathcal{E}$ if and only if

$$\Delta(P) := E^2\ell_2 - 4Pr_1\ell_1 \geq 0, \tag{7.6}$$

where

$$\ell_1 := r_3\bar{u}^2 + r_1 + r_2, \ \ell_2 := r_3\bar{u}^2 + r_2$$

and

$$\begin{aligned}
\bar{x}_1 &= \frac{1}{2r_1\ell_1}\left[E(\ell_2+2r_1)-\sqrt{\ell_2}\sqrt{\Delta(P)}\right],\\
\bar{x}_2 &= \frac{1}{2\ell_1}[\sqrt{\ell_2}\sqrt{\Delta(P)}+E\ell_2],\\
\bar{x}_3 &= \frac{1}{2\ell_1}\left(\frac{\sqrt{\Delta(P)}}{\sqrt{\ell_2}}+E\right),\\
\bar{x}_4 &= \frac{r_3\bar{u}}{2\ell_1}\left(\frac{\sqrt{\Delta(P)}}{\sqrt{\ell_2}}+E\right).
\end{aligned} \tag{7.7}$$

C2 The power dissipated at the shunt damper in steady state, *i.e.,* the quantity

$$\begin{aligned}
\mathcal{P}_{\mathrm{L}}(P) &:= r_2\bar{x}_3^2+\frac{1}{r_3}\bar{x}_4^2,\\
&= \frac{r_3\bar{u}}{4\ell_1^2}\left(\frac{\sqrt{\Delta(P)}}{\sqrt{\ell_2}}+E\right)^2
\end{aligned}$$

attains a maximum at $P=0$ if and only if $\Delta(P)>0$.

Proof. The proof of the first claim follows from straightforward algebraic calculations. For the second claim consider

$$\frac{d\mathcal{P}_{\mathrm{L}}(P)}{dP} = -\frac{2r_1r_3\bar{u}}{\ell_1\sqrt{\Delta(P)}}\left(\frac{\sqrt{\Delta(P)}}{\sqrt{\ell_2}}+E\right),$$

which is strictly negative if and only if $\Delta(P)>0$, implying that $\mathcal{P}_{\mathrm{L}}(P)$ is a strictly decreasing function of P. Hence, it attains a maximum at $P=0$. □□□

In [66], the equilibria $(\bar{x},\bar{u})\in\mathcal{E}$ are parametrized in terms of $\bar{x}_2$, not in terms of $\bar{u}$, as follows

$$\begin{aligned}
\bar{x}_1 &= \frac{E-\bar{x}_2}{r_1},\\
\bar{x}_3 &= -\frac{Pr_1-E\bar{x}_2+\bar{x}_2^2}{r_1\bar{x}_2},\\
\bar{x}_4 &= \frac{1}{r_1\bar{x}_2}\sqrt{r_3\kappa_1(\bar{x}_2,P)\kappa_2(\bar{x}_2,P)},
\end{aligned} \tag{7.8}$$

where

$$\begin{aligned}
\kappa_1(\bar{x}_2,P) &:= -\left[Pr_1+\bar{x}_2(-E+\bar{x}_2)\right],\\
\kappa_2(\bar{x}_2,P) &:= Pr_1r_2+\bar{x}_2[-Er_2+(r_1+r_2)\bar{x}_2].
\end{aligned}$$

Then, the equilibrium $\bar{x}$, associated to $\bar{x}_2=\frac{E}{2}$, is singled out for stabilization. This choice allows the stable operation of the network in a wide range of values of P. Unfortunately, the steady-state shunt-damper's power dissipation is given in this case by $E^2/4r_1-P$, which implies a very low energetic efficiency when P is small.

The parametrization proposed in equation (7.7) implies a more involved algebraic expression for the damper's power losses, nonetheless, with an appropriate selection of $\bar{u}$ these losses can be made considerable inferior with respect to the approach adopted in [66]. The effectiveness of this choice is illustrated in the numerical experiments presented in Section 7.6.

7.4.2 Design of a full information stabilizing control law

This subsection presents a static, state-feedback control law that renders asymptotically stable the equilibrium point (7.7). For its design it is assumed that $P \geq 0$ is *known* and $\bar{u} \in (0,1)$ is fixed so (7.6) holds.

Following the ideas presented in [24, Section IV], a new input is introduced:

$$w = x_4 u,$$

which allows rewriting the system (7.4) in the cascade form shown in Fig 7.3, where

$$\Sigma^{13} : \begin{cases} L_1 \dot{x}_1 &= -r_1 x_1 - x_2 + E \\ C_1 \dot{x}_2 &= x_1 - \frac{P}{x_2} - x_3 \\ L_2 \dot{x}_3 &= -r_2 x_3 + x_2 - w, \end{cases} \tag{7.9}$$

and

$$\Sigma^4 : C_2 \dot{x}_4 = -(\tfrac{1}{r_3}) x_4 + \tfrac{1}{x_4} w x_3. \tag{7.10}$$

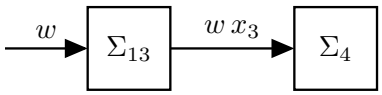

Figure 7.3: Block diagram for the cascaded interconnection between the subsystems (7.9) and (7.10).

The next proposition presents a control law that ensures voltage regulation and exponential stability of an equilibrium point of Σ^{13}.

Proposition 7.2. Fix the constant desired voltage $\bar{x}_2 > 0$. Consider the system (7.9) in closed-loop with the static-state feedback

$$\begin{aligned} w(x_1, x_2, x_3, P) &= -L_2 C_1 \left[\beta(x_2 - \bar{x}_2) + \alpha f_2(x_1, x_2, x_3)\right] \\ &+ x_2 - r_2 x_3 - L_2 \left[f_1(x_1, x_2) + \tfrac{P}{x_2^2} f_2(x_1, x_2, x_3)\right], \end{aligned} \tag{7.11}$$

where $\alpha > 0$ and $\beta > 0$ are design parameters, and the mappings f_i are defined in (7.5).

Then the output voltage error

$$y := x_2 - \bar{x}_2, \tag{7.12}$$

verifies

$$\ddot{y} + \alpha \dot{y} + \beta y = 0, \tag{7.13}$$

ensuring $\lim_{t\to\infty} y(t) = 0$ (exp.) Moreover, the equilibrium point $(\bar{x}_1, \bar{x}_2, \bar{x}_3)$ defined in (7.8) is exponentially stable.

Proof. See Appendix 7.A at the end of the chapter. □□□

The next proposition establishes the stability of the overall system.

Proposition 7.3. Fix the constant desired voltage $\bar{x}_2 > 0$. Consider the system (7.9), (7.10) in closed-loop with the static-state feedback (7.11). Assume the system's initial condition is sufficiently close to the equilibrium $\bar{x}$ defined in (7.8). Then, $x_4(t) > 0$, for all $t \geq 0$ and $\lim_{t\to\infty} x(t) = \bar{x}$, exponentially.

Proof. See Appendix 7.B at the end of the chapter. □□□

As a direct application of Propositions 7.2 and 7.3, the full-information input-output linearizing controller of the overall dynamics (7.4) is presented next.

Proposition 7.4. Consider the system (7.4) in closed-loop with the static state-feedback control law

$$u = \tfrac{1}{x_4} w(x_1, x_2, x_3, P), \tag{7.14}$$

where w is given in (7.11). Then, $\bar{x} \in \mathcal{E}$ is a locally, exponentially stable equilibrium point of the closed-loop system.

7.4.3 Stabilization with unknown CPL power

An adaptive version of controller (7.14) is established now by adding an *observer* for x_1 and an on-line *estimator* for the constant parameter P, which are now assumed to be unmeasured and unknown, respectively.

Proposition 7.5. Consider the system (7.1) and assume that x_2 is positive and belongs to the interval $[x_2^{\min}, x_2^{\max}]$. Define the adaptive observer

$$\begin{aligned}
\dot{q}_1 &= \frac{E}{L_1} - \frac{x_2}{L_1} - \frac{r_1}{L_1}\hat{x}_1 + k_1\hat{P} - k_1 x_2\hat{x}_1 + k_1 x_2 x_3,\\
\dot{q}_2 &= -k_2\hat{P} + k_2 x_2\hat{x}_1 - k_2 x_2 x_3,\\
\hat{x}_1 &= q_1 + \frac{1}{2}k_1 C_1 x_2^2,\\
\hat{P} &= q_2 - \frac{1}{2}k_2 C_1 x_2^2,
\end{aligned} \tag{7.15}$$

where k_1 and k_2 are such that

$$\begin{aligned}
-\frac{r_1}{x_2^{\max} L_1} < k_1 \leq 0,\\
T_1(x_2^{\max}) - 2T_2(x_2^{\max}) < k_2 < T_1(x_2^{\max}) + 2T_2(x_2^{\max}),
\end{aligned} \tag{7.16}$$

where

$$\begin{aligned}
T_1(\omega) &:= \frac{\omega k_1 L_1 + 2r_1}{\omega^2 L_1},\\
T_2(\omega) &:= \frac{1}{L_1\omega^2}\sqrt{\omega k_1 L_1 r_1 + r_1^2}.
\end{aligned}$$

Then

$$\lim_{t\to\infty} |\hat{x}_1(t) - x_1(t)| = 0, \quad \lim_{t\to\infty} \hat{P}(t) = P,$$

exponentially.

Proof. See Appendix 7.C at the end of the chapter. □□□

The stability of the system (7.4) in closed-loop with an adaptive version of the control law (7.14) is established next.

Proposition 7.6. Let k_1 and k_2 be such that (7.16) hold. Fix $\bar{u}$ and compute $\bar{x}$ from (7.7). Define the *adaptive* control law

$$u = \tfrac{1}{x_4} w(\hat{x}_1, x_2, x_3, \hat{P}), \tag{7.17}$$

where w is given in (7.11), and $\hat{x}_1$, $\hat{P}$ are generated by the adaptive observer (7.15). Then, $(x, \hat{x}_1, \hat{P}) = (\bar{x}, \bar{x}_1, P)$ is an asymptotically stable equilibrium point of the overall system.

Proof. See Appendix 7.D at the end of the chapter. □□□

Remark 7.1. A key extension with respect to the research done in [66] is the use of an adaptive, observer-based feedback law, the implementation of which requires only the measurement of the variables x_2 and x_3, which is easy to obtain in a physical setup.

Remark 7.2. The computation of the control law (7.11), (7.17) requires the knowledge of $\bar{x}_2$, which is dependent on the unknown P; see equation (7.7). In the experiments reported in Section 7.6, the value of $\bar{x}_2$ is computed from the estimate of P, *i.e.* $\hat{P}$, discretely, not continuously in time. This approach is common in hierarchical and supervisory control of AC and DC microgrids [42] and prevents introducing $\bar{x}_2$ to the controller if an overshoot of the time-varying signal $\hat{P}$ occurs, it also simplifies the controller design.

Remark 7.3. Through direct, but lengthy, computations, it can be shown that the condition (7.16) may be replaced by the conditions

$$\begin{aligned} 0 < k_1 < \frac{8 r_1 (x_2^{\min} + x_2^{\max})}{L_1 (x_2^{\max} - x_2^{\min})^2}, \\ T_1(x_2^{\min}) - 2T_2(x_2^{\min}) < k_2 < T_1(x_2^{\max}) + 2T_2(x_2^{\max}). \end{aligned} \tag{7.18}$$

7.5 Numerical simulations

This sections reports two simulations that illustrate the good performance of the proposed controller. The physical parameters of the system (7.4) are given in Table 7.1, and the parameters for the adaptive output-feedback controller of equation (7.11), (7.15), (7.17) are selected as

$$\alpha = 3 \times 10^4, \quad \beta = \frac{\alpha^2}{4}, \quad k_1 = 10, \quad k_2 = 25.$$

In all simulations a saturation function has been used to keep $u \in (0, 1)$.

7.5.1 Simulation 1

The value $\bar{u} = 0.5$ is fixed and the equilibrium point to be stabilized $\bar{x}$ is computed via (7.7) for $P = 0$. The initial condition has been fixed at that equilibrium point. Then, at $t = 3$ s, a step change in the CPL power, from $P = 0$ W to $P = 479$ W, is

introduced, this yields a *new* equilibrium point to be stabilized: $\bar{x}|_{P=479}$. Additionally, at $t = 6$ s, the CPL is stepped down to 0 W once again. It should be pointed out that $P = 479$ W still verifies the necessary and sufficient condition for existence of equilibria of the network *without* the shunt damper established in Subsection 7.2.2. However, it is well above the *necessary* bound for stability given in (7.3), which is given by

$$\frac{E^2 C_1 L_1 r_1}{(L_1 + C_1 r_1^2)^2} = 276.9 \text{ W}.$$

Hence, without the shunt damper the equilibria are unstable.

Table 7.1: Parameters for the circuit in Fig. 7.2

$r_1 = 0.3\ \Omega$	$L_1 = 85.0\ \mu$H	$C_1 = 200\ \mu$F	$E = 24.0$ V
$r_2 = 5\ m\Omega$	$L_2 = 100\ \mu$H	$C_2 = 1.0$ mF	$r_3 = 1\ k\Omega$

Fig. 7.4 shows the time history of each component of the state x against their equilibrium values, respectively; a zoom of these plots around the second transient is shown in Fig. 7.5. It is clear from these figures that fast convergence is achieved. In Figs. 7.6 and 7.7 are plotted the control variable u. It can be seen from the figures that, except from some peaks at the instants of power change where the saturation enters into play, the control signal remains all the time within the admissible bounds. The figures also show the errors in the state and parameter estimates, which converge to zero very fast. Finally, the plots of the power consumption of the shunt damper, *i.e.,* the product $\mathcal{P}_{\text{L}} = x_2 x_3$, shows that the controller is energetically efficient.

7.5.2 Simulation 2

This simulation shows in detail the performance of the adaptive observer. The simulation starts from the initial condition $x(0) = \bar{x}|_{P=10}$, then, at $t = 3$ s, a large step change in the CPL power, from $P = 10$ W to $P = 300$ W, is introduced. Figs. 7.8 and 7.9 show the excellent performance of the state observer and the slightly slower tracking of the power estimator.

7.6 Experimental validation

In order to investigate the practical feasibility of the proposed control scheme, an experimental setup has been designed and built according to the electrical scheme shown in Fig. 7.2. The test bench is composed of a DC voltage source Delta Elektronika SM-52-AR-60, the passive components of the RLC circuit (r_1, L_1 and C_1), a DC boost converter and a custom-designed and built CPL. The CPL has a maximum allowed current $I_{\max} = 40$ A and a maximum power in steady state of $P_{\max} = 900$ W. The physical setup of the experiments is shown in Fig. 7.10.

The measured parameters of the system are the same as in Table 7.1, except for r_1 that in the physical setup is $r_1 = 0.314\ \Omega$. The gains of the adaptive controller are the same as in section 7.5.

It is underscored that the CPL has been designed to approximate an ideal algebraic behavior, *i.e.*, with a much wider bandwidth than the expected dynamics of the whole system. Particularly, in a LTspice simulation with an ideal DC voltage

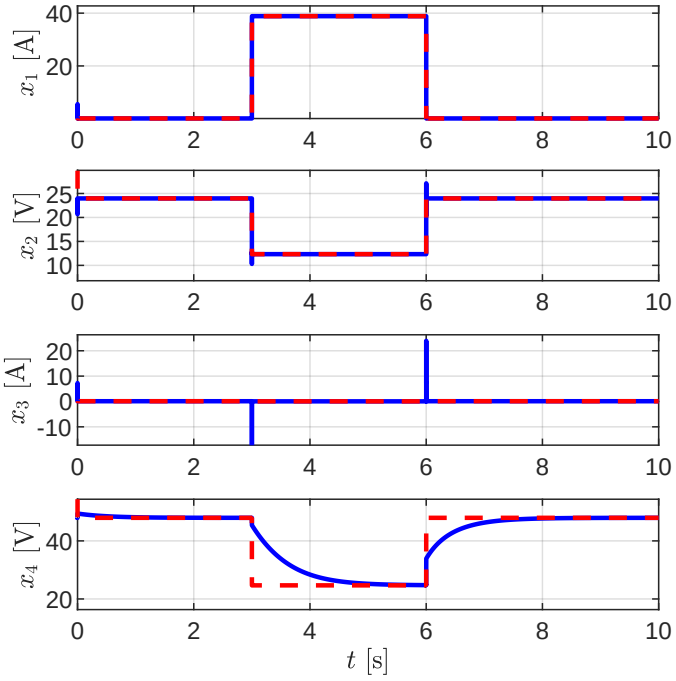

Figure 7.4: Time history of the components of x (blue curves) against their reference values (in dashed red) for Simulation 1. Convergence is achieved despite the step change in the CPL's power.

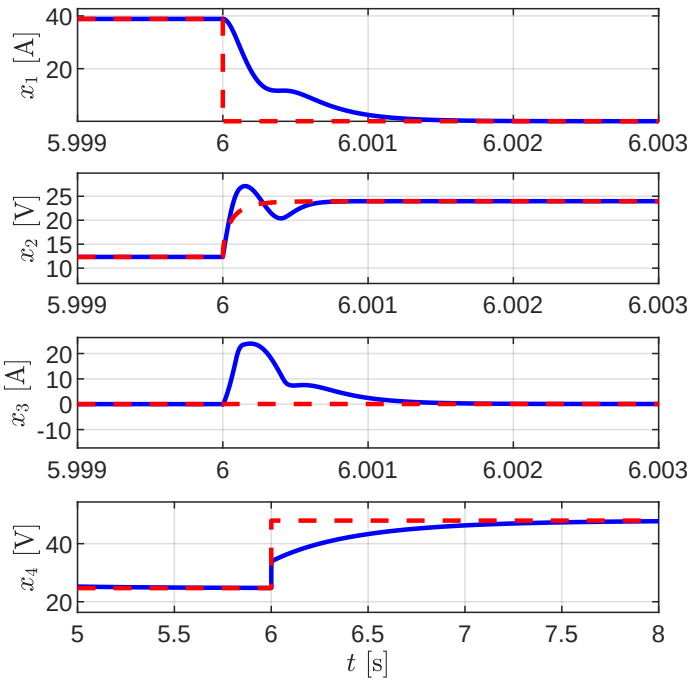

Figure 7.5: Zoom around the second transient of the plots in Fig. 7.4.

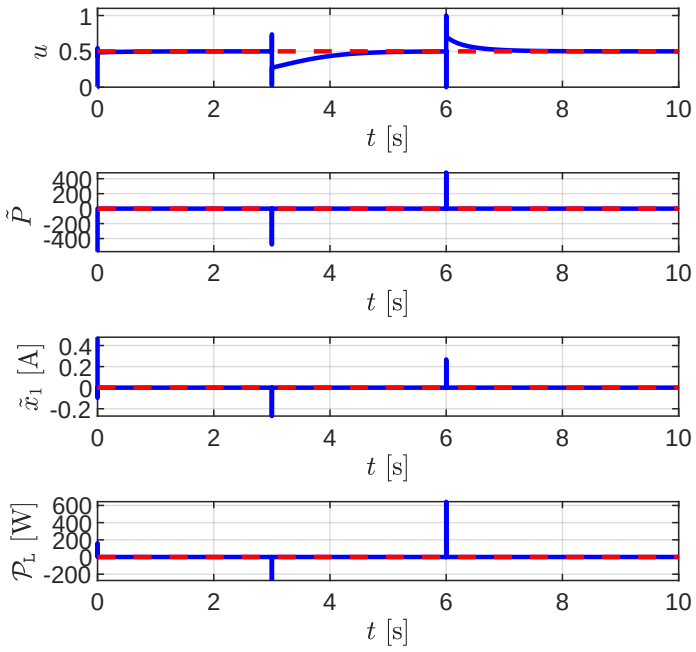

Figure 7.6: Time history of u, the power estimation error $\tilde{P}$, the observer error $\tilde{x}_1$ and the power losses $\mathcal{P}_\mathrm{L} = x_2 \cdot x_3$ (in blue) against their respective reference values (in dashed red) for Simulation 1.

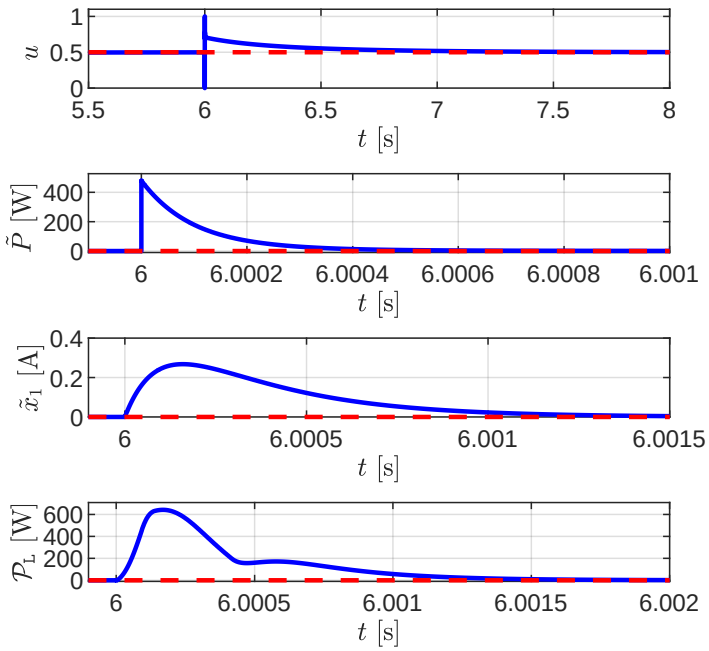

Figure 7.7: Zoom around the second transient of the plots in Fig. 7.6.

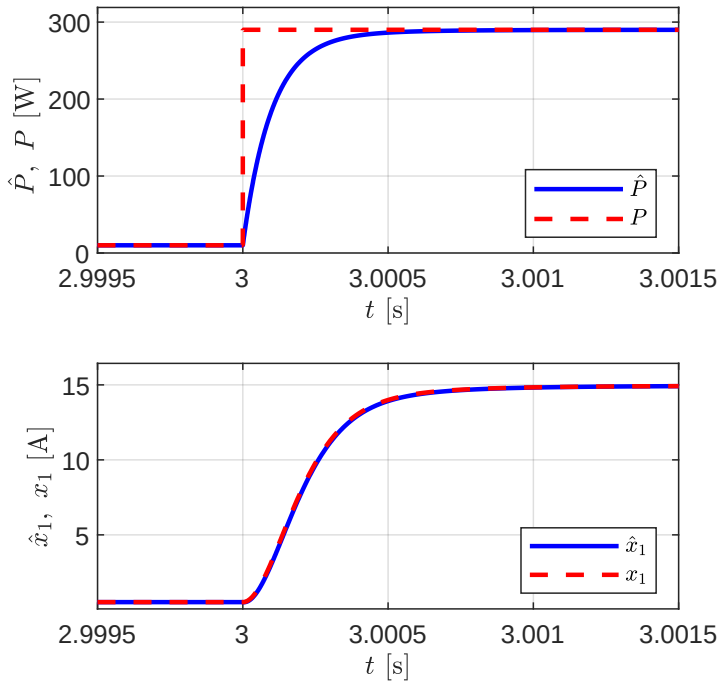

Figure 7.8: Time history of $\hat{x}_1$ and $\hat{P}$ (in blue) against their respective reference values, x_1 and P (in dashed red), in Simulation 2. Fast convergence is achieved after the step change in the CPL's power.

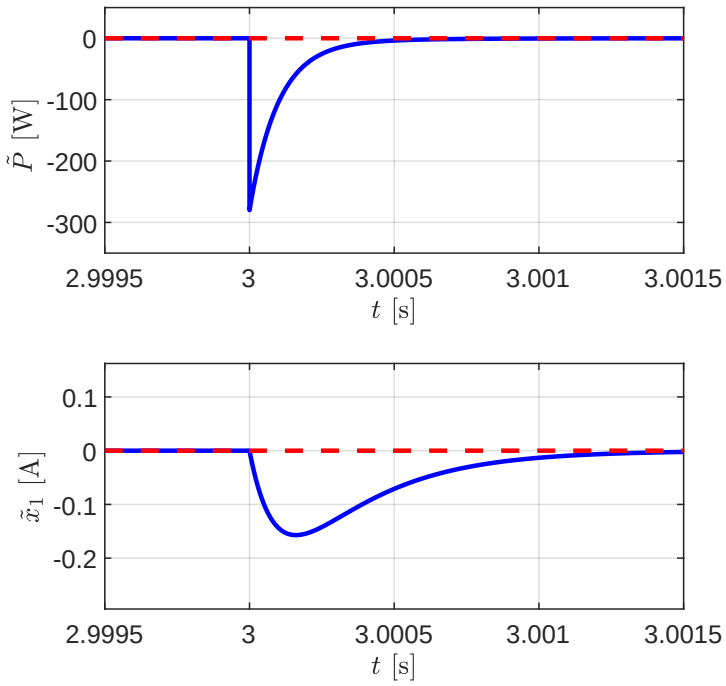

Figure 7.9: Zoom around the transient, now of the estimation errors, of the plots in Fig. 7.8.

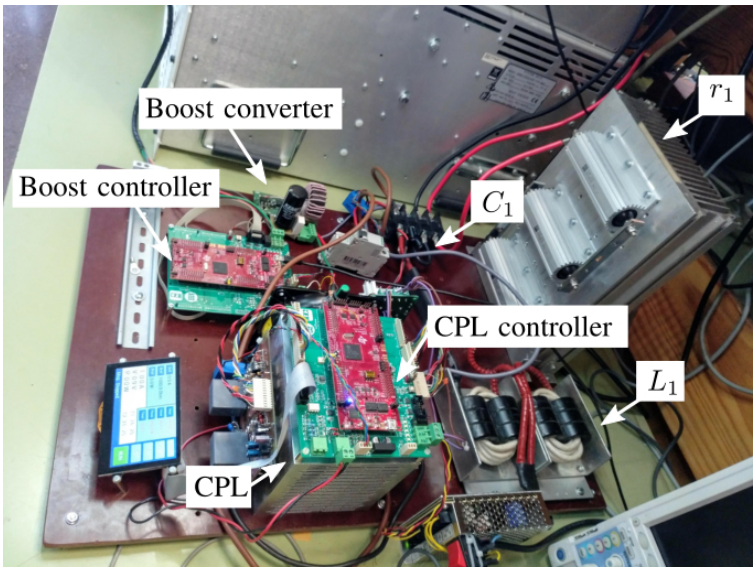

Figure 7.10: Experimental test bench. The DC voltage source is not shown here.

Table 7.2: Parameters of the experimental setup of Fig. 7.10.

$r_1 = 0.314\ \Omega$	$L_1 = 85.0\ \mu$H	$C_1 = 200\ \mu$F	$E = 24.0$ V
$r_2 = 5\ \text{m}\Omega$	$L_2 = 100\ \mu$H	$C_2 = 1.0$ mF	$r_3 = 1\ \text{k}\Omega$

source, the CPL settling time for a power step change is $t_s = 7\,\mu s$. In an experimental test, with the CPL directly connected to the DC voltage source, the time response to a power step change is under-damped, with an approximate settling time of $t_s = 75\,\mu s$. This change in the load dynamics stems from the non-ideal behavior of the DC voltage source, particularly due to its controlled output impedance.

The adaptive control law of equation (7.17) has been discretized in time using the bilinear transformation (trapezoidal integration) and implemented in a digital signal processor (DSP) TI TMS320F28379D using the automatic code generation tools of Simulink.[1]

7.6.1 Experiment 1: system without the shunt damper

The electrical system without shunt damper is tested first; see Fig. 7.1. The objective of this experiment is twofold: (1) to analyze the maximum power that can be demanded by the CPL before the system turns unstable and (2) to illustrate a reduced region of attraction with respect to the closed-loop system.

Fig. 7.11 shows the response of the system without the shunt damper to a step change of the load's power from $P = 250$ W to $P = 336$ W. The behavior is highly oscillatory, but *stable*, contradicting the predicted *necessary* bound for stability that is presented in (7.3), which reads as $P < 276.9$ W. This contradiction is explained due to the finite bandwidth of the real CPL.

In Fig. 7.12 the system response is shown for a step change of the CPL from $P =$

[1]The algebraic loops that appear in the equations after the discretization in time have been solved analytically before doing the automatic code generation.

250 W to $P = 338$ W, where an unstable behavior is observed.[2] It is concluded then that the upper bound for the system's stability is within the interval $[336, 338]$ W.

The unstable behavior of the system without the shunt damper to a power step change from $P = 10\,\mathrm{W}$ to $P = 300$ W can be observed in Fig. 7.13. Notice that even if the load's power is lower than the necessary upper bound for stability, a drastic load change can also destabilize the system. Clearly, in this scenario, the former system's equilibrium lies outside the domain of attraction of the latter one. This behavior is to be contrasted with respect to the operation with the controlled shunt damper, which is discussed next.

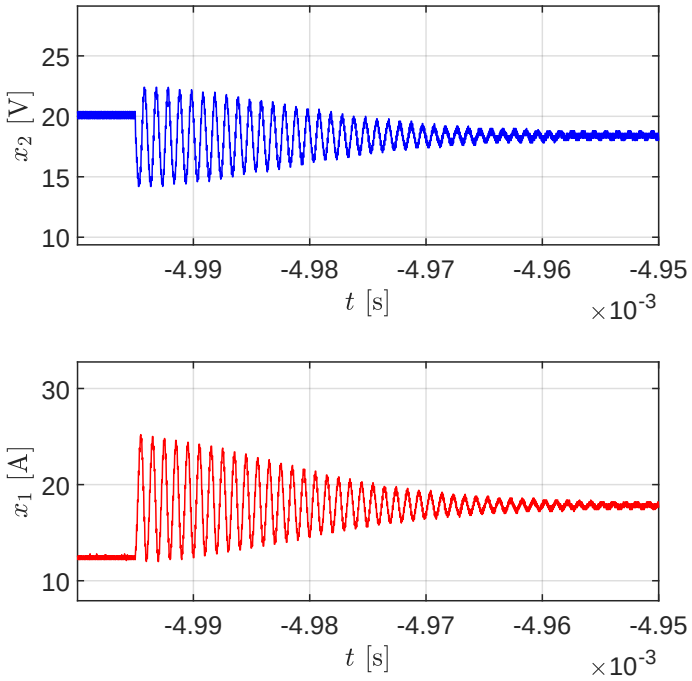

Figure 7.11: System response to a step from $P = 250\,\mathrm{W}$ to $P = 336\,\mathrm{W}$ without the controlled shunt damper. The blue curve (above) corresponds to the voltage x_2; the red curve (below), the current x_1.

[2] In all the unstable experiments the CPL stops, *i.e.,* abruptly goes to zero, either because the current goes outside of the operating range, which is $[0, 40]$ A, or because the voltage at the CPL input terminals falls below the safety limit, which has been situated at a value considerably lower than that corresponding to the maximum power (≈ 12 V).

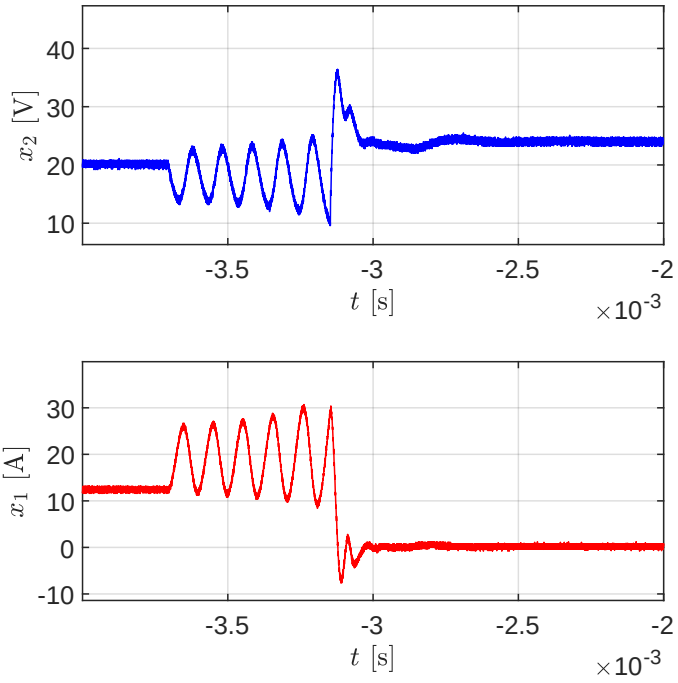

Figure 7.12: System response to a step from $P = 250\,\mathrm{W}$ to $P = 338\,\mathrm{W}$ without the controlled shunt damper. The blue curve (above) corresponds to the voltage x_2; the red curve (below), the current x_1.

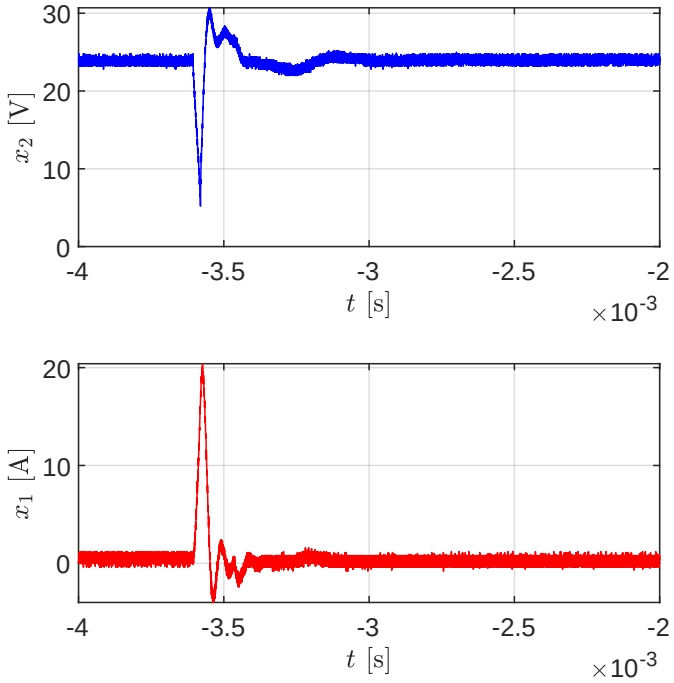

Figure 7.13: System response to a step from $P = 10\,\mathrm{W}$ to $P = 300\,\mathrm{W}$ without the controlled shunt damper. The blue curve (above) corresponds to the voltage x_2; the red curve (below), the current x_1.

7.6.2 Experiment 2: system with the controlled shunt damper

The stable response of the system with the controlled shunt damper in the presence of a step change in the CPL's power, from $P = 250\,\mathrm{W}$ to $P = 380\mathrm{W}$, is shown in Fig. 7.14. Notice that the CPL power is stepped up to a value much bigger than those reported for *Experiment 1*, yet the system is able to keep operating in a stable manner, which implies a relaxation of the necessary bound for stability of the system in without the shunt damper.

The system response to a CPL step change from $P = 10\,\mathrm{W}$ to $P = 300\,\mathrm{W}$ is shown in Fig. 7.15, where a stable behavior is observed. By making a comparison with the results reported in Fig. 7.13, it can be concluded that the domain of attraction of the system with the controlled shunt damper has been successfully increased with respect to its operation without the shunt damper.

To study the energetic efficiency of the proposed active damping scheme, Fig. 7.16 reports the measured power consumption of the shunt damper during its operation and in the presence of a step change in the CPL's power from $P = 10\,\mathrm{W}$ to $P = 300\mathrm{W}$. Clearly, a low power consumption is evidenced. Before the change in the CPL's power, when the system is in steady state, it can appreciated that the power losses are nearly zero (approximately 4 W), these losses are due to the passive components of the converter and the mosfets switching losses. During the first 2 ms of the transient, the average power is negative, that is, the shunt damper is injects power to the system to stabilize it. After the transient the system reaches another stable equilibrium and the average power losses of the damper return to a minimum.

Finally, from successive experiments with different power steps in the CPL, it has been determined that the experimental limit for the stable operation of the system with the controlled shunt damper is in the range [410, 420] W. This value represents, approximately, the 90% of the range of power for existence of equilibrium in the system, which from (7.2) reads as $P < 458.6$ W.[3] Clearly, the former value is drastically superior with respect to the operation of the network without the shunt damper.

[3]Without taking into account the power needed to supply the operating losses of the boost converter.

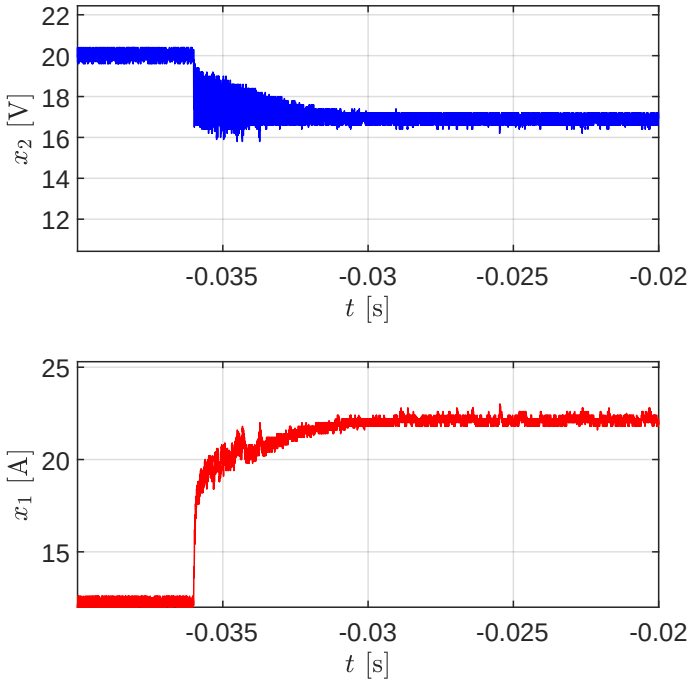

Figure 7.14: System response to a step from $P = 250\,\mathrm{W}$ to $P = 380\,\mathrm{W}$ with the controlled shunt damper. The blue curve (above) corresponds to the voltage x_2; the red curve (below), the current x_1.

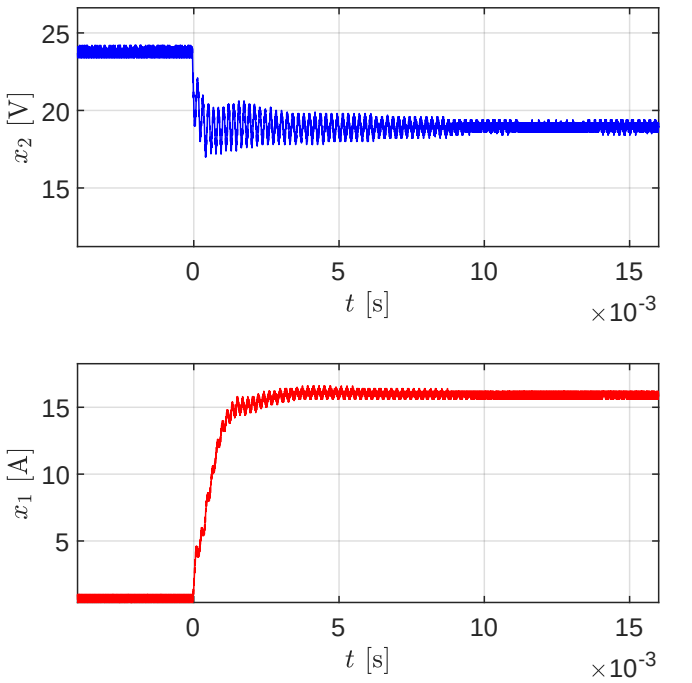

Figure 7.15: System response to a step from $P = 10\,\mathrm{W}$ to $P = 300\,\mathrm{W}$ with the controlled shunt damper. The blue curve (above) corresponds to the voltage x_2; the red curve (below), the current x_1.

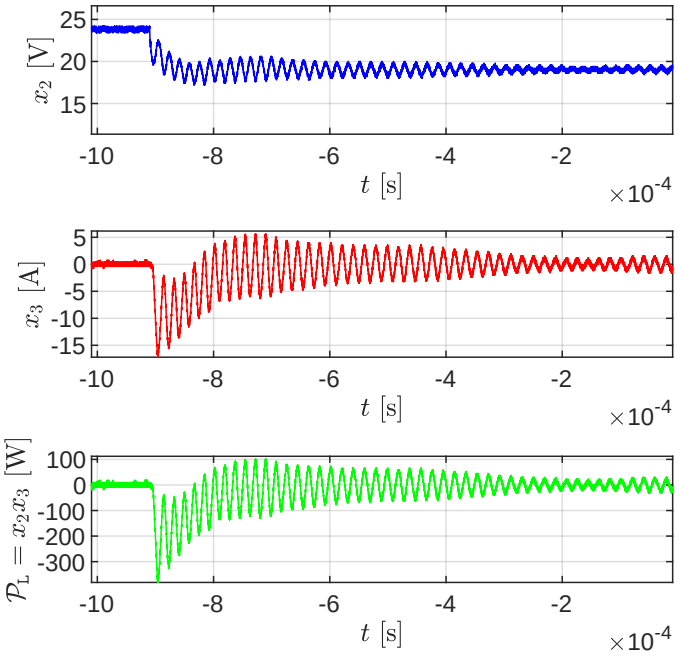

Figure 7.16: Measured power consumption of the shunt damper (Bottom figure). The closed-loop system is subject to a step change in the load's power from $P = 10\,\mathrm{W}$ to $P = 300\,\mathrm{W}$.

7.7 Summary

In this chapter, a nonlinear stabilization method for a DC small-scale power system that supplies electric energy to a CPL has been explored. By adding a controlled DC-DC power converter in parallel with the load and using standard input-output linearization with a suitable tailored adaptive observer, a nonlinear adaptive control law for the stabilization of the overall network has been proposed. Furthermore, the proposed design permits the stable operation of the network for a wide range of values of the CPL and is able to relax some necessary stability bounds that are imposed if the system were to be operated without the shunt damper. Finally, the good performance of the controller has been validated through experiments on a real small-scale DC network.

Technical Appendices of the Chapter

7.A Proof of Proposition 7.2

From (7.9) a and (7.12) it follows that

$$\dot{y} = \dot{x}_2 = \frac{1}{C_1}\left(x_1 - \frac{P}{x_2} - x_3\right) =: \mathcal{F}_2(x_1, x_2, x_3),$$

and

$$\ddot{y} = \nabla \mathcal{F}_2^\top \begin{bmatrix} \frac{1}{L_1}(-r_1 x_1 - x_2 + E) \\ \frac{1}{C_1}(x_1 - \frac{P}{x_2} - x_3) \\ \frac{1}{L_2}(-r_2 x_3 + x_2 - w) \end{bmatrix}. \tag{7.19}$$

If $w(x_1, x_2, x_3)$ is substituted from equation (7.11) into equation (7.19), then (7.13) is obtained, which clearly is an asymptotically stable system.

To show that the equilibrium $(\bar{x}_1, \bar{x}_2, \bar{x}_3)$ is asymptotically stable, the zero dynamics of Σ^{13} with output y is analyzed, which is the dynamics of Σ^{13} restricted to the set

$$\begin{aligned} \mathcal{Z} &= \{(x_1, x_2, x_3) : \ y = 0 \ \wedge \ \dot{y} = 0\} \\ &= \{x_1, x_2, x_3) : \ x_2 = \bar{x}_2 \ \wedge \ x_3 = x_1 - \frac{P}{\bar{x}_2}\}. \end{aligned}$$

Restricting the dynamics of x_1 to $\mathcal{Z}$ yields

$$\begin{aligned} L_1 \dot{x}_1 &= -r_1 x_1 - \bar{x}_2 + E, \\ &= -r_1 (x_1 - \bar{x}_1). \end{aligned}$$

Therefore, $x_1 \to \bar{x}_1$. Now, in $\mathcal{Z}$, it holds that $x_3 = x_1 - \frac{P}{\bar{x}_2}$, hence $x_3 \to \bar{x}_1 - \frac{P}{\bar{x}_2} = \bar{x}_3$.

7.B Proof of Proposition 7.3

With the change of coordinates $z = \frac{1}{2} C_2 x_4^2$, the system Σ^4 is equivalent to

$$\dot{z} = -\frac{2}{r_3 C_2} z + w x_3. \tag{7.20}$$

From Proposition 7.2, it follows that $\bar{x}_{13}$ is an exponentially stable equilibrium point of Σ_{13} in closed-loop with (7.11). Then, the term $w x_3$ remains bounded and converges, exponentially, to the value $\bar{u}\bar{x}_3\bar{x}_4$. The latter limit is computed from the steady state expression

$$-r_2 \bar{x}_3 - \bar{u}\bar{x}_4 + \bar{x}_2 = 0.$$

It follows trivially from equation (7.20) that

$$z \to \frac{r_3 C_2}{2} (w x_3) \to \frac{r_3 C_2}{2} (\bar{u}\bar{x}_4\bar{x}_3).$$

at an exponential rate. Using the steady state expression

$$\bar{u}\bar{x}_3 - \frac{1}{r_3}\bar{x}_4 = 0,$$

it can be concluded that any solution x_4 of Σ^4 is positive for all time and converges exponentially to $\bar{x}_4 > 0$ as long as it starts sufficiently close to $\bar{x}_4$.

7.C Proof of Proposition 7.5

The derivatives of the errors $\tilde{x}_1 := \hat{x}_1 - x_1$ and $\tilde{P} := \hat{P} - P$ are given by

$$\begin{aligned} \dot{\tilde{x}}_1 &= -\frac{r_1}{L_1}\tilde{x}_1 - k_1 x_2 \tilde{x}_1 + k_1 \tilde{P}, \\ \dot{\tilde{P}} &= -k_2 \tilde{P} + k_2 x_2 \tilde{x}_1. \end{aligned} \tag{7.21}$$

To show that the origin of (7.21) is exponentially stable, consider then the Lyapunov function candidate

$$V := \frac{1}{2}\tilde{x}_1^2 + \frac{1}{2}\tilde{P}^2$$

and its derivative with respect to t, along the trajectories of (7.21), given by

$$\begin{aligned} \dot{V} &= \tilde{x}_1 \dot{\tilde{x}}_1 + \tilde{P}\dot{\tilde{P}} \\ &= -\left(\frac{r_1}{L_1}\right)\tilde{x}_1^2 - k_1 x_2 \tilde{x}_1^2 + k_1 \tilde{P}\tilde{x}_1 \\ &\quad - k_2 \tilde{P}^2 + k_2 x_2 \tilde{x}_1 \tilde{P} \\ &= -\begin{bmatrix} \tilde{x}_1 \\ \tilde{P} \end{bmatrix}^\top \mathcal{M}(x_2) \begin{bmatrix} \tilde{x}_1 \\ \tilde{P} \end{bmatrix}, \end{aligned}$$

where

$$\mathcal{M}(x_2) = \begin{bmatrix} \frac{r_1}{L_1} + k_1 x_2 & -\frac{1}{2}(k_1 + k_2 x_2) \\ -\frac{1}{2}(k_1 + k_2 x_2) & k_2 \end{bmatrix}.$$

Clearly, V is a strict Lyapunov function if and only if $\mathcal{M}(x_2) > 0$. The latter is satisfied if and only if

$$\begin{aligned} \tfrac{r_1}{L_1} + k_1 x_2 &> 0, \\ \det\{\mathcal{M}(x_2)\} = k_2\left(\frac{r_1}{L_1} + k_1 x_2\right) - \frac{1}{4}(k_1 - k_2 x_2)^2 &> 0, \end{aligned}$$

hold simultaneously. Through lengthy but direct computations, it can be verified that these conditions hold—in the domain $x_2 \in [x_2^{\min}, x_2^{\max}]$— whenever (7.16) (or (7.18)) hold. This concludes the proof.

7.D Proof of Proposition 7.6

Recall from the proof of Proposition 7.5 that the observer's error dynamics is given by (7.21). On the other hand, it can be shown through lengthy (but straightforward) computations that (7.4) in closed-loop with (7.17) has the form

$$\dot{x} = \left[f(x) + g(x)\frac{w(x_1, x_2, x_3, P)}{x_4}\right] + g(x)\epsilon(x, \tilde{x}_1, \tilde{P}), \tag{7.22}$$

where the mapping ϵ is such that $\epsilon(x, 0, 0) = 0$ for all x.

From Proposition 7.4 it follows that if $\epsilon \equiv 0$ for all t, then $\bar{x}$ is an asymptotically stable equilibrium of (7.22). Furthermore, Proposition 7.5 establishes that the origin of the observer's error dynamics is exponentially stable. Consequently, invoking [102, Proposition 4.1], it is concluded that $(x, \tilde{x}_1, \tilde{P}) = (\bar{x}, 0, 0)$ is an asymptotically stable equilibrium point of the overall system.

Part IV

EPILOGUE

Chapter 8

Conclusions

This thesis has explored different problems that emerge in the analysis and control of electrical power systems with constant power loads. The novel contributions of the present document, which are aimed at better understanding and possibly solve these problems, are summarized in the following list.

- For general multi-port linear AC networks with constant power loads, necessary LMI-based conditions for the existence of a sinusoidal steady state regime have been established. For one- or two-port networks and free active (or reactive) power of the load's components, these conditions are also sufficient. Particularly, for single-port networks, the admissibility condition can be tested directly from the data of the problem.

  These results may be extended in two main directions: (i) establish if the proposed LMI test is also sufficient for existence of steady states, and (ii) if a steady state exists, study its stability or attractivity properties.

- For general models in modern and conventional AC and DC power systems, it has been shown that their steady states satisfy a system of nonlinear algebraic equations whose vector field, when associated to an ODE, possesses properties of monotonicity. It has been established that if these models do admit steady states, then there is a distinguished one that dominates, component-wise, all the other ones and that furthermore is asymptotically stable. An algorithm to verify if the solutions of the ODE will converge to the distinguished equilibrium or not has also been proposed. In the treated power system models, the latter results imply the existence of a high-voltage steady state that is also *voltage regular*.

  The analysis of diverse ODEs' integration technique to identify efficient ways of implementing the proposed numerical algorithm when dealing with large-scale systems is an interesting path of future research.

- A class of port-Hamiltonian systems, in which the control input directly acts on the power balance equation, has been extensively investigated. These systems, coined *power-controlled Hamiltonian systems*, have been shown to be shifted passive, as long as the trajectories remain in a clearly specified set. The exhibited shifted passivity properties have been used to establish the stability of the intrinsically non zero equilibrium and to even provide an easy

to compute domain of attraction of them, under some simplifying assumptions. The introduced framework has been applied to analyze the stability of DC power systems with constant power loads that include general multi-port networks and the synchronous generator.

As a line of further research, the design of simple, high-performance controllers with guaranteed stability domains may be explored. In addition, the more general case of state-dependent interconnection and dissipation matrices [75], needs to be further investigated. Also the applicability of the methodology to AC circuits with constant power loads and higher order models of the synchronous generator [39] may be addressed.

- The control problem of regulating the output voltage of a buck-boost converter supplying electric energy to a CPL with unknown power has been addressed. A control law designed following the IDA-PBC technique in combination of an online estimator for the load power, has been presented. Moreover, performance limitations of classical PD controller have also been reviewed. In addition, the effectiveness of the proposed control scheme has been verified through realistic simulations.

  The designed control law is of great algebraic complexity, which may stymie its practical application, hence further research can be carried out to simplify it. Furthermore, the design of a current observer to remove the need for its measurement, which is an issue of practical interest, may also be investigated.

- The nonlinear *active damping* of a DC small-scale power system with a CPL has been addressed. The proposed scheme considers the addition of a controlled DC-DC power converter for which a nonlinear adaptive control law is designed. The stable operation of the network for a wide range of values of the CPL is guaranteed, and a clear extension of the CPL's operation range, with respect to the open-loop case, is verified. Moreover, the performance of the controller has been validated through experiments on a real small-scale DC network.

  Some directions of further research include: (i) computation of estimates of the region of attraction, (ii) analyze the robustness against parameter uncertainty, and (iii) extend the analysis to networks with several loads distributed in a meshed topology.

Bibliography

[1] V. Ajjarapu and C. Christy. "The continuation power flow: a tool for steady state voltage stability analysis". In: *IEEE Transactions on Power Systems* 7.1 (1992), pp. 416–423 (cited on page 40).

[2] A. Alonso and B. Ydstie. "Stabilization of distributed systems using irreversible thermodynamics". In: *Automatica* 37.11 (2001), pp. 1739–1755 (cited on page 67).

[3] S. Anand and B. Fernandes. "Reduced-Order Model and Stability Analysis of Low-Voltage DC Microgrid". In: *IEEE Transactions on Industrial Electronics* 60.11 (2013), pp. 5040–5049 (cited on pages 4, 138).

[4] P. Anderson and A. Fouad. *Power System Control and Stability*. J.Wiley & Sons, 2002 (cited on pages 2, 3, 136, 138).

[5] A. Araposthatis, A. Sastry, and P. Varaiya. "Analysis of power-flow equation". In: *International Journal of Electrical Power & Energy Systems* 3 (1981), pp. 115–126 (cited on page 18).

[6] M. Arcak, C. Meissen, and A. Packard. *Networks of dissipative systems: compositional certification of stability, performance, and safety*. Springer, 2016 (cited on page 12).

[7] D. Ariyasinghe and D. Vilathgamuwa. "Stability analysis of microgrids with constant power loads". In: *IEEE International Conference on Sustainable Energy Technologies*. 2008, pp. 279–284 (cited on page 4).

[8] A. Astolfi, D. Karagiannis, and R. Ortega. *Nonlinear and Adaptive Control with Applications*. Berlin: Springer-Verlag, 2008 (cited on pages 83, 89).

[9] N. Barabanov, R. Ortega, R. Griñó, and B. Polyak. "On existence and stability of equilibria of linear time-invariant systems with constant power loads". In: *IEEE Transactions on Circuits and Systems I: Regular Papers* 63.1 (2016), pp. 114–121 (cited on pages 4, 19, 21–25, 27, 28, 33, 53, 54, 82, 138).

[10] M. Belkhayat, R. Cooley, and A. Witulski. "Large signal stability criteria for distributed systems with constant power loads". In: *Power Electronics Specialists Conference, 1995. PESC '95 Record., 26th Annual IEEE*. Vol. 2. 1995, pp. 1333–1338 (cited on pages 4, 77, 138).

[11] D. Bertsimas and J. Tsitsiklis. *Introduction to Linear Programming*. Athena Scientific, 1997 (cited on page 46).

[12] N. Biggs. *Algebraic graph theory*. Cambridge university press, 1993 (cited on page 9).

[13] B. Bollobás. *Modern graph theory*. Springer Science & Business Media, 1998 (cited on page 9).

[14] S. Bolognani and S. Zampieri. "On the existence and linear approximation of the power flow solution in power distribution networks". In: *IEEE Trans. Power Syst.* 31.1 (2016), 163–172 (cited on pages 4, 14, 18, 138).

[15] B. Bose. "Global warming: Energy, environmental pollution, and the impact of power electronics". In: *IEEE Industrial Electronics Magazine* 4.1 (2010), pp. 6–17 (cited on pages 2, 136).

[16] R. Brayton and J. Moser. "A theory of nonlinear networks. I". In: *Quarterly of Applied Mathematics* 22.1 (1964), pp. 1–33 (cited on pages 4, 138).

[17] L. Bregman. "The relaxation method of finding the common point of convex sets and its application to the solution of problems in convex programming". In: *USSR Computational Mathematics and Mathematical Physics* 7.3 (1967), pp. 200 –217 (cited on pages 12, 67, 69).

[18] F. Bullo. *Lectures on Network Systems*. 1st ed. With contributions by J. Cortes, F. Dorfler, and S. Martinez. CreateSpace, 2018 (cited on pages 57, 60).

[19] M. Carmeli, D. Forlani, S. Grillo, R. Pinetti, E. Ragaini, and E. Tironi. "A stabilization method for DC networks with constant-power loads". In: *IEEE International Energy Conference and Exhibition (ENERGYCON)*. Florence, Italy, 2012, pp. 617–622 (cited on pages 101–104).

[20] K. Cavanagh, J. Belk, and K. Turitsyn. "Transient stability guarantees for ad hoc DC microgrids". In: *IEEE Control Systems Letters* 2.1 (2017), pp. 139–144 (cited on pages 4, 77, 138).

[21] M. Cespedes, L. Xing, and J. Sun. "Constant-Power Load System Stabilization by Passive Damping". In: *IEEE Transactions on Power Electronics* 26.7 (2011), pp. 1832–1836 (cited on pages 4, 138).

[22] G. Cezar, R. Rajagopal, and B. Zhang. "Stability of interconnected DC converters". In: *IEEE 54th Annual Conference on Decision and Control (CDC)*. 2015, pp. 9–14 (cited on page 77).

[23] H. Chiang and M. Baran. "On the existence and uniqueness of load flow solution for radial distribution power networks". In: *IEEE Trans. Circuits Syst.* 37.3 (1990), 410–416 (cited on page 18).

[24] R. Cisneros, F. Mancilla, and R. Ortega. "Passivity-Based Control of a Grid-Connected Small-Scale Windmill With Limited Control Authority". In: *IEEE Journal of Emerging and Selected Topics in Power Electronics* 1.4 (2013), pp. 247–259 (cited on page 107).

[25] M. Coste. *An Introduction to Semialgebraic Geometry*. Institut de Recherche Mathematiques de Rennes, 2002 (cited on page 58).

[26] M. Cucuzzella, S. Trip, C. De Persis, X. Cheng, A. Ferrara, and A. van der Schaft. "A Robust Consensus Algorithm for Current Sharing and Voltage Regulation in DC Microgrids". In: *IEEE Transactions on Control Systems Technology* (2018) (cited on page 52).

[27] J. Danskin. "The Theory of Max-Min, with Applications". In: *SIAM Journal on Applied Mathematics* 14.4 (1966), pp. 641–664 (cited on page 62).

[28] G. Dantzig. *Linear Programming and Extensions*. Princeton university press, 1966 (cited on page 46).

[29] S. Davis and K. Caldeira. "Consumption-based accounting of CO2 emissions". In: *Proceedings of the National Academy of Sciences*. Vol. 107. 12. 2010, pp. 5687–5692 (cited on pages 2, 136).

[30] C. De Persis, E. Weitenberg, and F. Dörfler. "A power consensus algorithm for DC microgrids". In: *Automatica* 89 (2018), pp. 364 –375 (cited on pages 3, 137).

[31] C. Desoer and E. Kuh. *Basic Circuit Theory*. McGraw-Hill, 1969 (cited on page 13).

[32] C. Desoer and M. Vidyasagar. *Feedback Systems: Input-Output Properties*. SIAM, 2009 (cited on page 11).

[33] T. Dragičević, X. Lu, J. C. Vasquez, and J. M. Guerrero. "DC Microgrids—Part I: A Review of Control Strategies and Stabilization Techniques". In: *IEEE Transactions on Power Electronics* 31.7 (2016), pp. 4876–4891 (cited on page 39).

[34] K. Dvijotham, H. Nguyen, and K. Turitsyn. "Solvability regions of affinely parameterized quadratic equations". In: *IEEE Control Systems Letters* 2.1 (2017), pp. 25–30 (cited on page 40).

[35] M. Dyer, B. Gärtner, N. Megiddo, and E. Welzl. "Linear Programming". In: *Handbook of Discrete and Computational Geometry*. 3rd ed. CRC Press, 2018 (cited on page 46).

[36] O. Ellabban, H. Abu-Rub, and F. Blaabjerg. "Renewable energy resources: Current status, future prospects and their enabling technology". In: *Renewable and Sustainable Energy Reviews* 39 (2014), pp. 748–764 (cited on pages 2, 136, 137).

[37] A. Elsayed, A. Mohamed, and O. Mohammed. "DC Microgrids and Distribution Systems: An Overview". In: *Electric Power Systems Research* 119 (2015), pp. 407–417 (cited on page 39).

[38] A. Emadi, A. Khaligh, C. Rivetta, and G. Williamson. "Constant power loads and negative impedance instability in automotive systems: definition, modeling, stability, and control of power electronic converters and motor drives". In: *IEEE Transactions on Vehicular Technology* 55.4 (2006), pp. 1112–1125 (cited on pages 3, 82, 137).

[39] S. Fiaz, D. Zonetti, R. Ortega, J. Scherpen, and A. van der Schaft. "A port-Hamiltonian approach to power network modeling and analysis". In: *European Journal of Control* 19.6 (2013), pp. 477–485 (cited on pages 4, 124, 138).

[40] J. Glover, M. Sarma, and T. Overbye. *Power system analysis and design*. Cengage Learning, 2011 (cited on pages 2, 136).

[41] D. Gross, C. Arghir, and F. Dörfler. "On the steady-state behavior of a nonlinear power system model". In: *Automatica* 90 (2018), pp. 248–254 (cited on pages 4, 138).

[42] J. M. Guerrero, J. C. Vasquez, J. Matas, L. De Vicuña, and M. Castilla. "Hierarchical control of droop-controlled AC and DC microgrids—A general approach toward standardization". In: *IEEE Transactions on industrial electronics* 58.1 (2011), pp. 158–172 (cited on page 109).

[43] P. Hartman. *Ordinary Differential Equations*. Birkhäuser, 1982 (cited on pages 40, 42, 59–61, 63).

[44] W. He, R. Ortega, R. Cisneros, F. Mancilla, and S. Li. *Passivity- based control for DC-DC power converters with a constant power load*. Tech. rep. LSS-Supelec, 2017 (cited on page 95).

[45] D. Hill. "Nonlinear dynamic load models with recovery for voltage stability studies". In: *IEEE transactions on power systems* 8.1 (1993), pp. 166–176 (cited on pages 5, 50, 139).

[46] S. Huddy and J. Skufca. "Amplitude death solutions for stabilization of dc microgrids with instantaneous constant-power loads". In: *IEEE Transactions on Power Electronics* 28.1 (2013), pp. 247–253 (cited on page 4).

[47] A. Isidori. *Nonlinear Control Systems*. 3rd ed. Berlin: Springer-Verlag, 1995 (cited on page 83).

[48] A. Isidori. *Nonlinear control systems*. Springer Science & Business Media, 2013 (cited on page 105).

[49] B. Jayawardhana, R. Ortega, E. García-Canseco, and F. Castaños. "Passivity of nonlinear incremental systems: Application to PI stabilization of nonlinear RLC circuits". In: *Systems & Control Letters* 56.9 (2007), pp. 618–622 (cited on pages 12, 67–69).

[50] D. Jovcic, D. Van Hertem, K. Linden, J. Taisne, and W. Grieshaber. "Feasibility of DC Transmission Networks". In: *Proc. 2nd IEEE Power Energy Soc. Int. Conf. and Exhibit. Innovative Smart Grid Technol.* IEEE. 2011, pp. 1–8 (cited on page 39).

[51] J. Keenan. "Availability and irreversibility in thermodynamics". In: *British Journal of Applied Physics* 2.7 (1951), p. 183 (cited on page 67).

[52] A. Kettner and M. Paolone. "A Generalized Index for Static Voltage Stability of Unbalanced Polyphase Power Systems including Thévenin Equivalents and Polynomial Models". In: *IEEE Transactions on Power Systems* (2019) (cited on page 19).

[53] A. Khaligh, A. M. Rahimi, and A. Emadi. "Modified pulse-adjustment technique to control DC/DC converters driving variable constant-power loads". In: *IEEE Trans. on Ind. Electron* 55.3 (2008), pp. 1133–1146 (cited on page 82).

[54] H. Khalil. *Nonlinear Systems*. 3rd ed. Prentice Hall, 2002 (cited on page 10).

[55] H. Kim, S. Kang, G. Seo, P. Jang, and B. Cho. "Large-Signal Stability Analysis of DC Power System With Shunt Active Damper". In: *IEEE Transactions on Industrial Electronics* 63.10 (2016), pp. 6270–6280 (cited on page 101).

[56] P. Kundur. *Power system stability and control*. McGraw-Hill, 1994 (cited on pages 2–4, 15, 39, 41, 49, 50, 136, 138).

[57] P. Kundur et al. "Definition and classification of power system stability". In: *IEEE Transactions on Power Systems* 19.2 (2004), pp. 1387–1401 (cited on pages 4, 138).

[58] K. Kurdyka, P. Orro, S. Simon, and *et al.* "Semialgebraic Sard Theorem for Generalized Critical Values". In: *Journal of Differential Geometry* 56.1 (2000), pp. 67–92 (cited on page 58).

[59] A. Kwasinski and C. Onwuchekwa. "Dynamic Behavior and Stabilization of DC Microgrids With Instantaneous Constant-Power Loads". In: *IEEE Transactions on Power Electronics* 26.3 (2011), pp. 822–834 (cited on pages 3, 4, 137, 138).

[60] A. Kwasinski and P. Krein. "Stabilization of constant power loads in DC- DC converters using passivity-based control". In: *In Proc. 29th Int. Telecommun. Energy Conf.* 2007, pp. 867–874 (cited on pages 83, 86, 89).

[61] D. Langarica, R. Ortega, and D. Casagrande. "Transient stabilization of multimachine power systems: Towards a global decentralized solution". In: *European Journal of Control* 26 (2015), pp. 44–52 (cited on pages 4, 138).

[62] R. Lasseter. "Microgrids". In: *IEEE Power Engineering Society Winter Meeting* 1 (2002), pp. 305–308 (cited on pages 3, 137).

[63] F. Lima, M. Lopes Nunes, and J. Cunha. "Energy indicators framework and climate change policy implications". In: *IEEE 14th International Conference on the European Energy Market (EEM)*. 2017 (cited on pages 2, 136).

[64] J. Linares-Flores, A. Hernández-Méndez, C. Garca-Rodríguez, and H. Sira-Ramrez. "Robust nonlinear adaptive control of a boost converter via algebraic parameter identification". In: *IEEE Trans. Ind. Electron* 61.8 (2014), pp. 4105–4114 (cited on page 85).

[65] P. LÖf, D. Hill, S. Arnborg, and G. Andersson. "On the Analysis of Long-Term Voltage Stability". In: *International Journal of Electrical Power & Energy Systems* 15.4 (1993), pp. 229–237 (cited on pages 5, 50, 139).

[66] J. E. Machado, J. Arocas-Pérez, W. He, R. Ortega, and R. Griñó. "Active Damping of a DC Network with a Constant Power Load: An Adaptive Passivity-based Control Approach". In: *Congreso Nacional de Control Automático (CNCA)*. San Luis Potosi, Mexico, 2018 (cited on pages 102, 103, 106, 109).

[67] J. Machowski, J. Bialek, and J. Bumby. *Power system dynamics: stability and control*. J.Wiley & Sons, 2008 (cited on pages 2, 3, 14, 15, 136–138).

[68] P. Magne, B. Nahid-Mobarakeh, and S. Perfedierici. "A design method for a fault-tolerant multi-agent stabilizing system for DC microgrids with constant power loads". In: *IEEE Transportation and Electrification Conference and Expo (ITEC)*. 2012 (cited on page 4).

[69] D. Marx, P. Magne, B. Nahid-Mobarakeh, S. Pierfederici, and B. Davat. "Large signal stability analysis tools in DC power systems with constant power loads and variable power loads—A review". In: *IEEE Transactions on Power Electronics* 27.4 (2012), pp. 1773–1787 (cited on pages 4, 138).

[70] B. Maschke, R. Ortega, and A. van der Schaft. "Energy-Based Lyapunov Functions for Forced Hamiltonian Systems with Dissipation". In: *IEEE Transactions on Automatic Control* 45.8 (2000), pp. 1498–1502 (cited on pages 67, 68).

[71] Y. Massaoudi, E. Dorsaf, and J.P. Gaubert. "Experimental implementation of new sliding mode control law applied to a DC-DC boost converter". In: *Asian Journal of Control* 18.6 (2016), pp. 2221–2233 (cited on page 82).

[72] M. Mesbahi and M. Egerstedt. *Graph theoretic methods in multiagent networks*. Vol. 33. Princeton University Press, 2010 (cited on pages 8, 9).

[73] D. Molzahn, B. Lesieutre, and C. DeMarco. "A sufficient condition for power flow insolvability with applications to voltage stability margins". In: *IEEE Transactions on Power Systems* 28.3 (2013), 2592–2601 (cited on page 18).

[74] D. Molzahn, I. Hiskens, and *et al.* "A survey of relaxations and approximations of the power flow equations". In: *Foundations and Trends® in Electric Energy Systems* 4.1-2 (2019), pp. 1–221 (cited on pages 4, 138).

[75] N. Monshizadeh, P. Monshizadeh, R. Ortega, and A. van der Schaft. "Conditions on Shifted Passivity of Port-Hamiltonian Systems". In: *Systems & Control Letters* (2018). (accepted for publication) (cited on page 124).

[76] P. Monshizadeh, C. De Persis, N. Monshizadeh, and A. van der Schaft. "Nonlinear analysis of an improved swing equation". In: *IEEE 55th Conference on Decision and Control (CDC)*. 2016, pp. 4116–4121 (cited on pages 78, 79).

[77] P. Monshizadeh, C. De Persis, T. Stegink, N. Monshizadeh, and A. van der Schaft. "Stability and Frequency Regulation of Inverters with Capacitive Inertia". In: *arXiv preprint arXiv:1704.01545* (2017) (cited on page 78).

[78] P. Monshizadeh Naini. "Modeling and control of power systems in microgrids". PhD thesis. University of Groningen, 2018 (cited on page 7).

[79] H. Mosskull. "Optimal DC-Link Stabilization Design". In: *IEEE Transactions on Industrial Electronics* 62.8 (2015), pp. 5031–5044 (cited on page 102).

[80] H. Mosskull. "Optimal stabilization of constant power loads with input LC-filters". In: *Control Engineering Practice* 27 (2014), pp. 61–73 (cited on page 82).

[81] R. Ortega and E. Garcia-Canseco. "Interconnection and damping assignment passivity-based control: A survey". In: *European Journal of Control* 10.5 (2004), pp. 432–450 (cited on pages 83, 87, 95).

[82] R. Ortega, A. van der Schaft, B. Maschke, and G. Escobar. "Interconnection and damping assignment passivity-based control of port-controlled Hamiltonian systems". In: *Automatica* 38.4 (2002), pp. 585–596 (cited on pages 67, 83).

[83] R. Ortega, A. Loría, P. J. Nicklasson, and H. Sira-Ramirez. *Passivity-Based Control of Euler-Lagrange Systems: Mechanical, Electrical and Electromechanical Applications*. Communications and Control Engineering. Springer-Verlag, 1998 (cited on pages 83, 86).

[84] R. Ortega, A. van der Schaft, I. Mareels, and B. Maschke. "Putting energy back in control". In: *IEEE Control Systems* 21.2 (2001), pp. 18–33 (cited on page 67).

[85] A. Pavlov and L. Marconi. "Incremental passivity and output regulation". In: *Systems & Control Letters* 57.5 (2008), pp. 400–409 (cited on page 11).

[86] B. Polyak. "Convexity of quadratic transformations and its use in control and optimization". In: *Journal of Optimization Theory and Applications* 99.3 (1998), pp. 553–583 (cited on pages 4, 19, 24, 139).

[87] R. Quadrelli and S. Peterson. "The energy–climate challenge: recent trends in CO 2 emissions from fuel combustion". In: *Energy policy* 35.11 (2007), pp. 5938–5952 (cited on pages 2, 136).

[88] A. Rahimi and A. Emadi. "Active damping in DC/DC power electronic converters: A novel method to overcome the problems of constant power loads". In: *IEEE Trans. Ind. Electron.* 56.5 (2009), pp. 1428–1439 (cited on page 82).

[89] A. Rahimi, G. Williamson, and A. Emadi. "Loop-cancellation technique: A novel nonlinear feedback to overcome the destabilizing effect of constant-power loads". In: *IEEE Trans. Veh. Technol.* 59.2 (2010), pp. 650–661 (cited on page 83).

[90] S. Rahman and A. de Castro. "Environmental impacts of electricity generation: A global perspective". In: *IEEE Transactions on energy Conversion* 10.2 (1995), pp. 307–314 (cited on pages 2, 136).

[91] S. Sanchez, R. Ortega, R. Griñó, G. Bergna, and M. Molinas. "Conditions for existence of equilibrium points of systems with constant power loads". In: *IEEE Transactions on Circuits and Systems I: Regular Papers* 61.7 (2014), pp. 2204–2211 (cited on pages 19, 26, 33).

[92] S. Sanchez, A. Garces, G. Berna, and E. Tedeschi. "Dynamics and Stability of Meshed Multiterminal HVDC Networks". In: *arXiv preprint arXiv:1803.06892* (2018) (cited on pages 50, 51, 54, 56).

[93] A. van der Schaft. *L_2-Gain and Passivity Techniques in Nonlinear Control*. 3rd Revised, Enlarged Edition (1st edition 1996, 2nd edition 2000), Springer Communications, and Control Engineering series, Springer International, 2017 (cited on pages 67, 68, 70, 71).

[94] A. van der Schaft. *L_2-gain and passivity techniques in nonlinear control*. 2nd ed. Springer, 2000 (cited on page 11).

[95] A. van der Schaft and D. Jeltsema. *Port-Hamiltonian Systems Theory: An Introductory Overview*. Now Foundations and Trends, 2014 (cited on pages 11, 12, 67, 72).

[96] J. Schiffer. "Stability and Power Sharing in Microgrids". PhD thesis. Technical University of Berlin, 2015 (cited on pages 3, 7, 137).

[97] J. Schiffer, J. Zonetti, R. Ortega, A. Stanković, T. Seizi, and J. Raisch. "A survey on modeling of microgrids–From fundamental physics to phasors and voltage sources". In: *Automatica* 74 (2016), pp. 135–150 (cited on pages 3, 137).

[98] J. Schiffer, P. Aristidou, and R. Ortega. "Online Estimation of Power System Inertia Using Dynamic Regressor Extension and Mixing". In: *IEEE Transactions on Power Systems* (2019) (cited on pages 4, 138).

[99] J. Schiffer, T. Seel, J. Raisch, and T. Sezi. "Voltage Stability and Reactive Power Sharing in Inverter-Based Microgrids With Consensus-Based Distributed Voltage Control." In: *IEEE Trans. Contr. Sys. Techn.* 24.1 (2016), pp. 96–109 (cited on pages 15, 49).

[100] A. Schrijver. *Theory of Linear and Integer Programming*. John Wiley and Sons, 1998 (cited on page 46).

[101] R. Sepulchre, M. Jankovic, and P. Kokotovic. *Constructive Nonlinear Control*. London: Springer-Verlag, 1997 (cited on page 98).

[102] R. Sepulchre, M. Jankovic, and P. Kokotovic. *Constructive nonlinear control*. Springer Science & Business Media, 2012 (cited on page 121).

[103] J. Simpson-Porco. "A theory of solvability for lossless power flow equations—Part I: Fixed-point power flow". In: *IEEE Transactions on Control of Network Systems* 5.3 (2017), pp. 1361–1372 (cited on page 19).

[104] J. Simpson-Porco. "A theory of solvability for lossless power flow equations—Part II: Conditions for radial networks". In: *IEEE Transactions on Control of Network Systems* 5.3 (2017), pp. 1373–1385 (cited on page 19).

[105] J. Simpson-Porco. "Distributed Control of Inverter-Based Power Grids". PhD thesis. University of California Santa Barbara, 2015 (cited on pages 7, 15).

[106] J. Simpson-Porco, F. Dörfler, and F. Bullo. "On Resistive Networks of Constant-Power Devices". In: *IEEE Transactions on Circuits and Systems II* 62.8 (2015), pp. 811–815 (cited on pages 3, 4, 137, 138).

[107] J. Simpson-Porco, F. Dörfler, and F. Bullo. "On resistive networks of constant-power devices". In: *IEEE Transactions on Circuits and Systems II: Express Briefs* 62.8 (2015), pp. 811–815 (cited on page 18).

[108] J. Simpson-Porco, F. Dörfler, and F. Bullo. "Voltage Collapse in Complex Power Grids". In: *Nature communications* 7 (2016) (cited on pages 49, 50).

[109] S. Singh, A. Gautam, and D. Fulwani. "Constant power loads and their effects in DC distributed power systems: A review". In: *Renewable and Sustainable Energy Reviews* 72 (2017), pp. 407–421 (cited on pages 3, 101, 138).

[110] S. Singh, A. Gautam, and D. Fulwani. "Constant power loads and their effects in DC distributed power systems: A review". In: *Renewable and Sustainable Energy Reviews* 72 (2017), pp. 407–421 (cited on page 82).

[111] S. Singh, N. Rathore, and D. Fulwani. "Mitigation of negative impedance instabilities in a DC/DC buck-boost converter with composite load". In: *Journal of Power Electronics* 16.3 (2016), pp. 1046–1055 (cited on page 83).

[112] H. Sira-Ramirez, R. Perez-Moreno, R. Ortega, and M. Garcia-Esteban. "Passivity-based controllers for the stabilization of DC-to-DC power converters". In: *automatica* 33.4 (1997), pp. 499–513 (cited on page 84).

[113] H. Sira-Ramirez, A. Hernández-Méndez, J. Linares-Flores, and A. Luviano-Jurez. "Robust flat filtering DSP based control of the boost converter". In: *Control Theory Technology* 14.3 (2016), pp. 224–236 (cited on page 85).

[114] H. Smith. *Monotone Dynamical Systems: An Introduction to the Theory of Competitive and Cooperative Systems*. American Mathematical Society, 2008 (cited on pages 40, 42, 59, 60).

[115] J. Szarski. *Differential Ineqialities*. Państwowe Wydawnictwo Naukowe, 1967 (cited on page 66).

[116] A. Tahri, H. El Fadil, and F. Giri. "Nonlinear adaptive control of a hybrid fuel cell power system for electric vehicles-a Lyapunov stability based approach". In: *Asian Journal of Control* 18.1 (2016), pp. 166–177 (cited on page 82).

[117] S. Trip, M. Cucuzzella, C. De Persis, A. Ferrara, and J. Scherpen. "Robust load frequency control of nonlinear power networks". In: *International Journal of Control* (2018), pp. 1–14 (cited on pages 4, 138).

[118] F. Uhlig. "A recurring theorem about pairs of quadratic forms and extensions: A survey". In: *Linear Algebra and its Applications* 25 (1979), pp. 219–237 (cited on pages 4, 19, 34, 139).

[119] T. Van Cutsem and C. Vournas. *Voltage Stability of Electric Power Systems*. Springer Science & Business Media, 2007 (cited on pages 39, 49, 50).

[120] D. Van Hertem and M. Ghandhari. "Multi-Terminal VSC HVDC for the European Supergrid: Obstacles". In: *Renewable and Sustainable Energy Reviews* 14.9 (2010), pp. 3156–3163 (cited on page 39).

[121] V. Venikov, V. Stroev, V. Idelchick, and V. Tarasov. "Estimation of Electrical Power System Steady-State Stability in Load Flow Calculations". In: *IEEE Transactions on Power Apparatus and Systems* 94.3 (1975), pp. 1034–1041 (cited on page 49).

[122] D. Vilathgamuwa, X. Zhang, S. Jayasinghe, B. Bhangu, C. Gajanayake, and K. Tseng. "Virtual resistance based active damping solution for constant power instability in AC microgrids". In: *IECON 2011-37th Annual Conference of the IEEE Industrial Electronics Society*. IEEE. 2011, pp. 3646–3651 (cited on pages 3, 4, 137).

[123] C. Wang, A. Bernstein, J. Le Boudec, and M. Paolone. "Explicit conditions on existence and uniqueness of load-flow solutions in distribution networks". In: *IEEE Transactions on Smart Grid* 9.2 (2018), pp. 953–962 (cited on pages 4, 14, 40, 138).

[124] J. Wang, S. Li, Yang. J., B. Wu, and Q. Li. "Extended state observer-based sliding mode control for PWM-based DC-DC buck power converter systems with mismatched disturbances". In: *IET Control Theory & Applications* 9.4 (2015), pp. 579–586 (cited on page 82).

[125] J. X. Wang, C. L. Zhang, S. Li, J. Yang, and Q. Li. "Finite-time output feedback control for PWM-based DC-DC buck power converters of current sensorless mode". In: *IEEE Trans. on Control Systems Technology* 25.4 (2017), pp. 1359–1371 (cited on page 82).

[126] Z. Wang, B. Cui, and J. Wang. "A necessary condition for power flow insolvability in power distribution systems with distributed generators". In: *IEEE Transactions on Power Systems* 32.2 (2016), pp. 1440 –1450 (cited on page 18).

[127] M. Wu and D. Lu. "A Novel Stabilization Method of LC Input Filter With Constant Power Loads Without Load Performance Compromise in DC Microgrids". In: *IEEE Transactions on Industrial Electronics* 62.7 (2015), pp. 4552–4562 (cited on page 102).

[128] C. Zhang, J. Wang, S. Li, Wu. B., and C. Qian. "Robust control for PWM-based DC-DC buck power converters with uncertainty via sampled-data output feedback". In: *IEEE Trans. on Power Electron.* 30.1 (2015), pp. 504–515 (cited on page 82).

[129] X. Zhang, X. Ruan, H. Kim, and K. Chi. "Adaptive active capacitor converter for improving stability of cascaded DC power supply system". In: *IEEE Transactions on Power Electronics* 28.4 (2013), pp. 1807–1816 (cited on pages 101, 102, 104).

[130] J. Zhou and Y. Ohsawa. "Improved Swing Equation and Its Properties in Synchronous Generators". In: *Circuits and Systems I: Regular Papers, IEEE Transactions on* 56.1 (2009), pp. 200–209 (cited on page 78).

[131] D. Zonetti. "Energy-based modelling and control of electric power systems with guaranteed stability properties". PhD thesis. Université Paris-Saclay, 2016 (cited on page 7).

[132] D. Zonetti and R. Ortega. "Control of HVDC transmission systems: From theory to practice and back". In: *Mathematical Control Theory I: Nonlinear and Hybrid Control Systems*. Ed. by M.N. Belur, M.K. Camlibel, P. Rapisarda, and J.M.A Scherpen. Berlin/Heidelberg: Springer, 2015, pp. 153–177 (cited on page 51).

Part V

APPENDIX

Appendix A

Résumé substantiel en langue française

A.1 Introduction

Les besoins en énergie d'une société moderne sont principalement fournis sous forme d'énergie électrique [4]. L'utilisation commerciale de l'électricité a commencé à la fin des années 1870 avec des réseaux de très petite taille fournissant suffisamment d'énergie pour alimenter les lampes à arc destinées à l'éclairage des phares maritimes et à l'éclairage des rues [56]. Afin de satisfaire la demande croissante en énergie électrique, des societés industriellement développées ont construit des systèmes électriques très vastes et complexes pouvant s'étendre à des pays entiers [4, 56].

L'énergie électrique est traditionnellement produite dans des centrales thermiques, où un processus de combustion de combustibles fossiles libère de l'énergie thermique qui est transformée en énergie électrique utile pour le consommateur. Les combustibles les plus couramment utilisés dans la production commerciale d'électricité sont le charbon, le gaz naturel, le combustible nucléaire et le pétrole [56, 67, 40]. La combustion de combustibles fossiles dans les centrales électriques représente une source majeure d'émissions de gaz à effet de serre dans l'atmosphère [67, 90, 15, 29]. En outre, il est considéré que les émissions de gaz à effet de serre provenant des activités humaines sont l'un des principaux facteurs responsables du changement climatique et du réchauffement de la planète [15, 63, 87].

Différentes stratégies ont été proposées pour réduire les émissions de gaz à effet de serre dans l'industrie électrique, par exemple, augmenter le nombre de centrales nucléaires ou éliminer le dioxyde de carbone des gaz d'échappement de la génération thermique traditionnelle grâce à une technologie de captage et de stockage spécialisée [67] . Une alternative radicale à ces stratégies consiste à passer des centrales électriques traditionnelles alimentées aux combustibles fossiles aux énergies renouvelables. Les énergies renouvelables sont des sources d'énergie continuellement reconstituées par la nature et dérivées directement du soleil (thermique, photoélectrique, par exemple), indirectement du soleil (vent, énergie hydraulique, biomasse) ou d'autres mouvements et mécanismes naturels de l'environnement (géo thermique, par exemple) [36].

Les marchés des énergies renouvelables ont connu une croissance continue au cours des dernières années. Le déploiement de technologies éprouvées, telles que

l'hydroélectricité, ainsi que de nouvelles technologies, telles que l'éolien et le solaire, a rapidement augmenté, ce qui a renforcé la confiance dans les technologies et réduit les coûts [36].

La pénétration croissante des marchés des énergies renouvelables nécessite un changement majeur des pratiques de production électrique actuelles. Les centrales thermiques d'un système électrique traditionnel ont généralement une très grande puissance et se trouvent très loin des consommateurs. Pour transporter efficacement l'électricité sur de grandes distances, les tensions de fonctionnement doivent être augmentés à des niveaux très élevés à l'aide d'un système complexe de sous-stations et de réseaux de transport. Inversement, les sources d'énergie renouvelables tendent à être très petites en termes de capacité en ce qui concerne les centrales thermiques, ce qui implique que, pour fournir la même quantité d'énergie électrique, de nombreuses sources d'énergie renouvelables doivent être installées. Néanmoins, en raison d'une faible densité d'énergie, ces sources sont réparties d'une manière distribuée plutôt que centralisé comme dans les installations traditionnelles [67].

Les progrès récents de l'électronique de puissance ont élucidé les réponses possibles à la question de comment mieux intégrer les sources d'énergie renouvelables dans le reseaux eléctrique conventionnel. Le concept de *microréseaux* [62] a beaucoup retenu l'attention. Un microréseau est constitué d'un ensemble d'unités de production—principalement basées sur des sources d'énergie renouvelables—de charges résidentielles et d'éléments de stockage d'énergie qui pouvent être operés en connectés ou déconnectés du réseau eléctrique principal [62]. Le lecteur est invité à consulter les travaux [96, 97] pour une discussion plus approfondie sur les microréseaux.

A.2 Le problème

Dans de nombreux systèmes de distribution d'énergie électrique, en particulier dans les microréseaux, des problèmes de stabilité peuvent survenir lorsqu'une proportion importante des charges est constituée d'équipements électroniques. Ce type d'équipement est généralement alimenté par des architectures distribuées en cascade caractérisées par la présence de différents niveaux de tension et de convertisseurs électroniques de puissance. Ces convertisseurs agissent comme des interfaces entre des sections de tensions différentes dans lesquelles, au dernier étage, les charges sont une combinaison de convertisseurs électroniques de puissance régulant étroitement sa tension de sortie, se comportant comme des charges à puissance constante. Ces architectures sont communs dans les installations de technologies de l'information et de la communication où de nombreux commutateurs de télécommunication, stations de base de communications sans fil et serveurs de centres de données agissent comme des charges à puissance constante [38, 59, 122]. Il est bien connu que les charges à puissance constante introduisent un effet déstabilisateur qui provoque des oscillations importantes ou un effondrement du réseau [38]. Ils constituent donc le composant le plus difficile du modèle de charge standard, appelé ZIP. model [106, 30] dans l'analyse de la stabilité du système d'alimentation.

L'évaluation de la stabilité dans les réseaux contenant des charges à puissance constante est un défi de taille, principalement en raison des non-linéarités introduites par la dynamique de ce type de charge, mais également par la nature non linéaire des convertisseurs électroniques eux-mêmes. De plus, les incertitudes liées aux énergies

renouvelables et à l'interconnexion de plusieurs sous-systèmes aggravent encore le problème. Par conséquent, la stabilité globale du système peut être difficile à assurer, même si les sous-systèmes individuels sont stables [109].

Considérant les implications économiques et environnementales pertinentes de la compréhension des conditions assurant le fonctionnement stable et sûr des réseaux contenant des charges à puissance constante, cette thèse s'intéresse à cet objectif.

A.3 Une examination générale de la littérature

L'objectif principal d'un système électrique est de fournir de l'énergie électrique aux consommateurs de manière fiable, avec un coût minimal, un impact écologique minimal et des normes de qualité spécifiées [56, 67]. L'analyse de la stabilité d'un système électrique concerne sa capacité à résister aux perturbations tout en permettant de remplir son objectif principal [4]. Les perturbations typiques des systèmes électriques sont, par exemple, des modifications de la demande, des pannes de centrales ou des défaillances du système de transmission [56]. Compte tenu de la grande complexité du système énergétique d'une société moderne, le problème de la garantie d'un fonctionnement sûr et stable du système reste un domaine de recherche actif [39, 61, 98, 117, 41].

Une condition très importante pour effectuer des analyses de stabilité et pour le bon fonctionnement des systèmes électriques est l'existence d'un état stable qui, de plus, devrait être robuste en présence de perturbations [56]. L'analyse de ces équilibres est compliquée par la présence de charges de puissance constante, qui introduisent des "fortes" non linéarités. Cela motive le développement de nouvelles méthodes pour analyser l'existence d'états stationnaires. En [69, 9, 14] une analyse de *existence* d'équilibres est effectuée alors que, dans [106], des conditions suffisantes sont définies pour que tous les points de fonctionnement de réseaux purement résistifs soient maintenus. Il est à noter que la communauté des systèmes électriques débat actuellement de nouvelles définitions de la stabilité, qui s'éloignent du paradigme équilibre-perturbation-équilibre [57]. Cependant, l'analyse des équilibres dans les systèmes à courant continu et alternatif est toujours un domaine de recherche actif; voir, *e.g.*, [74] et [123].

Une analyse de stabilité a été réportée dans [3, 9] à l'aide de méthodes de linéarisation, voir aussi [69]. Dans [10] et récemment dans [20], la théorie du potentiel de Brayton-Moser [16] été employée, mais les contraintes qui garantissent la stabilité du système sont imposées aux composants individuels du même. De plus, comme indiqué dans [69], l'estimation fournie de la région d'attraction des équilibres basée sur le potentiel de Brayton-Moser est plutôt conservatrice.

Il existe deux méthodes principales de stabilisation des réseaux avec des charges de puissance constantes. Elles sont respectivement appelées méthodes d'amortissement actif et passif. Pour une stabilisation passive, un matériel supplémentaire est connecté au réseau, *e.g.*, une résistance peut être connectée en parallèle avec la charge à puissance constante ou un effet capacitif plus important peut être obtenu en incluant des filtres supplémentaires [59, 21]. Cependant, le principal inconvénient de ces approches est qu'elles sont généralement inefficaces du point de vue énergétique et que les coûts ou la taille supplémentaires risquent de ne pas être pratiques. D'autre part, les méthodes d'amortissement actif visent à obtenir le même comportement de

ces composants passifs par la modification de boucles de commande déjà existantes ou supplémentaires.

A.4 Principales contributions et organisation

Les principales contributions de cette thèse portent sur l'analyse et le contrôle de réseaux contenant des charges de puissance constantes. Elles peuvent être répertoriées comme suit.

C1 Le problème de l'existence d'équilibres d'une classe générale de réseaux à courant alternatif qui energize des charges à puissance constante est traité. Cette thèse fournit des conditions nécessaires sur les valeurs de puissance des charges pour l'existence d'équilibres, c'est-à-dire que si ces conditions ne sont pas remplies, le réseau n'admet pas de régime d'équilibre sinusoïdal. En exploitant le cadre de *formes quadratiques* [86, 118], ces conditions sont exprimées en termes de faisabilité d'inégalités linéaires de matrices, pour lesquelles des logiciels fiables sont disponible. De plus, un raffinement est apporté pour le cas des réseaux à port unique où une condition à la fois *nécessaire* et *suffisante* pour l'existence d'équilibres est signalée.

C2 On montre que des modèles généraux des réseaux de courant alternatif et de courant continu avec des charges à puissance constante—qui incluent des systèmes de transmission haute tension multi-terminaux et des microréseaux—sont décrits en régime stationnaire par un champ vectoriel non linéaire qui, lorsqu'il est associé à un ensemble d'équations différentielles ordinaires, présente des propriétés de monotonie. Ces propriétés sont ensuite utilisées pour établir que si les modèles susmentionnés admettent des solutions d'équilibre, l'un d'eux domine, en termes de composants, tous les autres. En outre, dans le cas de réseaux à courant alternatif sous certaines hypothèses plutôt standard, cet équilibre s'avère être *voltage regular*; voir [65, 45].

C3 Une classe de systèmes port-Hamiltoniens dans lesquels les variables de contrôle agissent directement sur l'équation du rapport de puissance est explorée; ces systèmes sont ensuite appelés *systèmes Hamiltoniens contrôlés par puissance*. Dans ces systèmes dynamiques, les points d'équilibre sont intrinsèquement non nuls, ce qui empêche l'utilisation des propriétés de passivité connues de systèmes plus classiques port-hamiltoniens (avec matrice à entrées constantes) pour analyser leur stabilité. Les conditions dans lesquelles ces systèmes sont *shifted passive* sont étudiées; Cette méthode est également utilisée pour effectuer une analyse de stabilité des équilibres du système. Fait intéressant, dans le cas où l'Hamiltonien est quadratique, une estimation de la région d'attraction peut être fournie. Ces résultats sont appliqués à l'étude de la stabilité d'une classe générale de réseaux électriques à courant continu et d'un générateur synchrone, avec des charges à puissance constante.

C4 Le problème de la régulation de la tension de sortie du très populaire et polyvalent convertisseur DC buck-boost est abordé, dans l'hypothèse où il fournit de l'énergie à une charge de puissance constante. Le modèle bilinéaire décrivant

ce réseau s'avère être une phase non minimale par rapport à chacune des variables d'état, ce qui complique la conception des contrôleurs linéaires. Une nouvelle loi de contrôle adaptatif, non linéaire, est conçue conformément à la méthodologie de conception IDA-PBC. Le contrôleur est rendu adaptatif en incorporant un estimateur en ligne pour la valeur—pratiquement difficile à mesurer—de la charge à puissance constante.

C5 La stabilisation d'un microréseau à courant continu dont la source d'alimentation principale est connectée à une charge à puissance constante est explorée. La source étant supposée non contrôlable, le réseau est d'abord augmenté par l'ajout d'un convertisseur de puissance contrôlable. Ensuite, une loi de commande non linéaire et adaptative, qui permet de stabiliser le réseau dans son ensemble, est proposée pour contrôler le convertisseur. La conception est particulièrement difficile en raison de l'existence d'états difficiles à mesurer dans un scénario pratique—le courant du réseau à courant continu—et en raison de la consommation d'énergie inconnue de la charge. Il convient de souligner que les développements théoriques ont été validés par des experiments physiques sur un réseau à courant continu à petite échelle; ces résultats expérimentaux sont rapportés dans la thèse.

Le reste de la thèse est structuré comme suit. Quelques préliminaires sur les systèmes dynamiques non linéaires et les systèmes électriques sont présentés au chapitre 2. Les principales contributions, de C1 à C5, sont rapportées dans les chapitres 3 à 7, respectivement. La thèse se termine par le chapitre 8, qui contient un bref résumé et une discussion sur les recherches futures plausibles.

A.5 Des publications

Cette thèse est basée sur les articles suivants, dont certains ont déjà été publiés ou sont en cours de révision.

J1 Juan E. Machado, Robert Griñó, Nikita Barabanov, Romeo Ortega, and Boris Polyak, "On Existence of Equilibria of Multi-Port Linear AC Networks With Constant-Power Loads,", *IEEE Transactions on Circuits and Systems I: Regular Papers*, Vol. 64, No. 10, pp. 2772–2782, 2017.

J2 Wei He, Romeo Ortega, Juan E. Machado, and Shihua Li, "An Adaptive Passivity-Based Controller of a Buck-Boost Converter With a Constant Power Load," *Asian Journal of Control*, Vo. 21, No. 2, pp. 1–15, 2018.

J3 Pooya Monshizadeh, Juan E. Machado, Romeo Ortega, and Arjan van der Schaft, "Power-Controlled Hamiltonian Systems: Application to Electrical Systems with Constant Power Loads," *Automatica*, 2019. (à apparaître)

J4 Alexey Matveev, Juan E. Machado, Romeo Ortega, Johannes Schiffer, and Anton Pyrkin, "On the Existence and Long-Term Stability of Voltage Equilibria in Power Systems with Constant Power Loads," *IEEE Transactions on Automatic Control*, 2019. (accepté provisoirement)

J5 Juan E. Machado, Romeo Ortega, Alessandro Astolfi, José Arocas-Pérez, Anton Pyrkin, Alexey Bobtsov, and Robert Griñó, "Active Damping of a DC Network with a Constant Power Load: An Adaptive Observer-based Design," *IEEE Transactions on Control Systems Technology*, 2019. (envoyé)

ÉCOLE DOCTORALE
université PARIS-SACLAY
Sciences et technologies de l'information et de la communication (STIC)

Titre : Quelques problèmes dans l'analyse et la commande des réseaux électriques avec des charges à puissance constante

Mots clés : Réseaux électriques, Charges à Puissance Constante, Analyse, Commande

Résumé : La croissante demande d'énergie électrique a conduit à la conception de systèmes électriques de grande complexité où les combustibles fossiles constituent la principale source d'énergie. Néanmoins, les préoccupations environnementales poussent à un changement majeur dans les pratiques de production d'électricité, avec un passage marqué des énergies fossiles aux énergies renouvelables et des architectures centralisées à distribuées. Les problèmes de stabilité dus à la présence de ce qu'on appelle les *Charges à Puissance Constante* (CPLs) constituent l'un des principaux défis auxquels sont confrontés les systèmes électriques distribués. On sait que ces charges, que l'on trouve couramment dans les installations de technologie de l'information et de la communication, réduisent l'amortissement effectif des circuits qui les alimentent, ce qui peut provoquer des oscillations de tension, voire une chute. Dans cette thèse, les principales contributions sont centrées sur la compréhension et la résolution de divers problèmes rencontrés dans l'analyse et le contrôle de systèmes électriques contenant des CPLs. Les contributions sont énumérées comme suit. (i) Des conditions simplement vérifiables sont proposées pour certifier la *non existence* d'états en régime permanent pour des réseaux multi-ports, à courant alternatif avec une distribution de CPLs. Ces conditions, qui reposent sur les inégalités matricielles linéaires, permettent d'écarter les valeurs des puissances des charges qui produiraient certainement un effondrement de la tension sur l'ensemble du réseau. (ii) Pour des modèles généraux de certains systèmes électriques modernes, y compris les réseaux de transmission à courant continu haute tension et les microréseaux, il est montré que, si des équilibres existent, il existe un équilibre caractéristique à haute tension qui domine tous les autres. En outre, dans le cas des systèmes d'alimentation en courant alternatif sous l'hypothèse de découplage standard, cet équilibre caractéristique s'avère stable à long terme. (iii) Une classe de systèmes port-Hamiltoniens, dans laquelle les variables de contrôle agissent directement sur l'équation de puissance, est explorée. Il est démontré que ces systèmes sont décalés de manière passive lorsque leurs trajectoires sont contraintes à des ensembles facilement définissables. Ces dernières propriétés sont exploitées pour analyser la stabilité de leurs équilibres intrinsèquement non nuls. Il a également été montré que la stabilité des réseaux électriques à courant continu multiports et des générateurs synchrones, tous deux connectés à des CPLs, peuvent naturellement être étudiée dans le cadre proposé. (iv) Le problème de la régulation de la tension de sortie du convertisseur buck-boost alimentant une CPL non connu est résolu. L'un des principaux obstacles à la conception de commandes linéaires classiques provient du fait que le modèle du système est de phase non minimale par rapport à chacune de ses variables d'état. Cette thèse rapporte un contrôleur adaptatif non linéaire capable de rendre un équilibre souhaité asymptotiquement stable; de plus, une estimation de la région d'attraction peut être calculée. (v) La dernière contribution concerne l'amortissement actif d'un système d'alimentation de petite taille à courant continu avec une CPL. Au lieu de connecter des éléments passifs peu pratiques et énergétiquement inefficaces au réseau existant, l'ajout d'un convertisseur de puissance contrôlé est exploré. La contribution principale rapportée ici est la conception d'une loi de contrôle non linéaire basée sur l'observateur pour le convertisseur. La nouveauté de la proposition réside dans le fait qu'il n'est pas nécessaire de mesurer le courant électrique du réseau ni la valeur de la CPL, soulignant ainsi son applicabilité pratique. L'efficacité du schéma de contrôle est ensuite validée par des expériences sur un réseau à courant continu réel.

Title: Some Problems on the Analysis and Control of Electrical Networks with Constant Power Loads

Keywords: Power systems, Constant Power Loads (CPLs), Analysis, Control

Abstract: The continuously increasing demand of electrical energy has led to the conception of power systems of great complexity that may extend even through entire countries. In the vast majority of large-scale power systems the main primary source of energy are fossil fuels. Nonetheless, environmental concerns are pushing a major change in electric energy production practices, with a marked shift from fossil fuels to renewables and from centralized architectures to more distributed ones. One of the main challenges that distributed power systems face are the stability problems arising from the presence of the so-called *Constant Power Loads* (CPLs). These loads, which are commonly found in information and communication technology facilities, are known to reduce the effective damping of the circuits that energize them, which can cause voltage oscillations or even voltage collapse. In this thesis, the main contributions are focused in understanding and solving diverse problems found in the analysis and control of electrical power systems containing CPLs. The contributions are listed as follows. (i) Simply verifiable conditions are proposed to certify the *non existence* of steady states in general, multi-port, alternating current (AC) networks with a distributed array of CPLs. These conditions, which are based on Linear Matrix Inequalities, allow to discard the values of the loads' powers that would certainly produce a voltage collapse in the whole network. (ii) For general models of some modern power systems, including High-Voltage Direct Current transmission networks and microgrids, it is shown that if equilibria exist, then there is a characteristic high-voltage equilibrium that dominates, entry-wise, all the other ones. Furthermore, for the case of AC power systems under the standard decoupling assumption, this characteristic equilibrium is shown to be long-term stable. (iii) A class of port-Hamiltonian systems, in which the control variables act directly on the power balance equation, is explored. These systems are shown to be shifted passive when their trajectories are constrained to easily definable sets. The latter properties are exploited to analyze the stability of their—intrinsically non zero—equilibria. It is also shown that the stability of multi-port DC electrical networks and synchronous generators, both with CPLs, can be naturally studied with the proposed framework. (iv) The problem of regulating the output voltage of the versatile DC buck-boost converter feeding an *unknown* CPL is addressed. One of the main obstacles for conventional linear control design stems from the fact that the system's model is non-minimum phase with respect to each of its state variables. As a possible solution to this problem, this thesis reports a nonlinear, adaptive controller that is able to render a desired equilibrium asymptotically stable; furthermore an estimate of the region of attraction can be computed. (v) The last contribution concerns the active damping of a DC small-scale power system with a CPL. Instead of connecting impractical, energetically inefficient passive elements to the existing network, the addition of a controlled DC-DC power converter is explored. The main contribution reported here is the design of a nonlinear, observer-based control law for the converter. The novelty of the proposal lies in the non necessity of measuring the network's electrical current nor the value of the CPL, highlighting its practical applicability. The effectiveness of the control scheme is further validated through experiments on a real DC network.

Université Paris-Saclay
Espace Technologique / Immeuble Discovery
Route de l'Orme aux Merisiers RD 128 / 91190 Saint-Aubin, France